

IV Russian-Mexican workshop on Nanoparticles, Nanomaterials and Nanoprocessing



May 6-9, 2014

CNYN-UNAM, Ensenada, Mexico.

IV Russian-Mexican workshop on Nanoparticles, Nanomaterials and Nanoprocessing



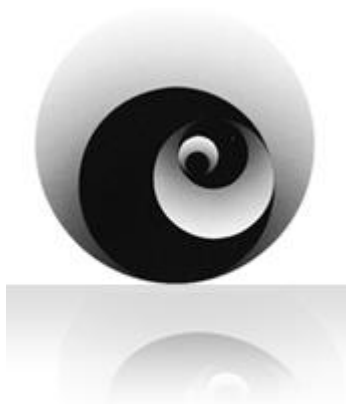
Book of abstracts

Edited by V. Petranovskii (Mexico)
and M. Shelyapina (Russia)

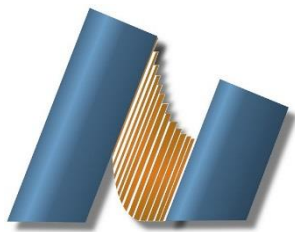
May 6-9, 2014

CNYN-UNAM

Ensenada, B. C., México.



Organizing committee acknowledges all-around support
of Coordination of Scientific Research, UNAM



The Organizing Committee is grateful to the CNyN for making 4th Workshop possible, and for financial support.



Agilent Technologies

Agilent Technologies helped us with their participation in the costs of Workshop conducting.

Board of Directors

Dr. José Narro Robles

President

Dr. Eduardo Bárzana García

General Secretary

Dr. Carlos Arámburo de la Hoz

Scientific Coordinator

Dr. Oscar Edel Contreras López

Director

Dr. Gustavo Alonso Hirata Flores

Academic Secretary

Dr. Jesus Antonio Diaz Hernandez

Technical Secretary

Lic. Jaime Oliver Sánchez

Administrative Secretary

Organizing Committee

Dr. Homero Galván, CNYN-UNAM, Mexico

Dr. Marina Shelyapina, St. Petersburg State University, Russia

Dr. Alexey Pestryakov, Tomsk Polytechnic University, Russia

Dr. Joel Antúnez-García, CETIS University, Mexico

Dr. Trino Zepeda-Partida, CNYN-UNAM, Mexico

MS Oscar Jaime-Acuña, CNYN-UNAM, Mexico

Dr. Vitalii Petranovski, CNYN-UNAM, Mexico

Opening remarks

From Director of the CNyN-UNAM

The Center of Nanoscience and Nanotechnology of the National Autonomous University of Mexico and the Department of Physics and Chemistry of the St. Petersburg State University have been developing intensive interactions in order to establish fruitful collaborations between both universities. The “Russian-Mexican workshop on Nanoparticles, Nanomaterials and Nanoprocessing” has been carried out three times so far alternatively between both Universities, being the first edition held in the St. Petersburg State University in July of 2012. These academic meetings have included advanced presentations from specialist in natural science, life science as well as on the health field. The 4th edition of this important meeting is held in the Center of Nanoscience and Nanotechnology in Ensenada City, Mexico and additionally to St. Petersburg State University the academic participation has expanded to Buryat State University at Ulan-Ude and Tomsk Polytechnic University at Tomsk, both cities from Russia. Now, considering the recent inauguration of new facilities in our Center, I hope that the 4th meeting becomes the appropriate occasion to establish great scale scientific, academic and technological projects.

We welcome all participants from the St. Petersburg State University, Tomsk Polytechnic University and Buryat State University to the Center of Nanoscience and Nanotechnology.



Dr. Oscar E. Contreras

Director of Center of Nanoscience and Nanotechnology

Preface

This is the “Book of abstracts” of *IV Russian-Mexican workshop on Nanoparticles, Nanomaterials and Nanoprocessing*.

The main topics in this “Workshop” are related with the synthesis, characterization and theoretical analysis of various aspects of studies touching NANO-world, in particular:

- Producing and Characterizations of Nanoparticles and Nanostructured Thin Films
- Nanomaterials Applications in Electronics, Spintronics and Photonics
- Nanomaterials Applications in Biotechnologies and Medicine
- Nanomaterials for Energy Applications
- Nanoparticles in Catalysis
- Russian-Mexican cooperation in the field of nanomaterial science and technology

Previous Workshops took place:

- 1st RuMex, Saint Petersburg, Russia, 24-26 June, 2012;
 - 2nd MexRu, Ensenada, Mexico, 5-8 November, 2012;
 - 3rd RuMex, Saint Petersburg, Russia, 14-17 October, 2013.
- Book of Abstracts of this Workshop is available for downloading at
<http://nmr.phys.spbu.ru/rumex/main>

We hope that the comprehensive and all- round cooperation between Russian and Mexican scientists in the field of nanomaterials science and technology will be fruitful for both countries.



IV Russian-Mexican workshop on Nanoparticles, Nanomaterials and Nanoprocessing

	Martes, 6 de mayo	Miércoles, 7 de mayo	Viernes, 9 de mayo
09:00-09:20	Opening ceremony		
09:20-09:40	K-01 -- Designing, Manipulation and Processing of Nanostructures for Applications in CNYN J.M. Romo-Herrera, O.E. Contreras et al.	K-04 Electronic properties of some crystalline compounds D. H. Galvan	K-07 Studying nanoparticles with light Catalina Lopez, Roberto Machorro
09:40-10:00			
10:00-10:20	O-01 Nanofabrication of ALD oxide nanotubes Hugo Tiznado et al.	O-07 A theoretical study of distinct sodalitic zeolite frameworks Joel Antúnez-García et al.	O-13 Optical properties of supported metal nanoparticles: Modeling zeolite based composites Catalina López Bastidas et al.
10:20-10:40	O-02 Nanostructured catalysts for hydrogen production in artificial photosynthesis Sergio Fuentes	O-08 Hybrid entanglement in a triple quantum dot shuttle system J. Mora, F. Rojas, E. Cota	O-14 Spectroscopic study on nanospecies prepared by thermal reduction in hydrogen followed by cooling in variable atmosphere for the Cu²⁺-Ag⁺-Zn²⁺/trimetallic system supported on mordenite I. Rodríguez-Iznaga, M. Herrera Zaldivar et al.
10:40-11:00	<i>Coffee Break</i>		
11:00-11:20	K-02 Methods of thermal analysis for the investigation of the hydration of nanostructural materials Irina Zvereva	K-05 Size effect on the stability of the MgH₂ and AlH₃ hydrides Marina G. Shelyapina	K-08 Nuclear Quadrupole Resonance: a review of applications to study bulk and nanoscale solids Elena Kurenkova
11:20-11:40			
11:40-12:00	O-03 Numerical study of a model plasmonic solar cell Margoth Córdova and Eugenio R. Méndez	O-09 NMR and EPR study of protonated and copper ion-exchanged mordenites. Y.M. Zhukov et al.	O-15 Using isotopes (²H, ¹⁸O, ³H) for water balance investigation in arid regions. 1. Estimation of groundwater resources in province Almería (south-east Spain) I.V. Tokarev et al.
12:00-12:20	O-04 Immobilized biocatalyst in mesoporous materials and its bionanotechnological applications Karla Juárez-Moreno et al.	O-10 Gold nanoparticles supported on nanostructured ceria A. Simakov et al.	O-16 Using isotopes (²H, ¹⁸O, ³H) for water balance investigation in arid regions. 2. Naryn river run-off investigation (Kyrgyzstan) I.V. Tokarev et al.
12:20-12:40	O-05 UV-Vis-mass in situ analysis of gold nanoparticles formation over χ-alumina Miguel Estrada et al.	O-11 CO oxidation over gold NP's supported on Mg(OH)₂ and MgO under different redox treatment E. Smolentseva et al.	O-17 Analysis of 4-Nitrophenol Reduction over Gold Catalysts: Effect of Catalyst Surface Brenda Acosta et al.
12:40-13:00	<i>Coffee Break</i>		
13:00-13:20	K-03 Geo-environmental and modelling resource center of the Saint-Petersburg State University (RC Geomodel) E. F. Mikhailov, I.V. Tokarev	K-06 Effect of various parameters on the growth of carbon nanotubes with different metal catalyst deposited Si substrate D.K. Tiwari, J. Valenzuela, M. Herrera	O-18 Synthesis of Plant-Derived Virus-Like Particles and his Potential Use as Vector Rubén Darío Cadena-Nava
13:20-13:40			O-19 Kinetic study of water absorption in plant germination while using MWCNT as a growth promoter D. K. Tiwari et al.
13:40-14:00	O-06 Chirality in Amino Acid Overlayers on Cu Surfaces M.L. Clegg, L. Morales de la Garza, et al.	O-12 Spontaneous formation of self-assembling, hierarchical and biomorphic SiO₂ nanostructures N. Bogdanchikova et al.	<i>Closing remarks, Closure</i>
14:00-16:00	<i>Lunch</i>		
16:00-18:30	Round Table	Poster session	
19:00	Informal Workshop meeting at Enoteca "L.A.Cetto"		

Tuesday, May 6

- K-01** *Designing, Manipulation and Processing of Nanostructures for Applications in CNYN*
J.M. Romo-Herrera, M. Cardoza, Omar Perez, Z. Bedolla, G. Alonso-Nuñez, D. Domínguez, F. Muñoz-Muñoz, H. Tiznado, Víctor García and O.E. Contreras
- O-01** *Nanofabrication of ALD oxide nanotubes*
Hugo Tiznado, Franklin Muñoz, David Domínguez, José Romo-Herrera, Oscar Contreras, Gabriel Alonso and Gerardo Soto
- O-02** *Nanostructured catalysts for hydrogen production in artificial photosynthesis*
Sergio Fuentes Moyado
- K-02** *Methods of thermal analysis for the investigation of the hydration of nanostructural materials*
Irina Zvereva
- O-03** *Numerical study of a model plasmonic solar cell*
Margoth Córdova and Eugenio R.Méndez
- O-04** *Immobilized biocatalyst in mesoporous materials and its bionanotechnological applications*
Karla Juárez-Moreno, Gabriel Alonso Núñez, Sergio Fuentes Moyado and Rafael Vazquez-Duhalt
- O-05** *UV-Vis-mass in situ analysis of gold nanoparticles formation over χ -alumina*
Miguel Estrada, Eunice Vargas, Elena Smolentseva, Sergio Fuentes, Andrey Simakov
- K-03** *Geo-environmental and modelling resource center of the Saint-Petersburg State University (RC Geomodel)*
E.F. Mikhailov, I.V. Tokarev
- O-06** *Chirality in Amino Acid Overlayers on Cu Surfaces*
M.L. Clegg, L. Morales de la Garza, S. Karakatsani, D.A. King, S.M. Driver

ROUND TABLE

Wednesday, May 7

- K-04** *Electronic properties of some crystalline compounds*
D. H. Galvan
- O-07** *A theoretical study of distinct sodalitic zeolite frameworks*
Joel Antúnez-García, D. Homero Galván Martínez, Vitalii Petranovskii
- O-08** *Hybrid entanglement in a triple quantum dot shuttle system*
J. Mora, F. Rojas, E. Cota
- K-05** *Size effect on the stability of the MgH_2 and AlH_3 hydrides*
Marina G. Shelyapina
- O-09** *NMR and EPR study of protonated and copper ion-exchanged mordenites.*
Y.M. Zhukov, A.Y. Kul'taeva, 2, A.N.Kovalyov, M.G. Shelyapina, V.P. Petranovskii
- O-10** *Gold nanoparticles supported on nanostructured ceria*
B. Acosta, M.A. Estrada, V. Evangelista, E. Smolentseva, S. Beloshapkin, I. Simakova,
A. Simakov
- O-11** *CO oxidation over gold nanoparticles supported on $Mg(OH)_2$ and MgO under different redox treatment*
E. Smolentseva, M. Estrada, M. López Cisneros, S. Beloshapkin, S. Fuentes and A. Simakov

- K-06** *Effect of various parameters on the growth of carbon nanotubes with different metal catalyst deposited Si substrate*
D. K. Tiwari, J. Valenzuela, M. Herrera
- O-12** *Spontaneous formation of self-assembling, hierarchical and biomorphic SiO₂ nanostructures*
N. Bogdanchikova, O. Martynyuk, A. Pestryakov, R. Luna Vázquez G., F. Ruiz Medina, A. Huerta-Saquero, T. Zepeda

POSTER SESSION

Friday, May 9

- K-07** *Studying nanoparticles with light*
Catalina Lopez, Roberto Machorro
- O-13** *Optical properties of supported metal nanoparticles: Modeling zeolite based composites*
Catalina López Bastidas, Elena Smolentseva, Roberto Machorro, Vitalii Petranovskii
- O-14** *Spectroscopic study on nanospecies prepared by thermal reduction in hydrogen followed by cooling in variable atmosphere for the Cu²⁺-Ag⁺-Zn²⁺/trimetallic system supported on mordenite*
I. Rodríguez-Iznaga, M. Herrera Zaldivar, V. Petranovskii, F. Castellón Barrasa, R. Machoro, F. Chávez Rivas
- K-08** *Nuclear Quadrupole Resonance: a review of applications to study bulk and nanoscaled solids*
Elena Kurenkova
- O-15** *Using isotopes (²H, ¹⁸O, ³H) for water balance investigation in arid regions.*
1. Estimation of groundwater resources in province Almeria (south-east Spain)
I.V. Tokarev, Carlos Ordóñez Peres, V.G. Rumynin
- O-16** *Using isotopes (²H, ¹⁸O, ³H) for water balance investigation in arid regions.*
2. Naryn river run-off investigation (Kyrgyzstan)
I.V. Tokarev, Carlos Ordóñez Peres, V.G. Rumynin
- O-17** *Analysis of 4-Nitrophenol Reduction over Gold Catalysts: Effect of Catalyst Surface*
Brenda Acosta, Viridiana Evangelista, Serguei Miridonov, Andrey Simakov
- O-18** *Synthesis of Plant-Derived Virus-Like Particles and his Potential Use as Vector*
Rubén Darío Cadena-Nava
- O-19** *Kinetic study of water absorption in plant germination while using MWCNT as a growth promoter*
D. K. Tiwari, N. Dasgupta-Schubert, L. M. Villaseñor Cendejas
- K-09** *Study of shear properties of nanoparticle suspensions*
Bair B. Damdinov, Tuyana S. Dembelova, B.B. Badmaev
- O-20** *Study of nanoparticles size distribution by acoustic method*
Kalashnikov Sergei, Nomoev Andrei, Romanov Nikolai, Damdinov Bair

Poster presentations: Wednesday, May 7, 16:00-18:30.

- P-01: Reactions of Protonated Layered Titanates for Synthesis of Nanomaterials
Liliia D. Abdulaeva, Irina A. Zvereva.

- P-02: Protonation and hydration of layered perovskite-like titanates and niobates
I.A. Rodionov, A.A. Burovikhina, T.D. Utkina, E.V. Mechtaeva, M.V. Chislov, I.A. Zvereva.
- P-03: Zirconia nanoparticles with different composition, size and morphology synthesized under hydrothermal conditions and their properties
A.N. Bugrov, I.A. Rodionov, R.Yu. Smyslov, O.V. Almjasheva, I.A. Zvereva.
- P-04: KKR-CPA study of hydrogen induced phase transitions in disordered Ti-V-Cr alloys
O.O. Bavrina, M.G. Shelyapina.
- P-05: First-principles estimation of hydrogen diffusion coefficient in magnesium
Konstantin Klyukin, Marina G. Shelyapina, Daniel Fruchart.
- P-06: DFT calculation of Cu(II) aqua complexes embedded in mordenite matrix
A.N. Kovalev, M.G. Shelyapina, V.P. Petranovskii.
- P-07: Chemical bonding in MoS₂: bulk, nanoparticles, MoS₂-G, and MoS₂-GO
E.P. Mikheenko, M.G. Shelyapina, D.H. Galvan Martinez.
- P-08: Unsupported Ni(Co)Niobium sulfides as catalysts for HDS of Dibenzothiophene
L. Pérez, C. Suresh, J.N. Díaz De León, T.A. Zepeda, G. Alonso, D.H. Galván, S. Fuentes.
- P-09: Ti content effect in CoMo/alumina-titania catalysts to dibenzothiophene HDS activity
René Obeso-Estrella, Eder Lugo-Medina, Sergio Fuentes, J.Noé Diaz de Leon, Trino A. Zepeda.
- P-10: Study of the support effects in ultra-deep hydrodesulfurization W catalysts
J.N. Díaz de León, G. Torres-Otañez, L.A. Zavala-Sánchez, T.A. Zepeda, V. Petranovskii, S. Fuentes, J.A. de los Reyes
- P-11: Experience of geothermal exploration on the Kamchatka Peninsula using the audiomagnetotelluric sounding method
Ksenia Antaschuk, Alexander Saraev, Igor Tokarev.
- P-12: Application of the radiomagnetotelluric sounding method for the solution of engineering and environmental tasks
Alexander Saraev, Alexander Simakov, Igor Tokarev.
- P-13: Characterization of Zirconium Oxide Films Deposited by Using the Atomic Layer Deposition Method
J.R. Martinez-Castelo, H. Tiznado, M.H. Farias.
- P-14: Synthesis of PVP stabilized Co and Ni nanoparticles for APR reaction
I. Simakova, Yu. Demidova, D.Yu. Murzin, A. Simakov.
- P-15: Preparation of PVP stabilized Ru nanoparticles for sugar alcohol APR
I. Simakova, Yu. Demidova, D.Yu. Murzin, A. Simakov.
- P-16: The reduction of 4-nitrophenol over Au@ZrO₂ and Au-Ce@ZrO₂ nanoreactors
Viridiana Evangelista, Brenda Acosta, Serguei Miridonov, Andrey Simakov.
- P-17: Modifier effect of metal oxides in CO oxidation over gold supported on silica
Y. Kotolevich, O. Martynyuk, J.E. Cabrera Ortega, V. Maturano Rojas, A. Aguilar Tapia, H.J. Tiznado, N. Bogdanchikova, A. Pestyakov, R. Zanella Spesia
- P-18: Semiconductor/MOR nanostructured composites: characterizations and photocatalysis
O. E. Jaime-Acuña, H. Villavicencio, V. Petranovskii, O. Raymond.
- P-19: Natural Iron-Exchanged Mordenite: UV-Vis Diffuse Reflectance and Mössbauer Characterization
D. Tito Ferro, I. Rodríguez Iznaga, B. Concepción Rosabal, F. Chávez Rivas, V. Petranovskii, F. F. Castellón Barraza, A. Penton Madrigal

- P-20: A theoretical study of Cu_2O and Cu_x clusters hosting in MOR dealuminated zeolite
Joel Antúnez-García, D. Homero Galván Martínez, Vitalii Petranovskii.
- P-21: Natural mordenite as an ionic exchanger of Cr^{3+} from alkaline solutions
 V. Córdova Rodríguez, I. Rodríguez Iznaga, R. M. Acosta Chávez, V. Petranovskii.
- P-22: Study of Ag nanoparticles growth over monometallic (Ag) and bimetallic (Fe/Ag) systems supported in mordenite
 P. Sánchez-Lopez, R. Obeso-Estrella, S. Miridonov, S. Fuentes, F.F. Castellón-Barraza, V. Petranovskii.
- P-23: Insight of the silver influence to hidrothermal stability of Cu-mordenite catalysts for selective catalytic reduction of NO_x .
 R.E. Ramírez-Garza, F.F. Castellón-Barraza, I. Rodríguez-Iznaga, A. Simakov.
- P-24: Synthesis and characterization of mordenite (MOR) dispersed into silica
 Z. Bedolla, J.N. Díaz, G. Alonso, V. Petranovskii.
- P-25: Mass to frequency change in frequency domain sensors coated with zeolites
 Fabian N. Murrieta-Rico, Vitalii Petranovskii, Oleg Yu. Sergiyenko.
- P-26: Specific features of the spin echo signal in ferromagnetic $\text{Fe}_{100-x}\text{V}_x$
 Elena Kurenkova.
- P-27: Unusual structures of aggregates of silica nanoparticles
 N. Bogdanchikova, O. Martynyuk, A. Pestryakov, R. Luna Vázquez G.F. Ruiz Medina, A. Huerta-Saquero, J.L. Calvario.
- P-28: Au seeds stability
 L. Avalos, J.M. Romo-Herrera, O.E. Contreras, E.I. Chaikina, E.R. Méndez.
- P-29: Effect of laser pulses overlapping on the yield of silver nanoparticles
 D.O. Oseguera-Galindo, M.A. Santana-Aranda, A. Martínez-Benítez, G. Gómez-Rosas, A. Pérez-Centeno
- P-30: Synthesis of Cu_2O nanoparticles by pulsed laser ablation of a Cu target submerged in water
 Juan J. Velarde, Roberto Machorro, Catalina López, Vitalii Petranovskii, Gabriel Alonso, Serguei Stepanov.
- P-31: Nonlinear optical properties and light guiding in spherical and elongated Ag nanoparticles.
 Bonifacio Can-Uc, Raúl Rangel-Rojo, Luis Rodríguez-Fernández, Alicia Oliver.
- P-32: Interaction of silver nanoparticles with *Candida albicans*
 Roberto Vazquez-Muñoz, Ernestina Castro-Longoria, Miguel Avalos Borja.
- P-33: Encapsulation of Interference RNA by the CCMV capsid proteins
 J.N. Zamudio-Ocadiz, R. Vazquez-Duhalt, R.D. Cadena Nava.
- P-34: Inhibitory effect of silver nanoparticles in bacteria of clinical interest
 Roberto Vazquez-Muñoz, Alejandro Huerta Saquero, Roxana Ortiz, Emiliano Ventura Macías, Nina Bogdanchikova.
- P-35: Enteral Administration of Bile Salt-Phosphatidylcholine Mixed Micelles Loaded with Clonazepam Improves the Anticonvulsant Response in Pentylentetrazole-Induced Seizures in Mice
 Chavez Ramirez Daniela Silem, Quintanar Guerrero David, González Trujano Eva, Leyva Gómez Gerardo.

- P-36: Tomsk Polytechnic University – National Autonomous University of Mexico: 14 years of collaboration in Nanoscience
A. Pestryakov, N. Bogdanchikova, A. Simakov, E Smolentseva, V. Petranovskii, C. Almonaci.
- P-37: Models of Porous Media Filling Using Sphere Packing Approach for Different Size Distributions
Larysa Burtseva, Alexey Pestryakov, Rainier Romero, Benjamín Valdez, Vitalii Petranovskii
- P-38: Second-Harmonic Generation from Gold Nanoparticles on Profiled Substrate
C.I. García-Gil, V.A. Verdugo-Gutiérrez, A.V. Khomenko, M.A. García-Zárate
- P-39: Time-resolved Z-scan technique for simultaneous measurements of nonlinear absorption, thermo-optic, and Kerr effect in nonlinear optical materials
Arturo S. Rojas, A. V. Khomenko, M.A. García-Zárate.

Author index

Designing, Manipulation and Processing of Nanostructures for Applications in CNYN

J.M. Romo-Herrera^a, M. Cardoza^{b,@}, Omar Perez^{c,@}, Z. Bedolla^{d,@}, G. Alonso-Núñez^e,
D. Domínguez^f, F. Muñoz-Muñoz^g, H. Tiznado^h, Víctor Garcíaⁱ and O.E. Contreras^j
CNYN-UNAM, Ensenada B.C., México.

[@] Posgrado en Física de Materiales CNYN-UNAM / CICESE.

^ajmromo@cyn.unam.mx, ^bmarlenohemi@hotmail.com, ^cantiderivada@hotmail.com, ^dsimha86@gmail.com,
^egalonso@cyn.unam.mx, ^fdavid@cyn.unam.mx, ^gfrankmm@cyn.unam.mx, ^hhtiznado@cyn.unam.mx, ⁱvvg@cyn.unam.mx,
^jedel@cyn.unam.mx

ABSTRACT

Conventional manufacturing methods are reaching their limits. Thus, innovative fabrication routes are being pursued. In this context, nanostructures design and manipulation to evaluate nano-devices properties is needed.

Here we present a summary of some of the recent results from our Group at CNYN. This includes the plugging-in of semiconductor devices into the macro-world, this by photolithography processes, followed by *in-situ* manipulation in the electron microscope of the device, to end up with the Focus Ion Beam assisted deposition of the micro-contacts. This allows to plug-in semiconductor nanowires to be applied as highly sensitive gas sensors among other applications.

Follow up, we present some our advances with Carbon Nanotubes (CNTs) doping and processing to make use of their electrical properties for application purposes. Thereafter, electrically insulation of CNTs by atomic layer deposition (ALD) and a route to obtain inorganic nanotubes in large quantities is described; these results include the use of CNYN electron microscopes to ensure the abrupt interface between the insulating coating and the conductor CNT wire needed for electrical wiring purposes.

Following, progress in our Group related to dye sensitized titania nanoparticles (NPs) is shown, as a crucial stage of energy harvesting with Gratzel Cells. To end up mentioning a current project in CNYN to establish a nanofabrication laboratory including a clean room.

ACKNOWLEDGEMENTS

We thank E. Aparicio, A. Tiznado, E. Murillo, I. Gradilla, F. Ruiz, J. Díaz and Eric Flores for technical assistance; and DGAPA-PAPIIT projects IN-109612, IN114209-3 and IN104714, and CONACyT 82984, 83275 and 174689 for financial support.

Methods of Thermal Analysis for the Investigation of the Hydration of Nanostructured Materials

Irina Zvereva

St. Petersburg State University, 198504 Russia, St. Petersburg, Universitetskiy pr.26.

The presentation focuses on the application of methods of thermal analysis and calorimetry in area of properties and processes of nanostructural materials and their thermal stability.

It will be considered the information on the behavior of wide range of layered oxides in aqueous medium or ambient air obtained by methods of thermal analysis and/or calorimetry.

Among objects of investigation there are nanostructural layered oxides promising for functional materials, especially in photocatalysis. They belong to layered perovskite-type structures built of fragments of different structural types by the intergrowth of alternating layers (Ruddlesden-Popper and Dion-Jacobson phases with various nano-size thickness of perovskite slabs).

Main attention will be devoted to new data on quantitative characteristics of water intercalation in layered structure and ion-exchange reactions in the water medium obtained by thermogravimetry (TGA), simultaneous thermal analysis (STA) coupling with mass-spectrometry (QMS) and differential scanning calorimetry (DSC). On the base of these sets of data the links to photocatalytic activity for $A_2Ln_2Ti_3O_{10}$ and $ALnTa_2O_7$ ($A = Li, Na, K, Rb, Cs$) will be discussed. Unexpected high photocatalytic activity of some layered oxides can be clear from point of a prominent role of the water intercalation into the interlayer space of the crystal structure.

Results of thermal analysis are supported by structure investigation (XRD phase analysis and structure calculations), IR-spectroscopy and the investigation of morphology (SEM).

Brief review will be done on modern technical opportunities and equipment of Resource center "Thermogravimetric and Calorimetric Research" of Saint Petersburg State University.

Geo-environmental and modelling resource center of the Saint-Petersburg State University (RC Geomodel)

E.F. Mikhailov, **I.V. Tokarev**
Saint-Petersburg State University, Resource Center “Geomodel”
tokarevigor@gmail.com

INTRODUCTION

Recent trend in Saint-Petersburg State University (SPbU) efforts are to form new generation of Russian scientists and community leaders. Establishing of new laboratories headed by leading scientists SPbU and well-known scientist from any leading university or research center from Russia or any countries is activity in that direction. Three years ago was launched process for the establishment of Research Centers by conditions of the open competition and 21 new research laboratories were set up according to the results of this competition. Research Center Geomodel (RC Geomodel) is one from these new structures of SPbU.

RESEARCH CENTER “GEOMODEL”

The definition for the climate system makes it clear that one has to have an understanding of all of that system’s components (atmosphere, ocean, land surface processes, cryosphere and biosphere) in order to understand it. In recent decades, more and more manifest anthropogenic interference with the natural processes in the geosphere, manifested by changes in Earth's climate, the increase in natural hazardous weather events, increase their impact on the economies of many countries.

Russia is no exception to that seen in many of the processes observed in recent years. Prediction of these phenomena is extremely difficult, due to both the complexity of the system itself Geosphere, insufficient knowledge of many processes occurring in them, the presence of numerous links between them and the lack of understanding of all factors determining the temporal variability of many processes. In a world of rapidly developing numerical models to predict the state of the geosphere, but these models require continuous availability of large quantities of data on state and processes occurring in the Geosphere.

Geo-environmental resource center of the Saint-Petersburg State University was founded with the aim to consolidate and expands the current analytical expertise in-situ and nano- to macro-scale analysis, and to initiate a new scientific and education projects. The long-term goal is a comprehensive numerical Earth system model, to be realized by modular integration of additional components focusing on land surface and biosphere processes. The need for progress in Earth system science is not just about climate change, but also about how the Earth as a whole works, and about the magnitude and rates of change that humans are causing.

MISSION STATEMENT

- To conduct ethical and innovative research in both experimental and theoretical aspects of Earth Science.
- To provide high-quality and timely publications of our research results.
- To encourage interested and qualified students to become involved in research projects.
- To act in accordance with contract and grant regulations

STRUCTURE OF RC GEOMODEL

Our principal focus is the experimental and theoretical research of the Earth’s geosphere. We conduct basic and applied research in atmospheric physics, ionospheric plasma, physics and chemistry of the earth. Scientists, engineers, and technicians, and support personnel, who develop and extend these capabilities, staff the center. Currently, the center’s staff consists of 29 persons.

Atmospheric research division provides a broad array of tools for studying Earth’s atmosphere, including ground-based instruments for local and remote sensing gas and aerosol composition of the atmosphere, and laboratory tools for studying physical and chemical properties of the aerosol particles.

Aerosol group examines the physical and chemical properties of the atmospheric aerosol particles. Our research includes laboratory studies and field measurements, data analysis and numerical modeling. The challenge will be bridging the different spatial and temporal scales: from the tenths of a nanometer to thousands of kilometers and from nanoseconds to years.

Spectroscopy group is focused on the determination of spectroscopy parameters of the interacting system relevant to atmospheric research. High-resolution laboratory molecular spectra are needed to retrieve the atmospheric trace gas concentrations, and to obtain accurate information about molecular interactions in condensed system.

Hydrological research division. A set of interrelated objectives forms the basis of hydrological researches. We try to improve scientific understanding of seasonal, interannual, decadal, and long-term changes of the groundwater and river discharge at local, regional, and continental scales. Using the monitoring of the stable isotope composition and tritium contents in atmospheric precipitations, river run-off and groundwater, and special field works we are trying to develop the prediction criteria for the natural hazardous weather events and safety of radionuclides disposal in geological formations with aim to decrease their negative impact on the economies and ecosystems of Russia and other countries. Isotope data are the basis for verification and calibration of the numerical hydraulic and mass-transport models.

MINERAL EXPLORATION GROUP

Geochemical group. A set of scientific equipment aims at to analyze mineralogical, petrographic, crystallographic and geochemical process in the lithosphere. It can be also used in other areas like Science of Material, Chemistry, Physics, Biology, Archeology, and Geomorphology.

X-ray fluorescence analysis group is focused on conducting of qualitative and quantitative analysis of materials in geological environment: lithosphere, hydrosphere and biosphere – with the aim of determination of chemical composition.

Paleomagnetic group studies the evolution of the Earth's magnetic field recorded in the remanent magnetization of volcanic, sedimentary, and metamorphic rocks, as well as mechanisms of remanent magnetization acquisition and magnetic properties of minerals. The results of paleomagnetic research are used for paleogeographic and paleoenvironmental reconstructions, study of the Earth's deep interior, and in exploration geophysics.

Partners of RC Geomodel

Russian Academy of Sciences:

- Institute of Earth atmosphere physics (Moscow),
- Institute of atmosphere optics (Tomsk),
- Institute of Earth's physics (Moscow),
- Institute of Pre-Cambrian geology and geochronology (Saint-Petersburg),
- Institute of crystallography (Moscow),
- Institute of environmental geo-sciences (Moscow – head office and Saint-Petersburg division),

Max-Planck Society (Germany):

- Institute of atmosphere chemistry (Mainz),
- Institute of biogeochemistry (Mainz),

Barcelona University (Spain),

Technische Universität Bergacademie Freiberg (Sachsen, Germany),

Le Centre de Recherches Pétrographiques et Géo-chimiques (Nancy, France),

University of Athens (Greece),

Geological institute of Chinese seismic bureau (Beijing, China),

National academy of sciences of Kyrgyz Republic (Bishkek),

University of Utah (Salt Lake City, US),

Geophysics institute National academy of sciences of Ukraine (Kiev), etc.

Electronic properties of some crystalline compounds

D.H. Galvan

Centro de Nanociencias y Nanotecnología, Universidad Nacional Autónoma de México, Apartado Postal 2681, CP 22800, Ensenada, B. C. México.'

Our work will be centered in the presentation of two investigations:

Electronic properties of $MNbS_2$ with $M = Ni, Co, Fe$ and Cu , located in the *surface* and in front of Nb : An experimental and theoretical study.

D.H. Galvan, L. Pérez Cabrera and S. Fuentes

ABSTRACT

In this study, we examine the effect of Ni, Co, Fe and Cu in NbS_2 catalyst prepared by sol-gel technique. The activity results, as shown in HDS of DBT reaction were comparable with the results provided by Alelli or Chianelli et al. for the same compounds. On the other hand, theoretical calculations under tight-binding methodology using YAeHMOP computer package were performed on all the structures under investigation. Energy Band analysis indicate that the system remain metallic no matter where the M atoms are located, either on the *surface* or in front the Nb. From Total and Projected DOS analysis, it was possible to obtain information regarding the contributions from each atom to the Total DOS, especially in the vicinity of the Fermi level. In addition, from Mulliken Population Analysis yielded information on how Nb d-orbitals are filled and if the $MNbS_2$ still remains in a trigonal-prismatic configuration.

$YbOs_4Sb_{12}$ filled skutterudite: Its Electronic Properties

D.H. Galvan

ABSTRACT

A theoretical calculation on $YbOs_4Sb_{12}$ filled skutterudite is reported. The calculated Energy bands yield indication of a semimetallic behavior, while the projected Density of States provide support for the existence of a hybridization formed by Yb f-, Os d-, and Sb p-states. From the analysis of the energy bands that crosses the E_f , it is possible to infer a high effective mass; this value is added to the existence of a strong hybridization yielded indication of the heavy Fermion behavior for this compound which agrees with the experimental information available. The absence of a minigap provides an indication that this compound is not likely to serve as good thermoelectric material, unless doped in a certain direction as to enhance the probability to open the necessary minigap between the valence and conduction bands. Crystal Orbital Population Analysis yielded indication for the absence of a ferromagnetic instability.

Size effect on the stability of the MgH_2 and AlH_3 hydrides

Marina G. Shelyapina

Department of Nuclear-Physics Research Methods, St. Petersburg State University,
198504, Ulyanovskaya 3, Peterhof, Russia
marina.shelyapina@spbu.ru

ABSTRACT

In the last decades, hydrogen storage in metal hydrides is the object of attention of researchers. To date, magnesium (reversible hydrogen sorption to 7.6 wt% in MgH_2) is one of the most promising materials for hydrogen storage. The main obstacle to the direct use of pure MgH_2 is its slow sorption kinetics, high oxidation in air and high thermodynamic stability. Aluminium is another attractive material from hydrogen storage perspective. Let us remember that it is the second highest production metal in the world and it exhibits extremely high corrosion resistance. Moreover, alane, AlH_3 potentially has a very high hydrogen sorption ability (10.1 wt%). However, it has no any practical use, as it is thermodynamically unstable.

It is known that the transition from macro- to the nanoscale structure elements is accompanied by fundamental changes in the physical properties of the compounds. The MgH_2 and AlH_3 hydrides provide two antipodal examples of the role of the size effect on the thermodynamic stability of the compounds: the stability of the magnesium hydride decreases with decreasing the particle size, whereas the stability of the alane increases. In both cases, such a behavior improve one of the most important characteristics of these hydrides, the temperature of hydrogen release, determined by the thermodynamic stability of the hydride.

Despite numerous experimental data of magnesium hydride, up to now basic physical aspects of these phenomena are not completely understood. As for AlH_3 , due to its instability any experimental study is a challenging task. Nevertheless, it is obvious that the metal-hydrogen bonding plays a major role in the stability of these hydrides. That is why a comprehensive insight in interatomic bonding is needed in finding further modifications of magnesium or aluminum based hydrides with better characteristics. Theoretical researches could provide such insight and predict further steps in improvement of these materials. To understand the intrinsic mechanism of size effects on metal-hydrogen bonding several theoretical studies within different approaches have been carried out recently. In this contribution, we provide a brief review of these studies.

Effect of various parameters on the growth of carbon nanotubes with different metal catalyst deposited Si substrate

D.K. Tiwari, J. Valenzuela, M. Herrera

Centro de Nanociencias y Nanotecnología, Universidad Nacional Autónoma de México

Ensenada, B.C. 22860, México.

dktpy@cryn.unam.mx

ABSTRACT

In the recent years, the Nanomaterials have generated much interest in scientific community. The production of nanomaterials and their characterization [1, 2] for technological development is revolutionary for wide applications like electronics, environmental and in medical applications [2]. Carbon based nanomaterials represents a radical alternative to the conventional filled polymers. Between all nanomaterials, carbon nanotubes (CNTs) are widely popular in nanoscience related groups because of their unique mechanical, electrical, thermal and chemical properties. These properties of CNTs give them an ability to be applied in various ranges of applications [3, 4]. Moreover, a lot of research has been done to grow single-walled (SWCNT) and multi-walled carbon nanotubes (MWCNT) [5, 6, 7].

Here we demonstrate the possibility of growing carbon nanotubes (single-walled and multi-walled) on metal evaporated surfaces of silicon oxide. To attain our goal a selective deposition of metals like Ni, Co, Au and Au-ZnO was done on the Si/SiO₂ substrate using PVD (physical vapor deposition) technique; after the metallic deposition CNT growth was performed inside a quartz tube oven at 700-900°C temperature using C₂H₂ (acetylene gas) as a precursor and Ar as the carrier gas. The flow of carrier gas was constant while the oven temperature and precursor flow was varied in the performed experiment. Initially Ar gas was passed for 15 min to make the quartz tube an inert medium, then the temperature was increased to the desired value. After attaining the desired temperature, acetylene was passed in the Q-tube oven with the flow rate of 4-8 ml/min for 5-30 min depending on the planned experiments.

Scanning Electron Microscope (SEM: JEOL JIB-4500) was used to characterize the growth of carbon nanotubes and surface morphology. The roughness of the growth materials was examined using Atomic Force Microscope (Park System Model XE-70). Finally, TEM observations were employed to measure the structure of catalysts and carbon nanotubes at 200 keV (TEM: JEOL JEM-2010).

The results show the growth of carbon nanotubes on Ni, Co, Au and Au-ZnO coated Si substrates. The growth of carbon nanotubes depend on the 3 factors; the time of growth, growth temperature and the flow rate of precursor gas. With increase in growth time, a dense black layer of amorphous carbon was formed due to an excess formation of carbon leading to less interaction with the metal ions on Si surface (~20 min or more). When growth time was less or equal to 5 min (C₂H₂ flow 4-5 ml/min), there was no formation of CNTs.

ACKNOWLEDGMENTS

We are grateful to UNAM for postdoctoral funding and facilities of CNyN are highly appreciated. Authors are thankful to Dr. José Juan Gervacio Arciniega for helping AFM measurement. We also thanks to M.C. Eloisa Aparicio Ceja and Mr. Francisco Ruiz Medina for their technical assistance.

REFERENCES

- [1] D. K. Tiwari et al., *Int. J. Thermophys*, **34**, 1838–1843, (2013).
- [2] D. K. Tiwari et al., *Nano Studies*, **8**, 53-62, (2013)
- [3] D. K. Tiwari et al., *Applied Nanoscience*, 10.1007/s13204-013-0236-7.
- [4] D. K. Tiwari et al., *Nano Studies*, **7**, 87-96, (2013)
- [5] Yung Joon Jung et. al., *Nano Letters*, **Vol. 3**, No. 4, 561-564, (2003)
- [6] Irene Taurino et al., *Nanoscale*, **5**, 12448-12455, (2013).
- [7] Kanchan M Samant et al., *Pramana – Journal of Physics*, **Vol. 68**, No. 1, (2007).

Studying nanoparticles with light

Catalina Lopez, **Roberto Machorro**

Centro de Nanociencias y Nanotecnología, Universidad Nacional Autónoma de México, Ensenada, B.C.
roberto@cny.nam.unam.mx

INTRODUCTION

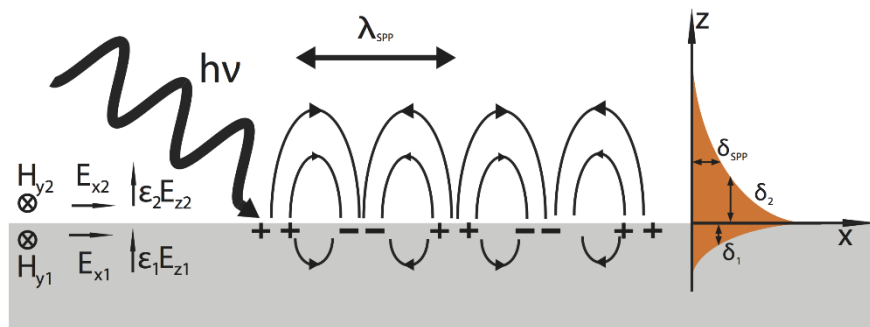
Characterization of metal nanoparticles is an important step towards its understanding, and derive useful applications. Among several options to characterize nanoparticles optical methods are very important and they are simpler to use than any others, with less or null sample preparation. Optical methods are, of course, complementary to electronic spectroscopies or imaging, they are not exclusive.

It may sound intriguing the fact that using a probe around 550 nm is possible to measure details of the order of few nanometers. Usually the probe should be smaller than sample detail. The quid is that we observe interactions, indirect responses.

In this report we discuss how to measure metal nanoparticles properties, based on optical spectroscopies. We make a tour on several techniques being used to localize and study particle size and shape. Some of our results, or other reported in literature, do not match perfectly with models, because simplified assumptions are used in modeling.

EXPERIMENTS

ATR.- Attenuated total reflection allows the coupling of electromagnetic waves with “free” electrons in a metal. Internally reflected light has its propagation vector along the surface of the metal, exciting surface plasmons. This effect is maximum at the surface because of the evanescent wave due to internal reflection and exponential absorption of the light in the metal. The reflected light is reduced in amount proportional to the light-metal coupling, this includes wavelength, angle of incidence, optical properties of the prism support, and very important, dielectric function and structure of the metal [1].



ELIPSOMETRY.- The transversal vector nature of the light provides a very sensitive form to measure optical properties of nanometric samples, usually thin films. Powders are not suitable for ellipsometry. Variation of a monolayer are measurable with ellipsometry. This technique is so sensitive that allows to perform microstructure studies. Of course, theoretical modeling of the results are essential to this purpose. Effective medium theory [2] is a key element to understand ellipsometric curves. With this powerful tool, we are able to study rough surfaces, composite materials, interfaces, etc. [3].

LSPR.- A particular situation arises when the electromagnetic field interacts with a metal nanoparticle. The electric field interacts with “free” electrons, moving them along the particle. A plasmon is excited, but restricted to the small volume of the particle, where plasmon is localized. The light energy is transfer to the particle via plasmon excitation. Measuring transmittance T with a UV-Vis spectrometer, reduction of T , or an increment in absorption gives a clear indication of a resonance of the light and the plasmon. Modeling the spectral response provides a way to study nanoparticles in metals [4].

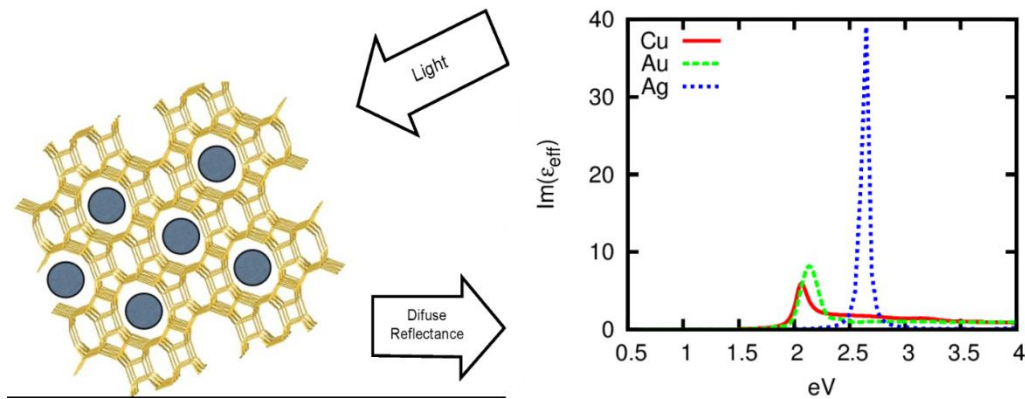
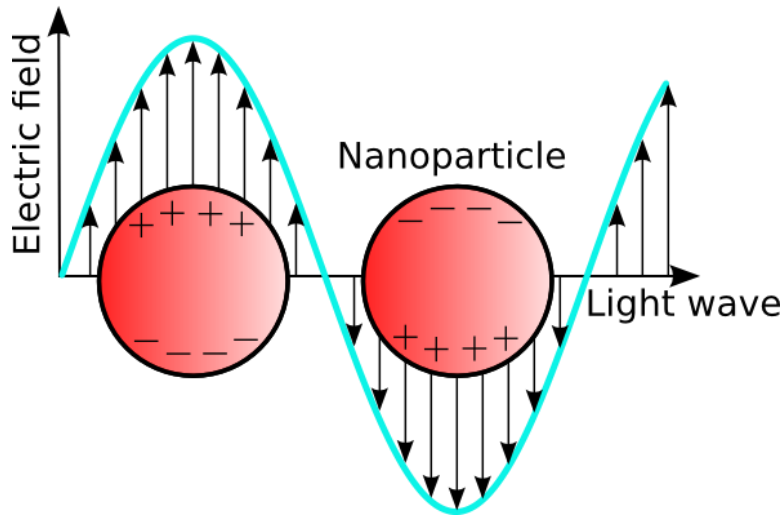


Figure taken from reference [4]

CONCLUSIONS

We review some optical spectroscopies, which are widely used to study nanoparticles. In the presentation, we will talk about the advantages and limitations of each one, with examples.

ACKNOWLEDGMENT

The authors wish to acknowledge partial support from CONACYT-Mexico Project No. 225166 and DGAPA-UNAM Project No. IN105914.

REFERENCES

- [1] L.E. Regalado, R. Machorro and J. Siqueiros, *Applied Optics*, 30, 3176 (1991)
- [2] D.E. Aspnes, *Am. J. Phys.* 50, 704 (1982)
- [3] D. Mateos, M. Curiel, et al, *Physica E* 51 111–114 (2013)
- [4] Catalina López-Bastidas, Elena Smolentseva, Vitalii Petranovskii and Roberto Machorro, *Plasmonics* (2013).

Nuclear Quadrupole Resonance: a review of applications to study bulk and nanoscaled solids

Elena Kurenkova

Center for Magnetic Resonance, Saint- Petersburg State University, Russia
e.kurenkova@spbu.ru

ABSTRACT

This work is a review of applications of methods of nuclear quadrupole resonance (NQR) on the basis of numerous experimental data in zero magnetic field. The lecture provides a brief overview of the basic theory of NQR necessary to treat experimental results. The NQR effect is possible to observe for nuclei with spin $I > \frac{1}{2}$ (as they have the quadrupole moment eQ) that occupy non-cubic symmetry (as that means that the electric field gradient (EFG) at the nucleus site is not equal to zero). The frequencies of the NQR transitions, are determined by the quadrupole coupling constant, e^2Qq_{zz}/h (here q_{zz} is the principal component of the EFG-tensor) and the asymmetry parameter $\eta = |(q_{xx}-q_{yy})/q_{zz}|$, which in their turn, strongly depend on the nearest neighboring. In such a manner, NRQ is a tool extremely sensitive to the charge distribution near the nucleus under study. It makes NQR very efficient and an exact method for studying the local structure of solids, chemical bonding, phase transitions of different nature and so on. In this report we will discuss a number of interesting problems related to NQR applications that include industrial catalysis research, spatial structure of minerals, drug control etc.

An important task of the NQR method is to systemize and accumulate experimental data to compare the chemical characteristics of the series of compounds in a class for understanding the changes in the properties of the sample under the influence of various factors. For example, NQR is very effective for express analysis of phase transitions [1, 2].

Sometimes, knowing the quadrupole coupling constant value is not sufficient, and the only reliable and informative source is the EFG asymmetry parameter η , which is extremely sensitive even for minor redistributions of the charge density near the nucleus under study, and can be used for identification of isomers [3, 4].

The temperature dependence of the NQR frequencies is another important issue about a character of the chemical bond, intra-and intermolecular interactions, including ionic interaction [5].

REFERENCES

- [1] Kravchenko E.A et al: Journal of Molecular Structure (1980). V.58. P.253-262
- [2] Kravchenko E.A et al: Temperature Dependence of NQR Spectra and Phase Transitions in' Complex Alkali Metal Hexaiodozirconates and Hafnates(IV), Zeitschrift fur Naturforschung: Physik. Physikalische Chemie. Kosmophysik. 1986. B. 41A. S.294-298.
- [3] J.N. Latoniska et al: Chemical Phys. Letters 462 (2008) 295-299
- [4] Feshin V.P. Main Group Metal Chemistry (1993). V.16. P. 377-413
- [5] Kravchenko E.A. et al: ^{209}Bi NQR Studies of Low-Temperature Spin-Lattice Relaxation in $\text{Bi}_4\text{Ge}_3\text{O}_{12}$ Single Crystal, Solid State Communications. 2008. V. 148. P. 319-321

Study of shear properties of nanoparticles suspensions

Bair B. Damdinov^{1,2}, Tuyana S. Dembelova¹, B.B. Badmaev¹

¹Institute of Physical Materials Science of the Siberian Branch of the Russian Academy of Sciences, Ulan-Ude, Russia; ²Physics of complex systems Lab, Buryat State University, Ulan-Ude, Russia
bdamdinov@bsu.ru



INTRODUCTION

Low-frequency (10^5) shear elasticity of liquids for the first time has been found by acoustic resonance method. Elasticity can be explained by the fact that in liquids there is unknown earlier low-frequency viscoelastic relaxation process. Therefore, detail investigation of the shear elasticity has fundamental importance for the correct understanding of the nature of liquid state as a whole.

METHOD

The resonance method [1-3] has high sensitivity to inhomogeneities of structure of investigated objects. Now viscoelastic properties of colloidal suspensions of nanoparticles are studied by using this method. We apply an acoustic resonance method for measuring of the shear visco-elastic properties (real and imaginary shear moduli) of various liquids and suspensions.

RESULTS

It was shown that tested materials have measurable shear moduli at experimental frequency 74 kHz. It was shown that its elastic and viscous properties depend on amplitude of resonator oscillation.

It is based on the our previous investigations (PhD dissertation at Acoustical Institute, Moscow, 2000; Doctor of Sciences dissertation at Buryat State University, Ulan-Ude, 2012) and collective research [4-6] at Buryat State University (2006-2013) and Institute of Physical Materials Science (1995-2013).

ACKNOWLEDGMENTS

This work was supported by several Grants of Russian Foundation for Basic Research (1999, 2004, 2005-2011).

REFERENCES

- [1] B.B. Badmaev and B.B. Damdinov, *Acoust. Phys.* **47**, 487 (2001).
- [2] B.B. Badmaev., T.S. Dembelova and B.B. Damdinov, *Adv. in Colloid and Interface Sci.* **104**, 299 (2003).
- [3] D.S. Sanditov, B.B. Badmaev and B.B. Damdinov, *Acoust. Phys.* **50**, 121 (2004).
- [4] B.B. Badmaev, O.R. Budaev, T.S. Dembelova and B.B. Damdinov, *Ultrasonics.* **44**, e1491 (2006).
- [5] B.B. Badmaev, S.A. Bal'zhinov, B.B. Damdinov and T.S. Dembelova, *Acoust. Phys.* **56**, 640 (2010).
- [6] B. Badmaev, T. Dembelova, B. Damdinov, D. Makarova and O. Budaev, *Colloids and Surfaces A: Phys. Chem. Eng. Aspests.* **383**, 90 (2011).

Nanofabrication of ALD oxide nanotubes

Hugo Tiznado¹, Franklin Muñoz¹, David Domínguez¹, José Romo-Herrera¹, Oscar Contreras¹, Gabriel Alonso¹ and Gerardo Soto¹

¹Universidad Nacional Autónoma de México – Centro de Nanociencias y Nanotecnología
tiznado@cnyun.unam.mx

ABSTRACT

Inorganic nanotubes have attracted substantial attention due to their potential application in a variety of technologies related to electronics, photonics, nanofluidics, medicine, sensing, catalysis, and controlled release.[1] A variety of processes has been developed to fabricate such tubes from a wide range of materials. Among those processes, the template-directed approach represents a straightforward route for the fabrication of nanostructures with hollow interiors. Carbon nanotubes (CNT) can be used as a sacrificial template for the fabrication of nanotubes of diverse materials with precise thickness and chemical composition[2], [3]. On the other hand, if the CNT is not removed the material can be used for other applications where the success depends on the deposition of insulating, passivating or functional films on the CNT.

In this work, we employ atomic layer deposition (ALD) on CNT as a direct mean to fabricate nanotubes with well-defined nanoscale walls composed of Al_2O_3 (Figure 1) and/or TiO_2 with/without a CNT core. TGA tests revealed an enhanced thermal oxidation resistance. The resulting structures observed through TEM confirmed that our strategy provides an attractive, high-fidelity and relatively low-cost route for nanotubes.

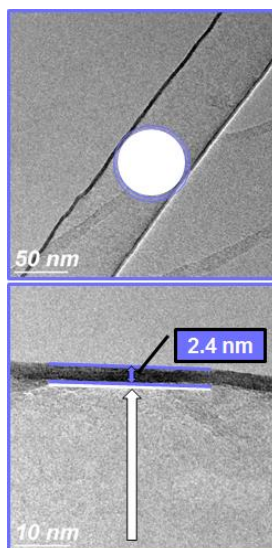


Figure 1. Al_2O_3 ALD nanotube.

ACKNOWLEDGMENTS

We thank the technical support of A. Tiznado and E. Medina. Financial support of projects PAPIIT IN114209 and CONACyT 83275.

References

[1] Y. Xia, P. Yang, Y. Sun, Y. Wu, B. Mayers, B. Gates, Y. Yin, F. Kim, and H. Yan, "One-Dimensional Nanostructures: Synthesis, Characterization, and Applications," *Advanced Materials*, vol. 15, no. 5, pp. 353–389, Mar. 2003.

- [2] Y.-S. Min, E. J. Bae, K. S. Jeong, Y. J. Cho, J.-H. Lee, W. B. Choi, and G.-S. Park, "Ruthenium Oxide Nanotube Arrays Fabricated by Atomic Layer Deposition Using a Carbon Nanotube Template," *Advanced Materials*, vol. 15, no. 12, pp. 1019–1022, Jun. 2003.
- [3] J. S. Lee, B. Min, K. Cho, S. Kim, J. Park, Y. T. Lee, N. S. Kim, M. S. Lee, S. O. Park, and J. T. Moon, "Al₂O₃ nanotubes and nanorods fabricated by coating and filling of carbon nanotubes with atomic-layer deposition," *Journal of Crystal Growth*, vol. 254, no. 3–4, pp. 443–448, Jul. 2003.

Nanostructured catalysts for hydrogen production in artificial photosynthesis

Sergio Fuentes Moyado

Universidad Nacional Autónoma de México, Centro de Nanociencias y Nanotecnología, Km. 107 Carretera Tijuana a Ensenada, C.P. 22860, Ensenada, Baja California, México
fuentes@cyn.unam.mx

ABSTRACT

Global problems as global warming, pollution of large urban areas, deforestation and water pollution, among others, are associated with the use of petroleum as the main source of energy and transport fuels. Therefore, the search of new energy sources and transportation fuels is very important to remediate these concerns.

The last decades the use of hydrogen as energy vector has been largely studied. It has been proposed for use in electronic devices, such as computers or cell phones, as well as transportation fuel for cars in either internal combustion engines or fuel cell driven electric motors.

The electrolytic dissociation of water is very well known, $2\text{H}_2\text{O} \rightarrow 2\text{H}_2 + \text{O}_2$ ($\Delta G^\circ = 237.17$ kJ/mol), and takes place in two redox steps: the reduction for production of hydrogen in the cathode; while the oxidation for production of oxygen in the anode. However, this is an expensive process and is not easy to scale for large production.

The natural process of photosynthesis carried out by the plants through a series of balanced thermodynamic steps has been successful since millions of years to dissociate water at room temperature under sunlight radiation by means of enzymes, producing oxygen and carbohydrates. Research groups in several countries are aiming to emulate nature by working in artificial photosynthesis based on photocatalysts.

In these heterogeneous processes different compounds are combined to carry out the different steps involved in photosynthesis, i.e., a photocatalyst that absorbs sunlight, a charge carrier material, a catalyst that dissociates water in O_2 and four protons, a protons transport material that moves these to the electrode, and the electrode that neutralizes the protons forming molecular hydrogen. The synthesis of nanostructured materials at the nanoscale allows a better control of the photosynthesis steps and important advances have been obtained to produce hydrogen at competitive prices.

Numerical study of a model plasmonic solar cell

Margoth Córdova¹ and Eugenio R. Méndez²
¹CNyN-UNAM, ²Optics Department, CICESE.
 rmargoth_cc@yahoo.com.mx

INTRODUCTION

Several techniques have been proposed to improve the efficiency of conventional silicon solar cells. Different roughening methods, for instance, have been proposed to decrease the first surface reflectance and help trap the solar radiation within the cell. The newer generations of solar cells attempt to save production cost in various ways. The so-called thin film solar cells, for instance, constitute one of these approaches. Due to the reduced thickness of these cells, roughening is not an option to reduce the first surface reflection and, in the near infrared, a good fraction of the light is transmitted (i.e. it is not absorbed).

The use of metallic nanoparticles, within the cell or on its surface, has been proposed as a means to improve the situation. These are the so-called plasmonic solar cells. The basic scheme is illustrated in Fig. 1. The idea is that the presence of the nanoparticles can, on the one hand, increase the local field intensity (through the excitation of plasmonic resonances [1]), and also help the coupling of the incident light into the active layer of the cell.

Initial reports of experiments with such arrangements indicate that the efficiency can be improved by the presence of metallic nanoparticles [2]. It is however important to analyze the characteristics that, in combination, will give greater efficiency to the cell. It is important to evaluate the effects that the material, the location of the particles, their shape distribution and density have on the efficiency of the cell. Moreover, it is necessary to take into account the optical properties of silicon in different regions of the solar spectrum.

In this work, we present calculations of the near field intensity in a model plasmonic solar cell. Our simplified model consists of a plasmonic particle placed on a silicon layer. To illustrate the results, we present, in Fig. 2, calculations corresponding to a disk-like particle with five-point-star shape. The system is illuminated with light at the wavelength of resonance of the isolated particle, which occurs at 690 nm. These results indicate that the presence of the particle intensifies the local field in some regions of the cell, improving thus the absorption properties.

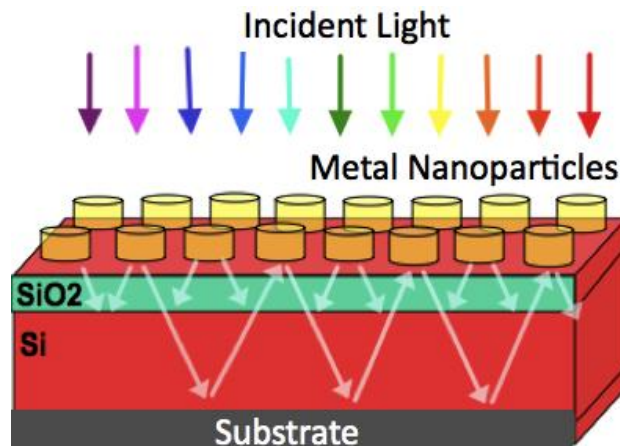


Fig. 1. Model of a plasmonic solar cell.

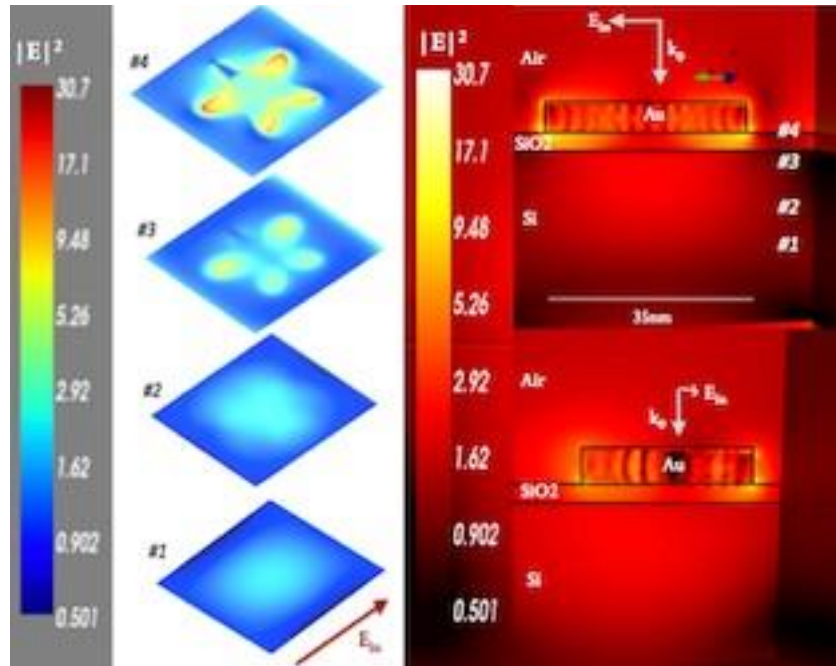


Fig. 2. Near field intensity maps calculations for our plasmonic solar cells model with a five-point-star Au particle.

To provide a more qualitative measure of the improvement, we have evaluated numerically the integral of the intensity within the silicon layer (I_i), and compared that quantity with the case in which the cell has no particle (I_0). The ratio of these two quantities $Q=I_i/I_0$, which can be called an “enhancement factor,” provides a measure of the improvement achieved by the presence of the particle. The results for particles with three different shapes and materials are shown in Table I. We observe that, in agreement with the intensification observed in the near field images, the total intensity within the cell has increased, leading to an increase in the fraction of the incident power that is absorbed by the cell. It is worth mentioning that the presence of the particle can also improve the absorption properties of the cell in regions of the spectrum that do not correspond to wavelengths of resonance of the particle.

Table I. Enhancement factor for different particles shapes.

Particle	wavelength(nm)	Q
cylinder Ag	430	1.41
cylinder Au	557	2.07
cylinder star cross section Au	690	3.04

REFERENCES

- [1] S. A. Maier *Plasmonics: Fundamentals and applications* (Springer, New York, 2007), p. 223.
- [2] K. R. Catchpole and A. Polman, *Appl. Phys. Lett.* **93**, 191113 (2008).

Immobilized biocatalyst in mesoporous materials and its bionanotechnological applications

Karla Juárez-Moreno, Gabriel Alonso Núñez, Sergio Fuentes Moyado and Rafael Vazquez-Duhalt
 Centro de Nanociencias y Nanotecnología, UNAM, Ensenada, BC, Mexico
 kjuarez@cny.unam.mx

INTRODUCTION

Immobilization of biological molecules in mesoporous materials has been possible through the developing of several strategies that took advantages of the physicochemical properties of either materials or biomolecules. Among all the known mechanisms, physical immobilization by adsorption represents the easiest and cheapest process of molecule anchoring. Bionanotechnology has taking advantage of this methodology and applied it in several processes such as drug delivery, cell targeting, biocatalysis and biorefinery.

In the biorefinery processes biomolecules such as biocatalysts (also known as enzymes) are used to oxidize reagents derived from crude oil, the most common enzymes for this purpose are peroxidases, like the enzyme chloroperoxidase (CPO) that was isolated from the black mold *Caldariomyces fumago*, this protein is a heme-glycoprotein of 42kDa containing ferriprotoporphyrin IX as prosthetic group. CPO catalyzes several reactions and acts as peroxidase, halogenase and in cytochrome P450-type reactions of dehydrogenation [1].

Previous results from our group indicated that the immobilization of CPO in mesoporous materials provide the enzyme with thermal and solvent stability [2]. Taken this in consideration, herein we present the usage of SBA-15 mesoporous materials and different metal-impregnated preparations with titanium, cobalt and molybdenum (SBA-15/Ti, SBA-15/CoMo and SBA-15/CoMoTi) as supports for physical immobilization of the chloroperoxidase enzyme. We have calculated the enzyme maximal load capacity for each material and their specific activity on monochlorodimedone (MCD) by UV spectrophotometry and on dibenzothiophene (DBT) by RP-HPLC. Our results indicated that CPO immobilization into SBA-15 preparations increase enzyme stability to catalytic concentrations of hydrogen peroxide. The biocatalytic transformation of organosulfur compounds such as dibenzothiophene, 4,6-dimethyldibenzothiophene; benzyl sulfide; 1,2-benzodiphenylene sulfide; thiophene and thianthrene were also tested by RP-HPLC, showing that immobilization of CPO into SBA-15 and metal-impregnated SBA-15 increases their capacity to transform all the organosulfur compounds, among metal-impregnated preparations, SBA-15/Ti exhibited better specific activity on organosulfur compounds than other preparations.

We conclude that CPO immobilization into SBA-15 mesoporous materials not only may provide to CPO with a favorable environment for catalysis but also provides the enzyme with a higher stability than free enzyme. Oxidation of organosulfur compounds is favored by CPO immobilized in SBA-15 impregnated with Ti (SBA-15/Ti) or CoMo (SBA-15/CoMo), suggesting that this materials may be used for further biodesulfurization processes.

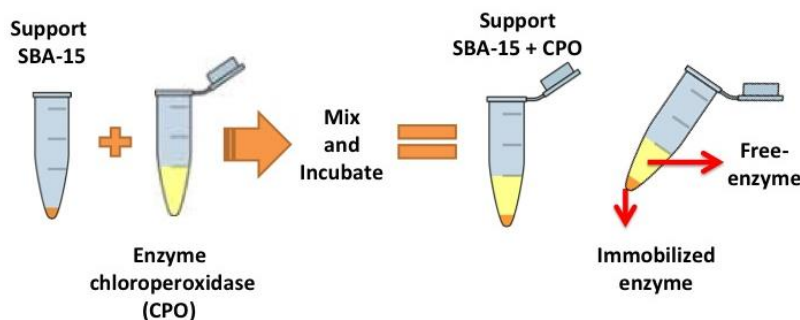


Fig. 1. Schematic representation of enzyme immobilization by physical adsorption in SBA-15 mesoporous material.

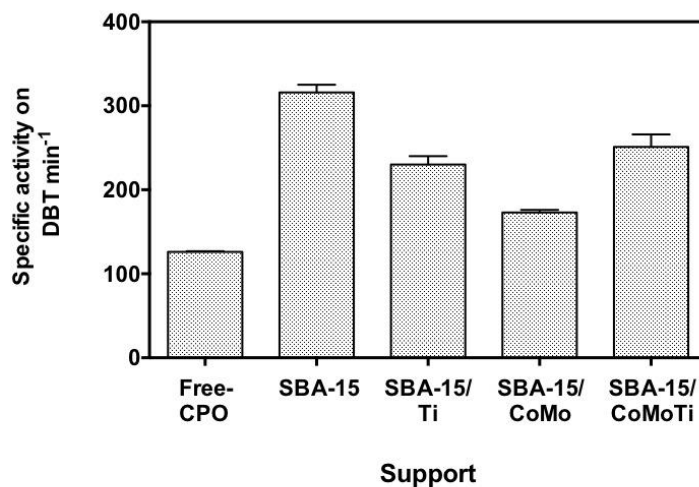


Fig. 2. Specific activity of Free-CPO and CPO immobilized in different metal-impregnated SBA-15 materials. Enzyme activity was calculated on dibenzothiophene (DBT) and measured by RP-HPLC.

ACKNOWLEDGMENT

K.J.M. thanks DGAPA-UNAM for a postdoctoral grant.

REFERENCES

- [1] Vázquez-Duhalt, R. and Quintero-Ramirez, R. 2004. Studies in Surface and Catalysis 151. Petroleum Biotechnology: Developments and perspectives. Elsevier, Amsterdam. The Netherlands. p. 545.
- [2] Aguila, S.V.-D., R.; Covarrubias, C.; Pecchi, G. and Alderete, J.B. Enhancing oxidation activity and stability of iso-1-cytochrome c and chloroperoxidase by immobilization in nanostructured supports. Journal of Molecular Catalysis B: Enzymatic. 2011. 70: p. 81-87.

UV-Vis-mass *in situ* analysis of gold nanoparticles formation over γ -alumina

Miguel Estrada¹, Eunice Vargas², Elena Smolentseva³, Sergio Fuentes³, Andrey Simakov³

¹Posgrado de Física de Materiales de CICESE-UNAM, Ensenada, B.C., 22860, México; ²Posgrado en Ciencias e Ingeniería, Área Nanotecnología, Universidad Autónoma de Baja California, Ensenada, B.C., 22860, México;

³Universidad Nacional Autónoma de México, Centro de Nanociencias y Nanotecnología, km.107 carretera Tijuana - Ensenada, Ensenada, B.C., 22860, México
mestrada@cnyun.unam.mx

INTRODUCTION

The gold-based catalysts are interest for several reactions such as CO oxidation, hydrogen peroxide production, water gas shift reaction, NO reduction and different organic compounds transformations [1]. After several decades of intensive investigation of gold catalysis, it has now been established that the catalytic properties of gold catalysts are related to the size of Au nanoparticles (NPs) and their interaction with the support [2]. The role of supports is to get required gold NPs dispersion and to avoid coalescence and agglomeration of particles. On other hand, support can be involved into the mechanism of catalytic reactions via the presence of hydroxyl groups, high density of structural defects on the support surface and adsorption of reactants and products.

The properties of supported Au NPs strongly depend on the method of their preparation. For example, supported Au NPs can be formed by decomposition/reduction of some gold compound previously deposited on the support. The technique most frequently used for gold deposition on oxides is deposition-precipitation (DP) method using NaOH or urea as precipitating agent. Indeed, this technique results in the formation of fine gold nanoparticles with narrow distribution and high efficiency of gold deposition [3].

The final step in the formation of supported gold metal NPs consists in the decomposition/reduction of supported gold compound. The transformation of gold compound to gold metal NPs can be performed under thermal treatment of freshly prepared sample with any gas. However, reducing gases such as hydrogen or carbon monoxide lead to smaller gold nanoparticles than those formed under calcination in air. However, the mechanisms of formation of Au NPs is still uncertain.

The aim of this work was to study the dynamics of Au NPs formation over alumina under thermal treatment in hydrogen or in oxygen, using UV-Vis-mass-*in situ* with analysis of the gas phase compounds. Selection of alumina as the support for gold catalyst was determined by the absence of any light adsorption in the 200-900 nm range, which helps to detect clear gold species transformation.

EXPERIMENTAL

Catalysts of 3 wt. % Au over pure aluminum oxide Al₂O₃, (Alfa Aesar) were synthesized by the deposition-precipitation technique using HAuCl₄ (Alfa Aesar) as gold precursor and urea as precipitating agent, similar to the procedure described elsewhere [4]. In order to remove the residual chloride, the samples were washed with a 25 M solution of NH₄OH (pH ca. 10), in accordance with [5]. Then, samples were washed with water, filtered, and dried at room temperature for 24h.

In situ UV-Vis-mass analysis of electronic transformations of the gold precursor during temperature-programmed treatments was performed in a homemade flow reactor with simultaneous analysis of gas phase components and analysis of UV-Vis spectra of the catalyst sample. The UV-Vis spectra were collected using an Avaspec-2048 UV-Vis spectrometer (AVANTES) equipped with an ALight-DHS light source and high temperature optic fiber reflection probe located close (4 mm) to the external wall of the quartz reactor. The spectra were collected each 15 seconds and the time of spectrum recording was 5 ms. Fifty mg of sample powders were heated from 25 to 350 °C with a temperature ramp rate of 20 °C per min. The total flow was 50 mL per min including 5 vol. % of hydrogen, 5 vol. % of argon and 90 vol. % of helium as balance. Spectra presented in the Results section were obtained by subtraction the first spectrum recorded at room temperature. The reactor packed with MgO was used as a reference for UV-Vis spectra measurements.

RESULTS

The *in-situ* UV -Vis analysis showed that there are 3 different steps of Au NPs formation as shown the Figure 1. The first stage begins at a temperature of 75 °C by the appearance in the UV -Vis spectra a signal of gold plasmon located at 520 nm characteristic for Au NPs. Formation of Au NPs at this temperature was accompanied with a desorption of water and CO₂ without any hydrogen consumption (see mass corresponding spectrometry profiles in Fig.1 (right)). It was proposed that at this step the metallic Au NPs were formed by thermal decomposition of gold precursor. The second step starts with further temperature increase above 225 °C. It is characterized with a high rate of Au NPs formation, intensive desorption of the products of gold precursor decomposition and consumption of hydrogen. The reduction of the external surface of gold hydroxide particles by hydrogen resulted in the formation of external metallic layer and desorption of ammonia because lower affinity of ammonia to the metal gold comparing to that for gold hydroxide. The third and final step begins at 285 °C when free Au NPs formed during first two steps can migrate on the catalyst surface and form agglomerates. After 300 °C, no significant changes in the UV -Vis spectra or in the profiles obtained by mass spectrometry were observed.

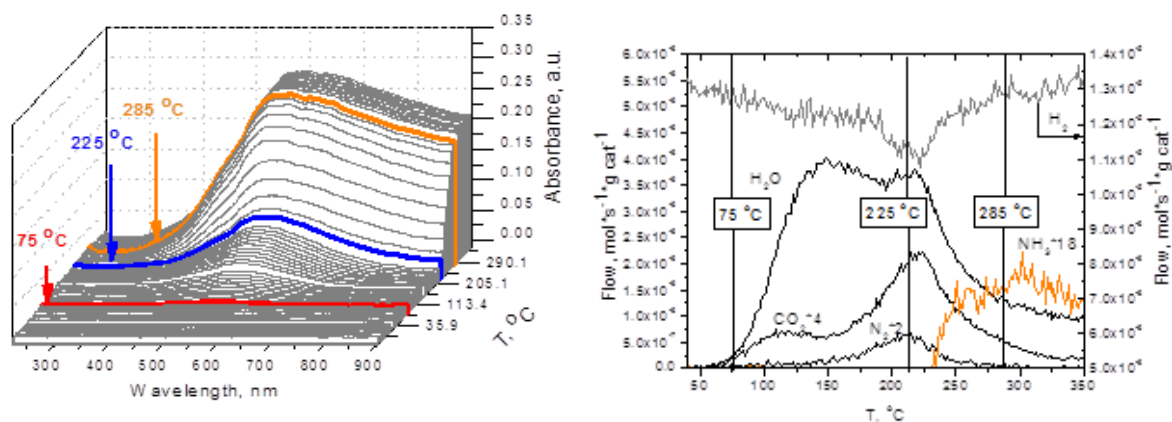


Fig. 1. In situ UV-Vis-mass analysis of Au/Al₂O₃ sample at TPR: UV-Vis spectra (left) and profiles of gas phase compounds (right) versus sample temperature.

CONCLUSIONS

In situ UV-Vis-mass analysis is a powerful technique allowing to monitor step by step the dynamics of Au NPs formation providing detailed information about the nature of each step.

REFERENCES

- [1] G.J. Hutchings, Appl. Catal. A: Gen. 291, 2–5 (2005).
- [2] M. Haruta, Catal. Today 36, 153-166 (1997)
- [3] R. Zanella, C. Louis, Catal Today 107–108, 768–777 (2005)
- [4] S. Ivanova, V. Pitchon and C. Petit, Appl. Catal. A 298, 57-64 (2006)
- [5] E. Smolentseva, B. T. Kusema, S. Beloshapkin Appl. Catal. A: Gen 392 69–79 (2011)

Chirality in Amino Acid Overlayers on Cu Surfaces

M. L. Clegg², L. Morales de la Garza¹, S. Karakatsani², D.A. King², S.M. Driver²,
¹Universidad Nacional Autónoma de México, Centro de Nanociencias y Nanotecnología,
Apdo. Postal 14, Ensenada, Baja California, México
²Department of Chemistry, University of Cambridge,
Lensfield Road, Cambridge CB2 1EW, UK
leonardo@cryn.unam.mx

INTRODUCTION

Chirality at surfaces has become a strong focus within the surface science community. A particular motivation is the prospect of using heterogeneous catalysis over chiral solid surfaces for asymmetric synthesis, a prospect which has clear relevance to the pharmaceutical industry. Small amino acids adsorbed on Cu surfaces have emerged as important model systems for studying the interaction of chiral molecules with metal surfaces. We review the current state of knowledge of these systems, and present the results of new experimental studies of alanine overlayers on Cu{311} and {531} surfaces. Our work on Cu{311} helps us to understand the interplay between different manifestations of chirality, especially “footprint chirality”, in the overlayers. Cu{531} is an intrinsically chiral surface orientation; our data reveal strongly enantiospecific alanine-induced restructuring of this surface. This points the way towards a promising route for obtaining strongly enantiospecific interactions with chiral adsorbates.

ACKNOWLEDGMENTS

The authors thank Dr. M. Blanco Rey, Prof. R. Raval and Drs. A. Mark, M. Forster and S. J. Jenkins for valuable discussions. The EPSRC is acknowledged for financial support, L. Morales de la Garza acknowledged financial support from DGAPA-UNAM.

REFERENCES

- [1] Topics in Catalysis (2011) 54:1429–1444.

A theoretical study of distinct sodalitic zeolite frameworks

Joel Antúnez-García^{1,2}, D. Homero Galván Martínez¹, Vitalii Petranovskii¹

¹Centro de Enseñanza Técnica y Superior, CINAP, Av. CETYS Universidad No. 4, Fracc. El Lago, Apdo. Postal 1196, C. P. 22210 Tijuana, B. C., México

²Centro de Nanociencias y Nanotecnología at UNAM, Km 107 Carretera Tijuana-Ensenada, Apdo Postal 14, C. P. 22800, Ensenada, B. C., México
joel.antunez@cetys.mx

INTRODUCTION

Zeolites are micro/nano porous aluminosilicate minerals that exhibits more than 180 different framework topologies well known [1]. Zeolites commonly are employed in heterogeneous catalysis [2], as molecular sieves [3] and in liquid and gas separation [4]. Although exists an arduous work at the experimental field, additional contributions becoming from theoretical calculations have provided useful information for the design of new technological applications.

On present work a systematic study of different sodalitic zeolites frameworks were developed, and the associated electronic properties were analyzed. As part of our study, aluminized frameworks with inclusions of water molecules, Na, and Cl atoms were mainly studied.

COMPUTATIONAL DETAILS

As starting point, the SOD unit cell at ground state was geometrically optimized by density functional theory (DFT) method, employing the Dmol³ [5–7] program package. For the exchange-correlation energy, was employed the Becke, Lee, Yang and Parr (BLYP) [8,9] gradient-corrected functional. For the expansion of wave functions of different atomic species under consideration, double numerical with d and p polarization (DNP) basis set (comparable to 6-31G, 6-31G(d) and 6-31G(d,p) Gaussian-type basis sets) [10] were used to take into account all core electrons interactions reasonably. After SOD unit cell was geometrically optimized, water molecules or Na and/or Cl atoms were disposed at the center of the main channel of it, and then this new framework was conducted to the minimal energy configuration under the parameterization early described.

RESULTS AND DISCUSSIONS

From configurational energy analysis shown in Fig. 1(a), is observed that pure siliceous SOD zeolite is energetically more stable than their aluminized counterpart. However, when water molecules or distinct atomic species (Cl or Na)

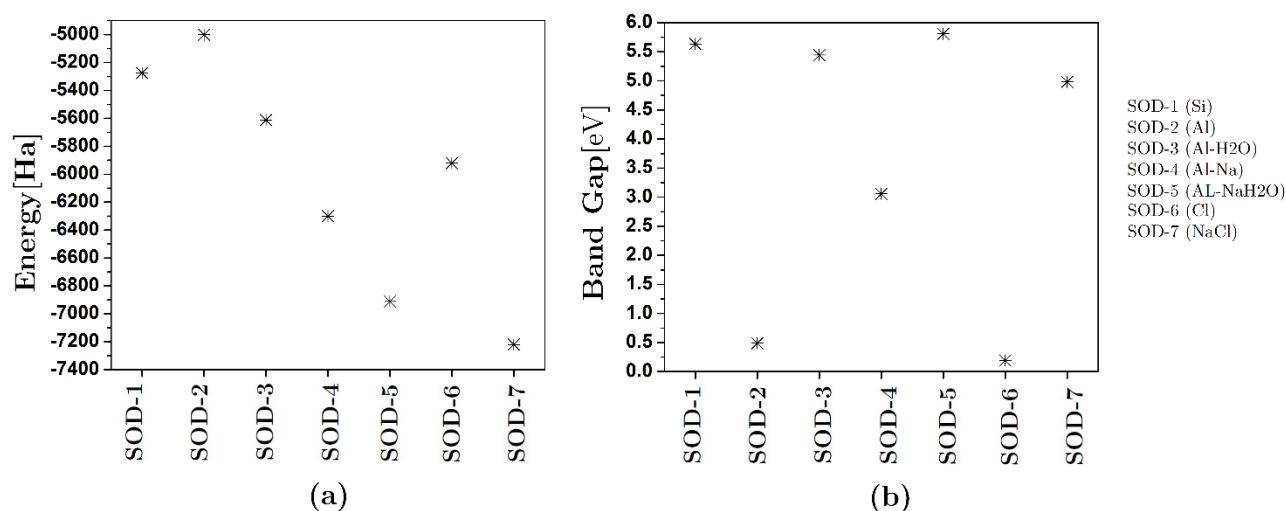


Figure 1. Graphs for (a) Configurational energy and (b) Band gap energy for distinct sodalitic zeolite frameworks.

are introduced inside of aluminized zeolite framework, the stability of the system is improved. On the other hand, on Fig. 1(b) is observed that the lowest energy band gap values corresponds for pure aluminized framework and when inside this framework just Cl atoms are present. Which agrees with the partial density of states (PDOS) analysis, that shows that on those cases the O[2p] and Cl[3p] orbital contributions contributes to diminish the band gap energy.

ACNOWLEDGMENT

This research was supported by CONACyT (México) under the grant No. 102907.

REFERENCES

- [1] <http://www.iza-structure.org/databases>.
- [2] F. Goovaerts, E. F. Vansant, J. Philippaerts, P. DeHulsters, and J. Gelan, J. Chem. Soc., Faraday Trans. 1 **85**, 3675 (1989).
- [3] D. W. Breck, *Zeolite Molecular Sieves*, Wiley, New York, (1974).
- [4] R. V. Jasra and S. G. T. Bhat, Sep. Sci. Technol. **23**, 945 (1988).
- [5] Software from Accelrys Inc.: <http://www.accelrys.com>.
- [6] B. Delley, J. Chem. Phys. **92** (1990) 508-517.
- [7] B. Delley, J. Chem. Phys. **113** (2000) 7756-7764.
- [8] A. D. Becke, PRA **38** (1988) 3098-3100.
- [9] C. Lee, W. Yang, and R. G. Parr, PRB **37** (1988) 785-789.
- [10] J. C. White and A. C. Hess, J. Phys. Chem. **97** (1993) 6398-6404.

Hybrid entanglement in a triple quantum dot shuttle system

J. Mora¹, F. Rojas² and E. Cota²

¹Centro de Investigación Científica y de Educación Superior de Ensenada,
Apartado Postal 2372, 22860 Ensenada, B.C., México

²Centro de Nanociencias y Nanotecnología – UNAM, Apartado Postal 356, 22860 Ensenada, B.C., México
frojas@cryn.unam.mx

ABSTRACT

Quantum entanglement is a central feature in quantum information processing [1]. Systems of two *qubits* have been extensively studied [2,3]. However, Hilbert spaces of higher dimensionalities are present in a variety of systems [4,5,6]. Hybrid entanglement refers to quantum correlations involving different degrees of freedom and can be measured experimentally [7]. The triple quantum dot shuttle (TQDS) device is a system of three series aligned quantum dots, where the central dot is oscillating [8,9,10]. It is a system whose dynamics are described by electronic and mechanical degrees of freedom. The eigenstates of this system are composite dot-oscillator states. Thus, we expect hybrid entanglement to be present. In this work, we characterize the degree of hybrid entanglement in the TQDS through the Schmidt number, and find an important correlation between this quantity and the measurable current through the TQDS. The time evolution of the degree of entanglement is also analyzed in the presence of an AC field giving rise to the phenomenon of coherent destruction of tunneling.

ACKNOWLEDGMENT

Support from DGAPA-UNAM project IN112012 is gratefully acknowledged.

REFERENCES

- [1] J. Audretsch, *Entangled systems: New directions in quantum physics* (Weinheim: Wiley-VCH, 2007)
- [2] A.C. Dada et al, *Nature Physics* **7**, 677 (2011)
- [3] A. Hichri et al., *Physica E* **24**, 234 (2004)
- [4] E. Rieffel and A. Polack, *ACM Computing Surveys* **32**, 300 (2000)
- [5] Luigi Amico et al., *Rev. Mod. Phys.* **80**, 517 (2008)
- [6] B. Rothlisberger et al., *Phys. Rev. Lett.* **100**, 100502 (2008)
- [7] E. Karimi et al., *Phys. Rev. A* **82**, 022115 (2010)
- [8] A.D. Armour and A. MacKinnon, *Phys. Rev. B* **66**, 035333 (2002)
- [9] J. Villavicencio et al., *New J. of Phys.* **13**, 023032 (2011)
- [10] J. Villavicencio et al., *Appl. Phys. Lett.* **92**, 19102 (2009)

NMR and EPR study of protonated and copper ion-exchanged mordenites.

Y.M. Zhukov¹, A.Y. Kul'taeva^{1,2}, A.N.Kovalyov¹, M.G. Shelyapina¹, V.P. Petranovskii³

¹St. Petersburg State University, 198504, Ulyanovskaya 3, Peterhof, Russia

²St. Petersburg State University, Center for Magnetic Resonance, 198504, Universitetskii 26, Peterhof, Russia

³Centro de Nanociencias y Nanotecnología, Universidad Nacional Autónoma de México, Apdo. Postal 2681, C.P. 22800, Ensenada, Baja California, México
yuri.m.zhukov@gmail.com

INTRODUCTION

Zeolites have a number of interesting, even unique properties, which may be utilized in various areas, especially in heterogeneous catalysis [1]. In the past few years it has been shown that the introduction of copper in the zeolite structure significantly improves the catalytic performance of the system [2]. Despite a considerable amount of both experimental and theoretical works, a fundamental and comprehensive understanding of intrinsic mechanisms that govern the catalytic processes in these materials still merits complementary investigations. Electronic paramagnetic resonance (EPR) is a powerful tool to study the copper ion state in zeolites [3, 4]. Magic angle spinning nuclear magnetic resonance (MAS NMR) helps to test the Si/Al framework imperfection caused by ion-exchange processes [5, 6]. Here we report on the results of our complementary study of protonated and copper-exchanged zeolites with mordenite structure and with the molar SiO₂/Al₂O₃ ratio equal to 10 (samples HMor10 and CuMor10, respectively).

SAMPLE PREPARATION AND EXPERIMENTAL METHOD

The protonated mordenite sample was supplied by TOSOH Corporation, Japan. Copper ion exchange was carried out from 0.1 M Cu(NO₃)₂ aqueous solution for 1 day. The excess of solution was removed; samples were dried under ambient conditions followed by heating in dry H₂ flow at temperatures from 150 to 450 °C for 4 h. The copper content in the obtained samples was determined by a JEOL 5200 Scanning Electron Microscope equipped with a Kevex Super Dry EDS (Energy Disperse Spectroscopy). Quantification was done using the standard Magic 5 software. Measurements showed ≈1.0 wt.% of copper for all samples.

EPR spectra were measured with an ELEXSYS E580 BRUKER X-band spectrometer (~ 9.5 GHz), at a power 4.74 mW and modulation frequency of 100 KHz. Field Sweeps 0.50 – 10000 G were acquired at 65536 points. The measurements were carried out at room temperature. MAS NMR spectra were measured with Bruker WB Avance III (400 MHz) spectrometer. ²⁷Al and ²⁹Si spectra were measured at rotation frequency equal to 9 kHz. The measurements were carried out at room temperature.

RESULTS

According to thermogravimetric analysis substitution of protons by copper ions changes both the character and the temperature of the adsorbed molecules release.

²⁷Al MAS NMR spectra of HMor10 and CuMor10 samples are shown in Fig.1. As one can see the ²⁷Al NMR spectrum of HMor10 contains three peaks at 52.6, 38.5 and -3.2 ppm. The peak at 52.6 ppm is ascribed to framework four-coordinated aluminum atoms. The signal at 0 ppm corresponds to extraframework six-coordinated aluminum atoms, which are formed during pretreatments. The line at 38.5 ppm is usually attributed to extraframework five-coordinated Al species. About 15% of Al atoms are six-coordinated, that means the aluminum-silicon framework is rather imperfect.

²⁷Al MAS NMR spectra CuMor10 show two peaks at 55 and 0 ppm that corresponds to four- and six- coordinated aluminum atoms, respectively. Their ratio of the integral intensities is 9/1. It means that the substitution Cu²⁺ for H⁺ leads to the Si/Al framework recovery.

The EPR spectrum of the CuMor10 sample is shown in Fig. 2. This is a spectrum of a paramagnetic ion Cu²⁺ with spin ½ with anisotropic g-tensor. The EPR studies showed that the copper ions are in the field close to the axial symmetry. Experimentally obtained parameters of the EPR spectrum (g-tensor components and hyperfine interaction tensor A) are following: (g_{xx}(g_⊥) = 2.115 ± 0.001, g_{yy} = 2.120 ± 0.001, g_{zz}(g_∥) = 2.370 ± 0.001; A_{xx} = 48 ± 1 MHz, A_{yy} = 3 ± 1 MHz, A_{zz} = 410 ± 1 MHz). To treat experimental data it is necessary to carry out DFT calculations of

Cu²⁺ ion clusters surrounded by water molecules (octahedral and square clusters [Cu(H₂O)₆]²⁺, [Cu(H₂O)₄]²⁺ respectively). The calculations are in progress.

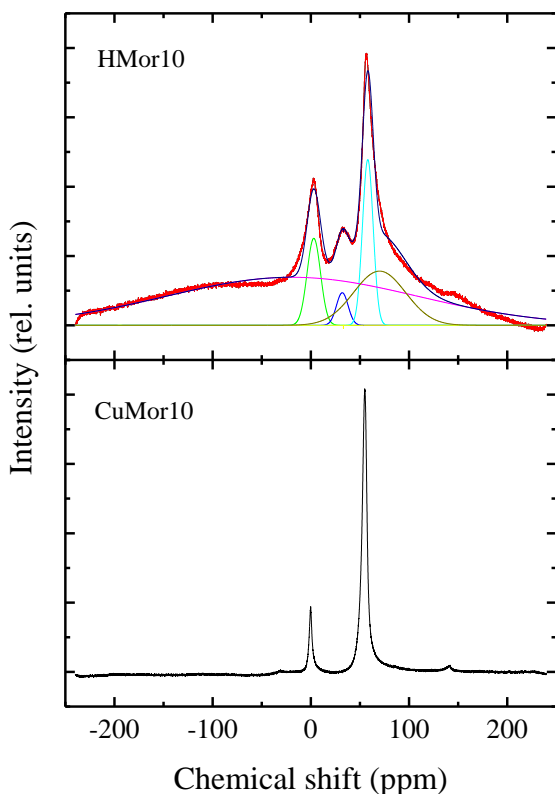


Fig. 1. ²⁷Al MAS NMR spectra of HMor10 and CuMor10.

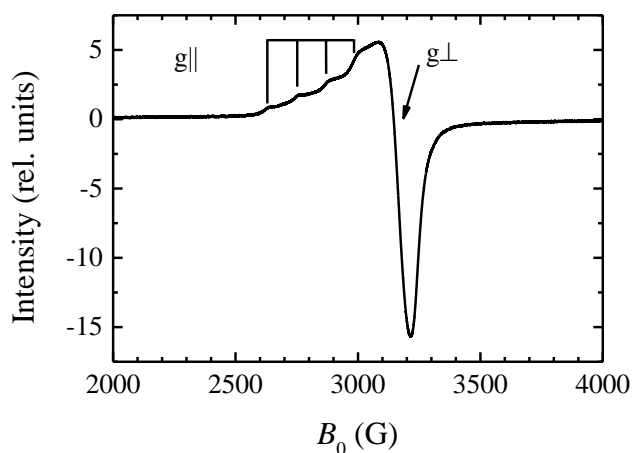


Fig. 2. EPR spectrum of polycrystal CuMor10

ACKNOWLEDGMENT

The studies were performed at the resource centers of Saint-Petersburg State University: Centre for Magnetic Resonance, Center of X-ray diffraction studies, Centre of Thermal Analysis and Calorimetry, Computer Center.

REFERENCES

- [1] J. Weitkamp. Solid State Ionics 131 (2000) 175-188.
- [2] P. Vanelderen, J. Vancauwenbergh, B.F. Sels, R.A. Schoonheydt. Coordin. Chem. Rev. 257 (2013) 483-494.
- [3] D. Berthomieu, G. Delahay. Catal. Rev. 48 (2006) 269-313.
- [4] A.C. Saladino, S.C. Larsen. Catal. Today 105 (2005) 122-133.
- [5] Hunger, M. and Brunner, E. (2004) Characterization I – NMR spectroscopy, in Molecular Sieves – Science and Technology (eds. H.G. Karge and J. Weitkamp), Springer, Berlin, pp. 201–293.
- [6] G.J. Kennedy, M. Afeworki, S.B. Hong. Micropor. Mesopor. Mat. 52 (2002) 55-59.

Gold nanoparticles supported on nanostructured ceria

B. Acosta¹, M.A. Estrada¹, V. Evangelista¹, E. Smolentseva², S. Beloshapkin³, I. Simakova⁴, A. Simakov²

¹Posgrado en Física de Materiales, Centro de Investigación Científica y de Educación Superior de Ensenada (CICESE), Ensenada, B.C., 22860, (México), ²Universidad Nacional Autónoma de México, Centro de Nanociencias y Nanotecnología, C.P. 22860, Ensenada, B. C., (México), ³Materials and Surface Science Institute, University of Limerick, Limerick (Ireland), ⁴Boreskov Institute of Catalysis, Novosibirsk (Russia).
andrey@cryn.unam.mx

INTRODUCTION

The remarkable ability of gold catalysts to catalyze different reactions at low temperatures is attributed both to Au nanospecies and the nature of the oxide supports [1-3]. Recent studies revealed that nanocrystalline CeO₂ used as support increases the activity of gold species in CO oxidation by two orders of magnitude in comparison with conventional CeO₂ [4, 5]. At the present time, there are different techniques to prepare nanostructured ceria as nanotubes, nanorods, fine nanocrystals using organic templates [6, 7] or rearrangement of freshly prepared wet cerium hydroxide at high pressure and temperature.

The aim of the present work was to prepare nanostructured ceria by hydrothermal treatment of solid CeO₂ in alkaline solution at high pressure and to evaluate the influence of ceria structural modification in the CO oxidation on gold-ceria catalysts.

MATERIALS AND METHODS

The ceria nanotubes with different size have been prepared via a hydrothermal treatment of solid CeO₂ at two different temperatures (120 °C and 150 °C) keeping constant residence time (36 h) and NaOH concentration (10 M). The synthesized ceria samples have been characterized by means of SEM, TEM, XRD and UV-Visible spectroscopy. The obtained ceria samples were used as supports for Au (3 wt. %) catalysts preparation by deposition precipitation technique using urea as a precipitating agent. The nature of gold species has been studied by means of TEM, *in situ* UV-Visible-Mass analysis and XPS spectroscopy.

RESULTS

The prepared nanostructured ceria samples were characterized with different amount of active surface oxygen species and different mobility of bulk oxygen. Decomposition of gold precursor supported on ceria depends on the nature of gas (oxygen or hydrogen) used for sample activation. Three distinguishable steps in the Au NPs formation on ceria: i) slow thermal decomposition of gold hydroxide; ii) fast formation of Au NPs due to thermal decomposition of Au(OH)₃ and its reduction with hydrogen, and, iii) slow transformation of residual part of gold precursor were found. The size of gold particles prepared in flow of oxygen does not depend on the support while

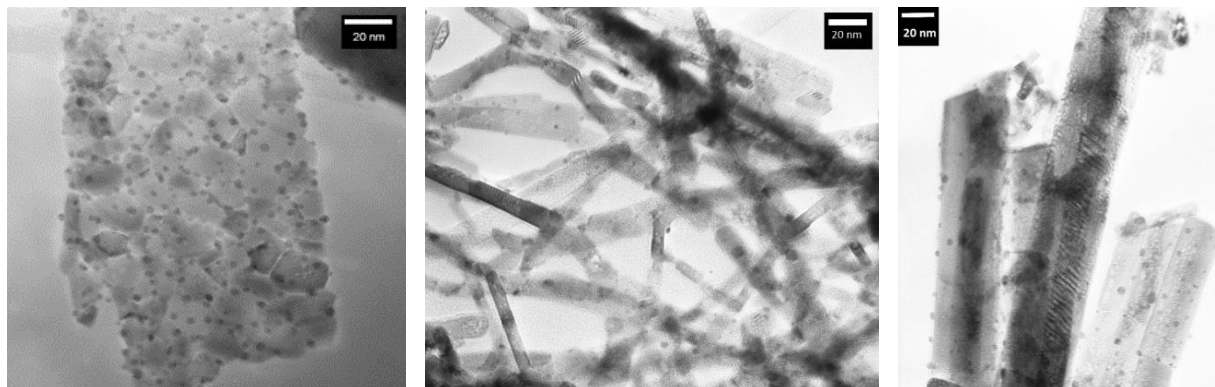


Fig. 1. TEM images for Au/CeO₂-SG (left), Au/CeO₂-HT1 (middle), Au/CeO₂-HT2 (right) samples reduced in hydrogen at 350 °C.

sample reduction in hydrogen flow leads to formation of gold nanoparticles with different size due to partial reduction of ceria samples that provokes gold species redistribution. The correlation between structural properties of ceria and the activity of gold catalysts in CO oxidation have been discussed.

Manipulation with ceria morphology and its electronic properties makes possible to control the relative content of different gold species in Au-ceria supported catalysts and their catalytic activity in CO oxidation.

ACKNOWLEDGMENTS

The authors would like to thank O. Callejas, E. Flores, F. Ruiz, J. Peralta and M. Sainz for technical assistance. This research project was partly supported by CONACyT (México) and PAPIIT-UNAM (México) through grants 179619 and 203813, respectively.

REFERENCES

- [1] M. Haruta, N. Yamada, T. Kobayashi, S. Iijima, *J. Catal.* 115 (1989) 301-309.
- [2] M. Schubert, S. Hackenberg, A. van Veen, M. Muhler, V. Plzak, R. Behm, *J. Catal.* 197 (2001) 113-122.
- [3] G.C. Bond, D.T. Thompson, *Catal. Rev. Sci. Eng.* 41 (1999) 19-388.
- [4] S. Carrettin, P. Concepción, A. Corma, J.M.L. Nieto, V.F. Puentes, *Angew. Chem. Int. Ed.* 43 (2004) 2538-2540.
- [5] J. Guzman, S. Carrettin, A. Corma, *JACS* 127 (2005) 3286-3287.
- [6] M. Yada, S. Sakai, T. Torikai, T. Watari, S. Furuta, H. Katsuki, *Advanced Mater.* 16, (2004) 1222-1226.
- [7] Z. Yuan, V. Idakiev, A. Vantomme, T. Tabakova, T. Ren, B. Su, *Catal. Today* 131 (2008) 203-210.

CO oxidation over gold nanoparticles supported on Mg(OH)₂ and MgO under different redox treatment

Elena Smolentseva¹, Miguel Estrada², Martin López Cisneros³, Sergey Beloshapkin⁴, Sergio Fuentes¹, Andrey Simakov¹

¹Universidad Nacional Autónoma de México, Centro de Nanociencias y Nanotecnología, Km. 107 Carretera Tijuana a Ensenada, C.P. 22860, Ensenada, Baja California, México, ²Posgrado en Física de Materiales, Centro de Investigación Científica y de Educación Superior de Ensenada, C.P. 22860, Ensenada, Baja California, México,

³Posgrado en Ciencia e Ingeniería de Materiales, Universidad Nacional Autónoma de México, Km. 107 Carretera Tijuana a Ensenada, C.P. 22860, Ensenada, Baja California, México, ⁴Materials & Surface Science Institute, University of Limerick, Limerick, Ireland.

elena@cny.unam.mx

INTRODUCTION

CO processing is required in many devices such as gas masks, CO gas sensors, air-purification equipment for indoor spaces, and catalytic converters for automotive exhaust gases. Hence, the CO oxidation reaction has attracted much interest in the areas of fundamental and applied catalysis.

The catalytic activity of gold catalysts in CO oxidation strongly depends on the gold particle size, method of gold deposition, pretreatment conditions, and the chemical nature and morphology of the supports [1, 2]. Gold nanoparticles (Au NPs) supported on Mg(OH)₂ and MgO have shown high catalytic activity in CO oxidation [3-5].

It is well-known that the MgO can be easily converted to Mg(OH)₂ in the presence of water at room temperature, especially under acidic conditions [6]. Usually the hydrolysis of MgO occurs during the gold deposition by deposition precipitation technique from aqueous solutions [7]. Complete back transformation of Mg(OH)₂ to MgO requires thermal treatment at temperature not less than 480 °C [8]. However, in some papers this factor is not controlled well [9, 10] and conclusions concerning the effect of MgO or Mg(OH)₂ on the catalytic activity of supported Au NPs may be not reliable.

The aim of the present work was to study the catalytic activity in CO oxidation during transformation of Au/Mg(OH)₂ to Au/MgO. The effect of phase transition on the Au NPs formation was studied by *in situ* UV-Visible spectroscopy with on-line mass analysis of the gas products. The obtained catalysts were tested on CO oxidation at different temperatures after sample reduction or oxidation in order to reveal the role of the electronic state of gold species.

MATERIALS AND METHODS

Gold (Au ~ 2.6 wt. %) was supported by deposition precipitation on commercial magnesia (Mallinckrodt) with following thermal treatment of selected samples in hydrogen or in oxygen at 350 or 500 °C. The phase transition of Mg(OH)₂ to MgO and formation of Au NPs under different redox treatments (reduction with hydrogen or oxidation with oxygen) were monitored by *in situ* UV-Visible spectroscopy, on-line mass analysis, XRD, TEM and XPS technique.

RESULTS

The phase transition of Mg(OH)₂ to MgO (350-450 °C) provoked the reconstruction of gold/magnesia catalyst and appearance of new portion of accessible Au NPs (diameter ~ 3.5 nm) formed from the gold species being encapsulated under catalyst preparation. The application of *in situ* UV-Visible analysis to study the catalyst transformation under different thermal treatments permitted to estimate the fraction of encapsulated gold species (~30 %). Estimation was done on the base of dynamics of plasmon intensity and plasmon position change during thermal treatment of Au/Mg(OH)₂ sample (Fig. 1).

The study of the effect of Mg(OH)₂ to MgO phase transition under different redox treatments on CO oxidation over Au NPs revealed that the initial activity in CO oxidation was similar for Au NPs supported on Mg(OH)₂ or MgO, and practically independent on the type of sample redox pre-treatment. On the other hand, the observed catalytic

activity delay with reaction time strongly depended on the type of redox pre-treatment (reduction or oxidation), which affected the acid-base properties of the catalyst surface (Fig. 2). Pre-oxidized catalysts were characterized with higher stability in CO oxidation compared to that for pre-reduced catalysts in spite of similar size of gold nanoparticles for both samples and almost equal amount of adsorbed CO₂ during the reaction.

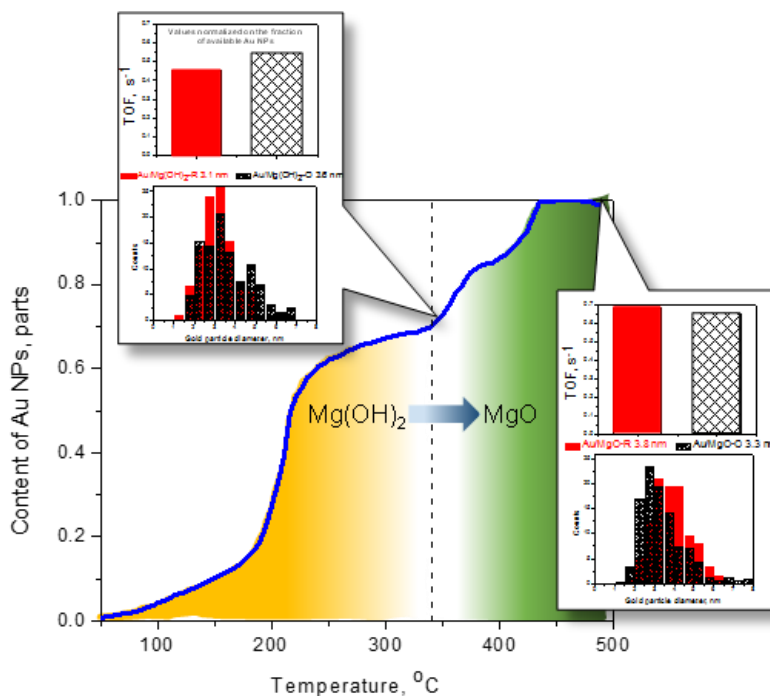


Fig. 1. The diagram of Mg(OH)₂ to MgO phase transition according to UV-Visible spectroscopy data. Left insert: TOF values for Au/Mg(OH)₂-R (reduced in H₂ at 350°C) and Au/Mg(OH)₂-O (oxidized in O₂ at 350°C) samples in CO oxidation at 30 °C and gold particle size distribution for these samples, according to TEM analysis. Right insert: TOF values for Au/MgO-R (reduced in H₂ at 500°C) and Au/MgO-O (oxidized in O₂ at 500°C) samples in CO oxidation at 30 °C and gold particle size distribution for these samples according to TEM analysis.

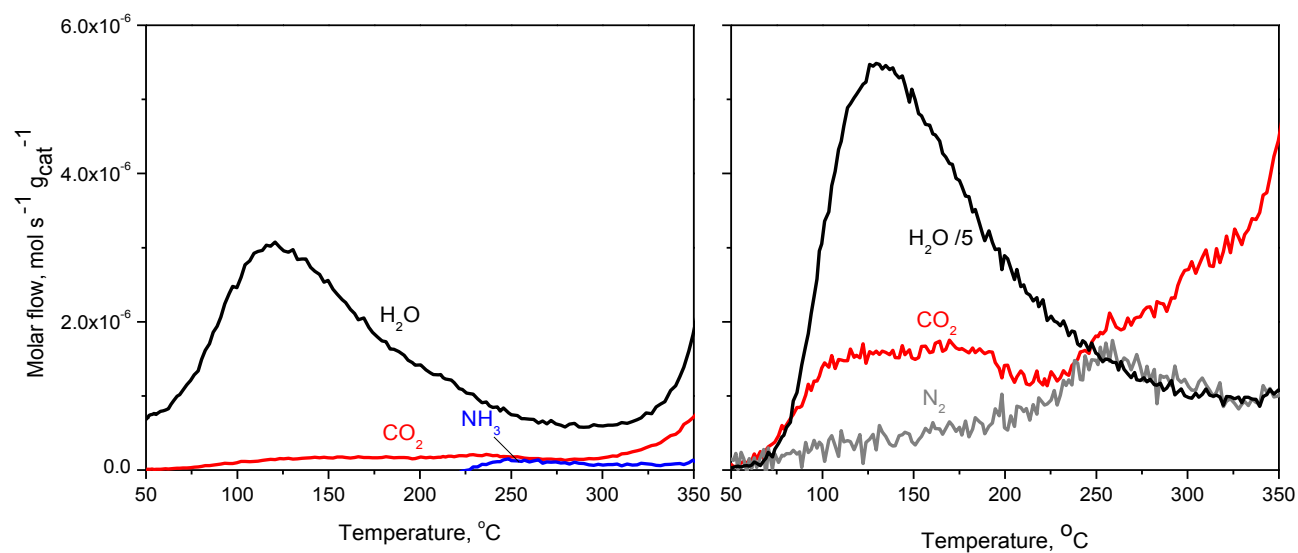


Fig. 2. Profiles of products desorption during temperature programmed reduction (left) or oxidation (right) of Au/Mg(OH)₂-F sample under temperature increase up to 350 °C with ramp rate of 20 °C/min.

ACKNOWLEDGMENT

The authors thank E. Flores, P. Casillas, V. García, F. Ruiz, E. Aparicio, M. Vega, M. Sainz and J. Peralta for their kind technical support in this work. I. Perez Montfort corrected the English version of the text. Financial support was from CONACyT (Mexico) and DGAPA-PAPIIT (UNAM, Mexico) through the grants 179619 and 203813, respectively, and SENER-CONACyT through the grant 117373.

REFERENCES

- [1] M. Haruta, N. Yamada, T. Kobayashi, S. Iijima, *J. Catal.* 115 (1989) 301-309.
- [2] G.C. Bond, D.T. Thompson, *Catal. Rev. Sci. Eng.* 41 (1999) 19-388.
- [3] M. Haruta, T. Kobayashi, S. Tsubota, Y. Nakahara, *Chem. Express*, 3 (1998) 159-162.
- [4] D.A.H. Cunningham, W. Vogel, H. Kageyama, S. Tsubota, M. Haruta, *J. Catal.* 177 (1998) 1-10.
- [5] M. Okumura, S. Nakamura, S. Tsubota, T. Nakamura, M. Azuma, M. Haruta, *Catal. Lett.* 51 (1998) 53-58.
- [6] A.V. Radha, P. Vishnu Kamath, G.N. Subbanna, *Mater. Res. Bull.* 38 (2003) 731-740.
- [7] M. Haruta, *J. New Mater. Electrochem. Syst.* 7 (2004) 163-172.
- [8] K. Itatani, K. Koizumi, S. Howell, A. Kishioka, M. Kinoshita, *J. Mater. Sci.* 23 (1988) 3405-3412.
- [9] J.L. Margitfalvi, A. Fási, M. Hegedus, F. Lónyi, S. Gobölös, N. Bogdanchikova, *Catal. Today* 72 (2002) 157-169.
- [10] K. Layek, M.L. Kantam, M. Shirai, D. Nishio-Hamane, T. Sasaki, H. Maheswaran *Green Chem.*, 14 (2012) 3164-3174.

Spontaneous formation of self-assembling, hierarchical and biomorphic SiO₂ nanostructures

N. Bogdanchikova¹, O. Martynyuk^{1,2}, A. Pestryakov², R. Luna Vázquez G.³, F. Ruiz Medina¹, A. Huerta-Saquero¹, T. Zepeda¹

¹Centro de Nanociencias y Nanotecnología-UNAM, Ensenada, México, ²Tomsk Polytechnic University, Tomsk, Russia, ³Universidad Autónoma de Baja California, Ensenada, México
nina@cryn.unam.mx

INTRODUCTION

Mesoporous silica is widely used in catalysis, drug delivery and imaging. Geometrical structures of the hexagonal mesoporous silica (HMS) usually have a form of short nanotubes, which are organized in honeycomb shape. However, our experiments showed that under certain conditions silica formed unorganized short nanotubes, which during storage spontaneously without any template form hierarchically self-assembled structures, resembling some biological molecules (DNA and proteins) and other bio forms (virus-like). In the literature there are works dedicated to one of these three phenomena; however, we did not find the description of observation of two or three of them simultaneously in one system. The closest analogous material with similar biomorphic structures for mixture of SiO₂ and BaCO₃ were reported in [1]. In this case, Ba carbonate played a role as template; while in our work we do not apply any template substance. Moreover, in [1] biomorphic structures with sizes $\geq 300 \mu\text{m}$ were formed; while in the present work size of biomorphic SiO₂ structures is at least three orders of magnitude smaller ($\sim 80 \text{ nm}$).

EXPERIMENTAL

The synthesis of silica nanoparticles was made according to method described in [2, 3] with low concentration of dodecylamine surfactant in alcohol. Preparation method included neutral S⁰T⁰ templating route as a first step. Dodecylamine was used as neutral primary amine surfactants (S⁰), tetraethylortosilicate as neutral inorganic precursor (T⁰) and mesitylene as a swelling organic agent. The final step included template removal by calcination at 550°C for 3.5 h in air. After calcination, storage of synthesized material was carried out in closed vials.

RESULTS AND DISCUSSION

Preparation of silica support included self-assembling of the HMS nanotubes with length 9 nm, external diameter 8.5 nm and internal diameter 5 nm. It was observed that after synthesis silica nanoparticles are chaotically distributed, but during their storage, the formation of spontaneously self-assembled nanoparticle aggregates with great multiplicity of morphologies was revealed. In Fig. 1 chain and branched chains with different level of complexity are presented. This diversity of observed structures allowed us to suggest the morphologic multiplicity of prepared hexagonal mesoporous silica, which is consisted in short curved nanorings with parallel and not parallel entrances. Such structures are not crystals but have rather high level of order that is not typical for inorganic materials, especially self-assembled without template as was in our case. In this work we show that different biomorphic silica structures have extraordinary similarity with biological molecules of comparative size.

Moreover, hierarchical formation of HMS nanostructures similar to deoxyribonucleic acid was found. Such hierarchic structures are combinations of self-assembled spirals and toroids consisted of deformed nanotubes. In the literature there is the hypothesis that DNA has shape of double helix influenced by repeating of spiral shape of water structure in very narrow spaces. If this hypothesis is correct SiO₂ nanotubes revealed in this work probably repeat the water structure too and consequently may act as sensors of water structure.

Existence of such quasi-bio structures was reproduced in the present work for 25 samples of HMS prepared by the same method varying different parameters such as temperature, time of storage, etc. Self-assembled hierarchic biomorphic silica structures were not observed during the first days after their synthesis. The structures were observed after several weeks if a small amount of water was added or after several months without water addition.

The spontaneous formation of self-assembled and biomorphic SiO₂ nano-structures represents an attractive challenge for various research areas: 1) formation of quasi-biological molecules based on silicon/silica; 2) development of visual and convenient instrument for investigation of water associates morphology; 3) existence

of microfossils of abiotic origin; 4) processes analogous to that presented during the early formation of organic molecules preceding evolution of biological systems; 5) important features developed in the early events of the origin of life.

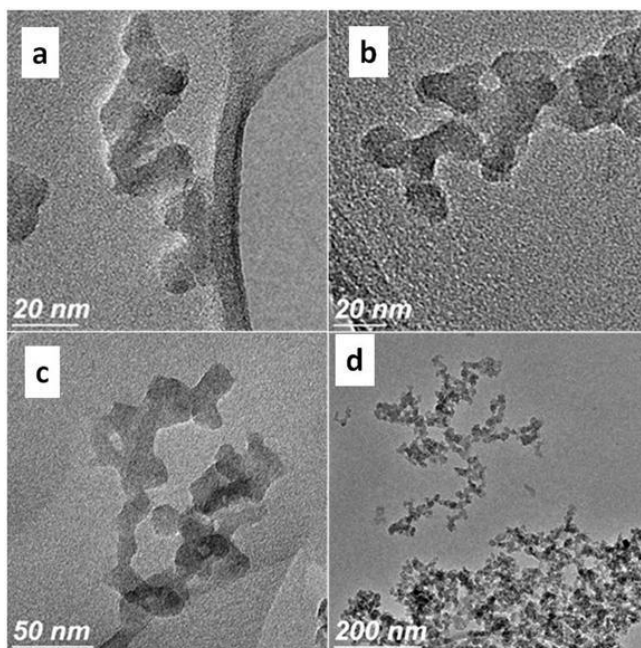


Fig. 1. Self-assembled silica nanoparticles in form of (a) chain and (b-d) branched chains with different levels of complexity

ACKNOWLEDGMENTS

The authors thank Dr. M. Avalos Borja for helpful comments on the manuscript and fruitful discussions. We are further grateful to Yu. Kotolevich, E. Flores, Sh. Sandoval, J. Mendoza, J. Peralta, M. Sainz for technical assistance. Financial support by CONACYT Project No 79062, PAPIIT-UNAM Projects IT200311, IT200114 (Mexico) and Russian Science Foundation is greatly appreciated.

REFERENCES

- [1] N. Sanchez-Puig, E. Guerra-Flores, F. López-Sánchez, P. A. Juárez-Espinoza, R. Ruiz-Arellano, R. González-Muñoz, R. Arre-guín-Espinosa, A. Moreno. *J. Mater.Sci.* 47 (2012) 2943.
- [2] Tanev, P., Pinnavaia, T.J. *Science* 267, 865-867 (1995).
- [3] B. Pawelec, P. Castano, T.A. Zepeda. *Appl. Surf. Sci.* 254, 4092–4102 (2008).

Optical properties of supported metal nanoparticles: Modeling zeolite based composites

Catalina López Bastidas¹, Elena Smolentseva, Roberto Machorro and Vitalii Petranovskii
CNyN, UNAM Ensenada, México
clopez@cyn.unam.mx

INTRODUCTION

The optical spectra of supported metal nanoparticles is of interest from both a fundamental and a practical point of view. The information obtained from the spectra combined with an appropriate theoretical model leads to better understanding of the influence of the environment on the fundamental collective electronic states, such as the localized plasmons that are available to electrons of the nanoparticle. Furthermore, the dynamic screening properties of the substrate can also be identified and studied. The knowledge of these properties can then be applied to the development of optical tools to monitor the synthetic path and in the future will hopefully aide the development of controlled synthesis of materials with predetermined properties. In this work, we present the experimental and theoretical analysis of optical spectra of gold, silver and copper nanoparticles supported on zeolite templates [1], [2]. The main topic of discussion will be the theoretical modeling of such a complex system, and what can be learned by working with an average field approximation. We will present experimental UV-visible spectra of varied host-guest combinations and respective theoretical modeling.

MAXWELL-GARNETT MODEL

In this work, we employ an average field approach to describe the physics relevant to the optical response of the zeolite (host)-metal (guest) system. The macroscopic dielectric response of the complete system will then be described by an effective dielectric function. Within this approach, a cluster or inclusion is considered to be immersed in a non absorbing homogeneous host medium described by a dissipation free, real valued dielectric function. The scheme is widely used to describe composite media. An important consideration when modeling such multipart systems is the interaction between the components. In the Maxwell-Garnett (MG) approach only direct dipole interactions between inclusions is accounted for [3]. Higher order interaction terms can be included systematically using generalized formulas available in the literature. Extension to such a treatment have been widely developed considering variations in shape and composition of the guest particles.

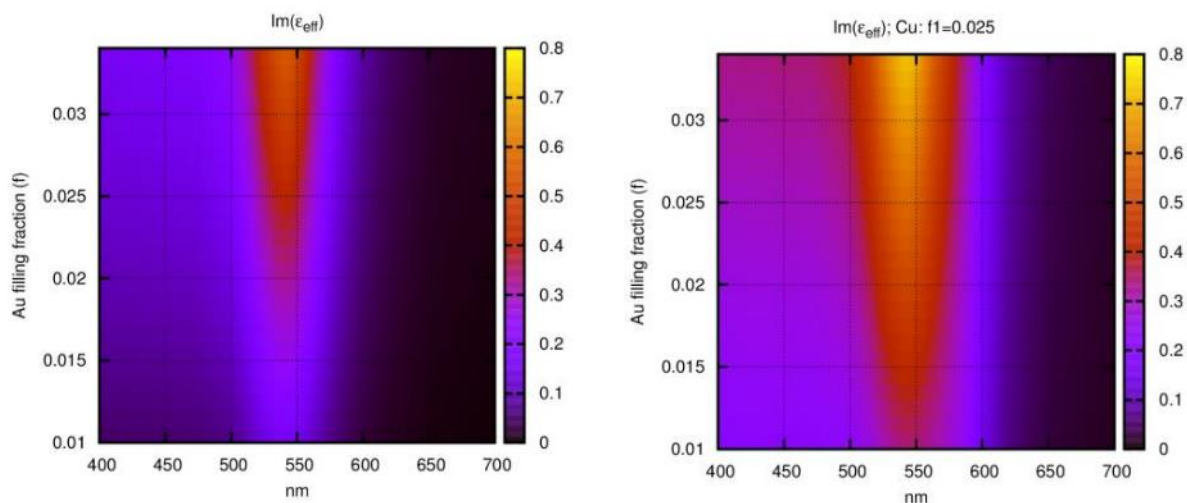
The basic MG model using ϵ_z for the dielectric response of the host and $\epsilon(\omega)$ for the frequency dependent metal dielectric function present with a volume filling fraction of f gives an effective dielectric function of

$$\epsilon_{eff}(\omega) = \epsilon_z \frac{\epsilon(\omega)(1+2f) + 2\epsilon_z(1-f)}{\epsilon(\omega)(1-f) + (2+f)\epsilon_z}$$

Once the effective dielectric response of the system is known it can be employed to calculate quantities such as reflectance, absorbance, etc. The imaginary part of the effective dielectric function will correlate directly with the absorbing channels present in the composite such as the plasmon excitation [4].

TWO METAL COMPOSITE

The Maxwell-Garnett (MG) model can be extended to include guest nanoparticles of different species [5]. The treatment is straight forward and only the respective filling fractions and dielectric functions need to be supplied. In Fig. 1 we show the imaginary part of the effective dielectric function for varying values of the filling fraction. In the left panel the results obtained with the MG model for a zeolite template with Au nanoparticles and in the right panel the results with a modified MG model for a composite containing a fraction of 0.025 of the total volume of Cu nanoparticles. We can see that the resonant wavelength is not noticeably shifted with the presence of the Cu nanoparticles but the magnitude of the signal is enhanced. Furthermore, the plasmon resonance can be observed for lower filling fractions of Au.



CONCLUSIONS

The absorbance spectra of metal nano particles embedded in zeolite template presents a plasmon resonance for sufficiently high values of temperature treatment. A thermal treatment modifies the diffusion coefficient of the metal within the structure changing the nano particle size, which can be correlated to the filling fraction of metal within the composite.

- The zeolite matrix screens the electromagnetic fields that excite the plasmon and modifies the resonant frequency.
- This screening depends on the chemical composition of the structure.
- The presence of a precursor metal within the composite enhances the plasmon both aiding in the formation of larger nanoparticles and by screening.

Some features can be explained qualitatively with an average field approach, modified Maxwell-Garnett model. We show that optical spectroscopy can be a useful tool to study nano particles supported on zeolites.

ACKNOWLEDGMENT

This work was supported by CONACYT, Mexico, through the grant 102907, SENER-CONACYT through the grant 117373 and UNAM-PAPIIT through the grants IN110713 and IN111013.

REFERENCES

- [1] C. Lopez-Bastidas, E. Smolentseva, V. Petranovskii, R. Machorro, Plasmonics **8**, 1551-1558 (2013)
- [2] C Lopez-Bastidas, V. Petranovskii, R. Machorro J. Colloid and Interface Sci. **375**, 60-64 (2012)
- [3] J.C. Maxwell-Garnett, Philos. Trans. Roy. Soc. London, Ser. B **203**, 385 (1904)
- [4] Craig F. Bohren, Donald R. Huffman, Absorbition and Scattering of Light by Small Particles, Wiley, (1983)
- [5] Ququan Wang, Decheng Tian, Guiguong Xiong, Zhengguo Zhou, Physica A **275** , 256–261 (2000)

Spectroscopic study on nanospecies prepared by thermal reduction in hydrogen followed by cooling in variable atmosphere for the $\text{Cu}^{2+}\text{-Ag}^+\text{-Zn}^{2+}$ /trimetallic system supported on mordenite

I. Rodríguez-Iznaga^{1,a}, M. Herrera Zaldivar^{2,a}, V. Petranovskii², F. Castellón Barrasa², R. Machoro² and F. Chávez Rivas³.

¹Instituto de Ciencia y Tecnología de Materiales (IMRE) - Universidad de La Habana, Cuba. ²Centro de Nanociencias y Nanotecnología, Universidad Nacional Autónoma de México, Ensenada 22800, México.

³Departamento de Física, Escuela Superior de Física y Matemáticas del IPN, D.F., México.

^ainocente@imre.oc.uh.cu, ^bzaldivar@cnyun.unam.mx

ABSTRACT

Modification of zeolites with metallic nanospecies is an important approach to the development of materials with new properties for different uses. Metal ions, clusters and nanoparticles can be confined into the channels and cages of nanometer or sub nanometer size, those are inherent to crystalline structure of zeolites. Stabilization of such species is crucial for the development of metal/zeolite materials with important properties such as catalytic or antimicrobial activity. Between other metals, copper, zinc and silver as well as their compounds are of great interest due to both catalytic properties and oligodynamic activity [1,2].

The ion exchange and reduction are more frequently used processes to obtain modified zeolites with metal nanospecies. Reports are mainly known for monometallic systems obtained by conventional ion-exchange procedure. Significant differences in the metal nanospecies obtained by thermal reduction are observed in multimetallic systems respect to the monometallic, which in line influences to their properties. In addition, an important aspect of nanospecies preparation is the atmosphere type used for the reduction and cooling of the samples. However, studies are mainly performed using thermal reduction in hydrogen flow, followed by cooling in the same atmosphere. In this work, the thermal reduction in hydrogen followed of cooling in air as well as in hydrogen of ternary $\text{Cu}^{2+}\text{-Ag}^+\text{-Zn}^{2+}$ /Mordenite system was evaluated using ultraviolet-visible diffuse reflectance (UV-Vis DRS) and Cathodoluminescence (CL) Spectroscopies.

For the studies, synthetic Na-Mordenite (NaMor) was exchanged at 100°C during 120 min under microwave-radiation with $\text{Cu}(\text{NO}_3)_2$, $\text{Zn}(\text{NO}_3)_2$, AgNO_3 and mixed solutions, with 1g/10mL solid/solution ratio. Mixed solutions used to obtain trimetallic samples were prepared by mixing of AgNO_3 , $\text{Cu}(\text{NO}_3)_2$ and $\text{Zn}(\text{NO}_3)_2$ solutions, in 1:1:1, 1:1:2, 1:2:1, 1:2:4, 1:2:6 and 1:2:8 ratios, respectively. These numbers placed after each metal encode the obtained trimetallic samples. The Cu, Ag and Zn content in monometallic CuMor, AgMor and ZnMor samples was 4.07%, 12.75% and 3.58%, respectively. The respective Cu, Ag and Zn contents in the trimetallic samples were 1.39%, 8.08% and 0.67% to Ag1Cu1Zn1Mor; 1.51%, 7.15% and 1.77% to Ag1Cu1Zn2Mor; 2.79%, 6.79% and 0.10% to Ag1Cu2Zn1Mor; 1.56%, 4.70% and 1.15% to Ag1Cu2Zn4Mor; 1.08%, 3.88% and 1.75% to Ag1Cu2Zn6Mor and 1.11%, 2.37% and 3.55% to Ag1Cu2Zn8Mor.

The resulting monometallic (CuMor, AgMor and ZnMor) and mixed trimetallic (Cu-Ag-Zn/M) samples were reduced in H_2 flow at 350°C, during 4 h. The reduced samples were cooled to room temperature, using two different atmospheres: H_2 and air. The UV-Vis diffuse reflectance and Cathodoluminescence spectra of the samples, before and after the reduction and cooling, were obtained. X-ray diffraction (XRD) patterns of the starting mordenite and ion-exchanged samples were achieved, too.

The changes observed in the metal contents in the ion-exchanged samples are results of the ion exchange between Na^+ from NaMor and the Cu^{2+} , Ag^+ and Zn^{2+} cations from used exchange solutions.

XRD patterns of the NaMor, as well of the ion-exchanged monometallic and trimetallic samples do show that the use of microwave radiation does not affect the structure of the mordenite.

The obtained by UV-Vis and CL results allows to outline that the use both of trimetallic Cu-Ag-Zn/M systems with different metal contents and variable atmospheres (air and H_2) for cooling of reduced trimetallic samples

leads to a diversity in obtained nanospecies. Copper and silver nanoparticles and silver cluster are obtained for the samples reduced and cooled in H₂. A lower silver content is in line with the formation of silver cluster, while the formation of nanoparticles of bigger size take place in the trimetallic samples with higher silver content. A cooling in air of the reduced trimetallic samples causes the oxidation of the silver and copper nanospecies (cluster and nanoparticles). This oxidation takes place by two ways: 1) oxidation to ionic species (Cu²⁺, Ag⁺) and 2) oxidation to nanoparticles of metal oxides. These results are different for the reported earlier [3,4] on oxidation of samples reduced and cooled in hydrogen and stored under ambient conditions. In this last case, the reduced nanospecies are re-oxidized to ionic species (Cu²⁺ and Ag⁺) or nanospecies of smaller size are originated before final complete oxidation.

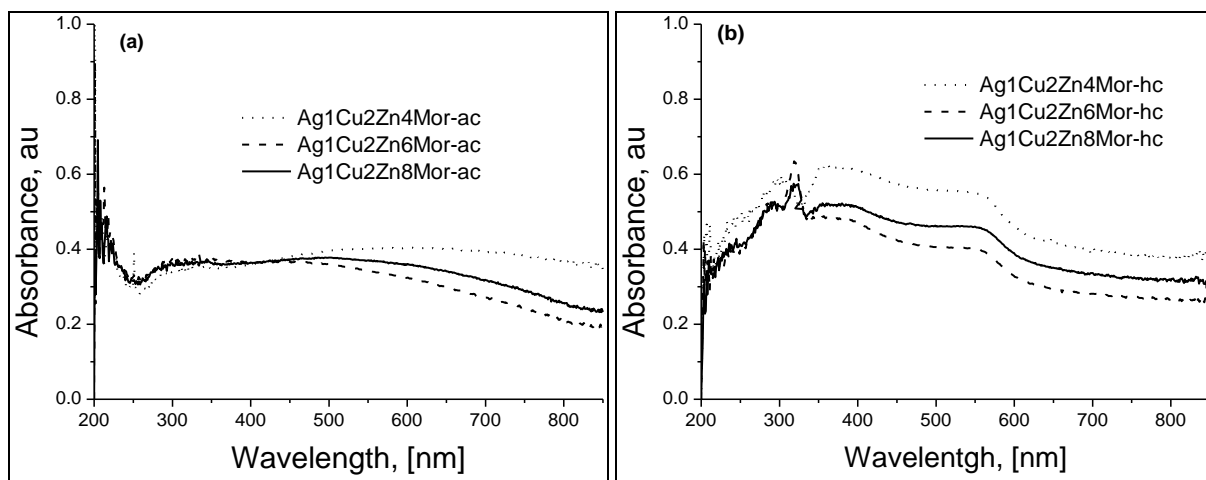


Fig. 1. UV-Vis diffuse reflectance spectra of selected samples reduced in hydrogen followed by cooling in air (a) or in hydrogen (b).

ACKNOWLEDGMENTS

Thanks are given to E. Aparicio, I. Gradilla, J. Peralta and E. Flores for the technical assistance. This research was supported by CONACYT, México, through grant 102907 and UNAM-PAPIIT through the grants IN207511, IN110713 and IN104414.

REFERENCES

- [1] A. Nezamzadeh-Ejhieh and M. Karimi-Shamsabadi. Chem. Eng. J. 228, 631 (2013).
- [2] P. Kaali, M. M. Pérez-Madrigal, E. Strömberg, R. E. Aune, Gy. Czél and S. Karlsson. eXPRESS Polym. Lett. 5, 1028 (2011).
- [3] V. Petranovskii and N. Bogdanchikova. Stud. Surf. Sci. Catal. 141, 569 (2002).
- [4] I. Rodríguez Iznaga, V. Petranovskii, F. Castellón Barraza, M.A. Hernández Espinosa and B. Concepción Rosabal. Proceedings of International Symposium on Zeolites and Microporous Crystals. Hiroshima, (2012)

Using isotopes (^2H , ^{18}O , ^3H) for water balance investigation in arid regions.

1. Estimation of groundwater resources in province Almeria (south-east Spain)

Tokarev I.V.¹, Carlos Ordóñez Peres², Rumynin V.G.³

¹Saint-Petersburg State University, Resource Center “Geomodel”; ²Técnicas de investigación hidrogeológica, S.A., Madrid; ³Institute of Environmental Geo-sciences of RAS, Saint-Petersburg Div.
tokarevigor@gmail.com

INTRODUCTION

Quantifying water budget is crucial to understanding the possibility of the water supply in arid region. The general approach is based on computation a partial water balance for each of landscape units and then calculation an aggregated water balance for the catchment. Such water balance study requires the long-term monitoring of the hydrology and hydrogeology of a watershed (including the high- and low water years). However often the peculiarity of raining and runoff formation, and change in groundwater storage do not allow get not only the average parameters, but also correctly find the upper and lower estimation of groundwater resources. Always two measuring values are ill-defined. Firstly, it is winter precipitations, which occur predominantly as snow in the mountains, have a high spatial and temporal variability and, secondly, it is evapotranspiration, which take up for 90-95% of the effective precipitations in arid zones. In addition, calculation of melt-water amount from the thawing glaciers is the labor-intensive work. However, it is very important information for prediction models, taking into account the climate changes and continued glaciers degradation.

This work demonstrates an approach for quantifying runoff and groundwater resources, which is based on the isotope technique in complex with other, for example geophysical investigation and remote sensing, in case of need.

Case study 1. Estimation of groundwater resources in province Almeria (south-east Spain)

The province of Almería, as also Alicante, Granada and Murcia, has many partially desert areas, which combine mountains and coast plains. Sierra Nevada (Granada province), which is the highest altitude of the Iberian Peninsula, blocks the water vapor transfer from Atlantic ocean toward the south-east part of Peninsula. There are some catchments with very little precipitation, for example, less than 50 mm per year in Tabernas municipio. Only the Andarax and Almanzora rivers have all-year significant flow, but the their runoff was decreased from 0.55 to 0.27 m³/s and from 1.14 to 0.38 m³/s for periods 1974-1980 and 1981-2004, respectively, as the result of climate and anthropogenic negative impact. Winter cold period, when the water reserve is refreshed, occurs from October to March (or to April for mountains). It is divided on wet (October-January) and dry (February-March) parts. In warm time of year from May to September, water storage is only spent to evapotranspiration.

In focus of this study was the Sierra de los Filabres (highest point is Calar Alto, 2 168 m), which is an eastern prolongation of the Sierra de Baza mountain range (this ridge is located parallel and to north from the Sierra Nevada) and forms the southern limit of the Almanzora valley. There are numerous small catchments, which have very steep altitude gradients due to Quaternary lifting of earth surface, giving rise to deep, narrow river valleys. These ephemeral, gravel streambeds (ramblas in the Mediterranean Spanish) are dry for most of the year. So, mainly groundwater is used for potable supply and agricultural irrigation. Groundwater had been traditionally used by tapping springs and diverting river base-flow, but now the major quantities are abstracted through wells and horizontal galleries.

The hydrogeological complexity of Sierra de los Filabres is caused by the existence and interaction of different aquifers and aquitards due to active tectonic moving in Quarter. Generally, three main hydrogeological units can be differentiated as aquifers.

1. The Nevado-Filabrides unit generally is an aquiclude being composed of mica-schists and quartzites. Weak aquifers sporadically distributed only in fissured rocks near earth surface as phreatic water and it is confined because of overlaying impermeable strata such as shale.

2. The Alpujarran unit represented by limestone, dolomite and quartzite intercalations. The aquifer has mostly local character, but sometimes this unit demonstrates high water content, as it is in Cobdar municipio, where horizontal gallery in marble mountain gives the water also for neighboring municipio Albanches.
3. A detritus strata consists of several layers of conglomerates and superposed Quaternary continental deposits. These porous rocks and sediments (especially alluvium) functions as most reliable aquifer.

The main goal of work was the estimation of groundwater resources for improving potable water supply in 22 municipios. Territory of each municipio usually takes one or several elementary catchments. In April-May (in the end of wet period) and in September-October (low water time) of 2002 water samples were taken from several wells, boreholes, springs, and the main stream and tributaries of Rio Almanzora. The exploited wells and boreholes mainly were chosen for testing. During sampling the pH-value, temperature and electrical conductivity of water were measured and in lab the chemical (major components and microelements) and isotope (deuterium – $\delta^2\text{H}$ and oxygen-18 – $\delta^{18}\text{O}$) composition of water, and activity of radon (^{222}Rn) and tritium (^3H) were analyzed. Abundance $\delta^2\text{H}$ and $\delta^{18}\text{O}$ was measured by mass-spectrometry. Province Almeria is not far from Atlantic Ocean, so electrolytic enrichment was used for ^3H concentration before liquid scintillation counting. Degasation of water and gas scintillation chamber was used for ^{222}Rn activity measuring.

Assignment of "input function", which describes temporal and spatial variations of $\delta^2\text{H}$, $\delta^{18}\text{O}$ and ^3H amounts in atmospheric precipitations, is the indispensable condition for interpretation of isotope data. In this work On-line Isotope in Precipitation Calculator (OIPC, by G. Bowen et al., Perdue University, LA, US) is used for definition of seasonal variation and altitude effect for $\delta^2\text{H}$, $\delta^{18}\text{O}$ in precipitations. For identify altitude effect the calculated values of $\delta^2\text{H}$ and $\delta^{18}\text{O}$ were compared with sampling of small catchments, which characterized the fast movement of water, on different altitudes of Sierra de los Filabres in spring and autumn. Published data (monitoring points Vera, Almeria and Thonon, France) were used for describe of ^3H temporal variation.

Obtained data show, as expected, that the river flow is replenished by precipitation throughout from the watershed to mouth of Rio Almanzora in winter and early spring and only by water of mountain origin in fall. Influence of evaporation is little bit visible for autumn samples from river.

In contrast to surface water, the groundwater has usually isotope composition, which is close to winter precipitations of the coldest months (December and January). Elevation of recharge area, which was calculated from function ($\delta^2\text{H}$ and $\delta^{18}\text{O}$) vs. altitude, as a rule, is similar to highest mark of watershed. It was interpreted, that the first portions of winter rains in October and November are spent to replacement of water storage in the root zone and soils. Also this may be indicates, that precipitations are efficiently absorbed and percolated to groundwater level only on the areas, there are no Quaternary sediments, that is on crest of ridges. In several cases watershed was located in 12-14 km from the sampled boreholes, so residence time of water in aquifer may be very high.

Isotope composition of water sample demonstrates wide spacing on classical diagram $\delta^2\text{H}$ vs. $\delta^{18}\text{O}$. Points are scattered as from the typical West Mediterranean trend, which characterized by shift of isotope composition to left from Global Meteoric Water Line (GMWL), both to right from GMWL. So, deuterium excess is varying from about 20 down to 0, which indicates the strong influence of evaporation to groundwater isotope composition in some cases. Note, the strongly evaporated water samples could not be used for calculation of recharge area elevation.

Tritium activity was measured for determination of groundwater residence time in aquifer. Unfortunately, due to very low input activity, several times ^3H has not been measured by liquid scintillation counting. Usually it was in case, when examined catchment was large. The lumped parameter model with calculated ^3H input function was used for estimation of groundwater residence time (τ). This parameter varied from one year (lower dating limit for applied procedure) up to 30 years (upper limit).

Calculation of groundwater resources was done from equation $Q = V/\tau$, where V is volume of water in catchment (m^3) and τ is age of groundwater (year). Volume of water was calculated in the following way. The size of recharge area (S) was estimated from the $\delta^2\text{H}$ and $\delta^{18}\text{O}$ data and using topography and partially from geology map. Thickness of water-saturated formation (h) was estimated by vertical electrical sounding and the volume of water-bearing porosity (p) by nuclear magnetic resonance technique, whence $V = S \times h \times p$.

Though foregoing estimation of potable groundwater resources is raw count, but there are several reasons take it for using. Firstly, it is estimation of lower limit of water resources, as only autumn sampling and measurements (low water period) were taken into account. Secondly, it was spent only six months as total time on whole work, so it is rapid method. At last, this technique could be appreciable enhanced due to (1) all-year monitoring of groundwater, (2) using tritium/helium-3 method for groundwater dating and mass-spectrometry measuring both ^3H and tritiogenic ^3He , (3) calculation of water resources by numerical models.

Using isotopes (^2H , ^{18}O , ^3H) for water balance investigation in arid regions. 2. Naryn river run-off investigation (Kyrgyzstan)

Tokarev I.V.

¹Saint-Petersburg State University, Resource Center "Geomodel"
tokarevigor@gmail.com

INTRODUCTION

An equitable apportioning of water resources is one of most important condition of economic development of five former soviet republics in Central Asia. Geographically these countries are divided on two groups. Kyrgyzstan and Tajikistan are located in area of mountain landform and have an excess of water. Kazakhstan, Turkmenistan and Uzbekistan have large desert areas and problems with water resources. Main contradiction is that highland countries use river water for electricity generation in winter, and last three countries use the water for irrigation in summer. Kyrgyzstan and Tajikistan have no possibility to redistribute run-off from year to year. Degradation of mountain glaciers due to climate changes causes concern, that river run-off will be proportionally declines.

Case study 2. Naryn river run-off investigation (Kyrgyzstan)

This work includes the results of two projects of International Scientific-Technical Center (ISTC KR-330.3 and KR-1430), which were done in 2003-2006 and 2007-2010 in cooperation of Russian and Kyrgyzian teams. Catchments of Issyk-Kul, which is closed lake, and Naryn, which forms Syr-Darya River after junction with Kar-Darya River, were in a focus of work. These rivers are the main source for agricultural irrigation of Fergana valley, there are about 10-12 millions of country people. Catchments of Naryn River and Issyk-Kul Lake together occupy about of 40 % of Kyrgyzstan area. There are four energy-producing reservoirs and one dispositive reservoir (its name is "Toktogul") on Naryn River.

During the term of the Project, the following activities were realized:

- (a) archive of meteorological and hydrological data was analyzed (in some cases it were records from 1897); the prediction of changes in climate characteristics up to 2100 was done using regional models (MAGICC/SCENGEN);
- (b) geological and hydrogeological structure of Naryn river basin and isotope characteristics of mountain glaciations were analyzed by using published information;
- (c) field-works on Toktogul reservoir and on Naryn catchment (up to river head and its tributaries), and monitoring stable isotopes ($\delta^2\text{H}$ and $\delta^{18}\text{O}$) in atmospheric precipitations, in river, reservoir and ground water were done;
- (d) conceptual model of water balance and mathematical model of run-off, which takes into account a snow-melt dynamics, were created (verification of model by isotope and calibration by remote sensing data were done);

Average weighted isotope composition of precipitation is $\delta^{18}\text{O} = -12.3$ и $\delta^2\text{H} = -91$ ‰ for weather station on altitude about 1700 m, and there are significant seasonal variations due to continental climate:

- summer precipitations (June – July – August) are subjected to evaporation, therefore the average composition of summer precipitation is considered with some degree of conventionality $\delta^{18}\text{O} = -9.5$ и $\delta^2\text{H} = -70$ ‰;
- spring (March – April – May in this period maximum of annual precipitations is usually observed) and autumn (September – October – November) precipitations have akin isotope composition $\delta^{18}\text{O} = -11.6$ and $\delta^2\text{H} = -83$ ‰, and $\delta^{18}\text{O} = -11.0$ and $\delta^2\text{H} = -79$ ‰, respectively;
- winter precipitation (December – January – February) have the lightest isotopic composition $\delta^{18}\text{O} = -17.3$ and $\delta^2\text{H} = -130$ ‰ and $\delta^{18}\text{O} = -16.1$ и $\delta^2\text{H} = -120$ ‰ on altitude about 900 m (on level of Toktogul reservoir).

Direct measurement of ice core isotope composition on Nylchek glacier (altitude of ice-tongue is 3300 m and average elevation of ice-catchment area is about 4000 m), which located to east from Toktogul reservoir on watershed of Naryn river, gives average values of $\delta^{18}\text{O} = -16.5$ and $\delta^2\text{H} = -105$ ‰ (Aizen et al., 2001; Mann et al. 2008). These values are noticeable heavier, than snow, not fit on GMWL and significantly shift to left from GMWL. Likely, in winter, water vapor is freezing on the glacier. Water steam should come to watershed from valleys, where it arises due to evaporation from surface Toktogul reservoir and Issyk-Kul Lake. Both ponds stay open during all winter and only in very harsh winter Toktogul reservoir is partially covered by ice.

Fractionation of isotopic composition of river water was sometimes revealed by sampling of Naryn headwater (on altitude about 2800–3200 m). This effect could arise due to partial freezing of water and consists in weighting of ice isotopic composition (and melt-water, which produced from this ice) in comparison with initial composition of precipitations. Likely this process occurs in early spring, when soil and rocks retain negative temperature, therefore rain and snow-melt water is partially freeze on stones during percolation from the surface. Later this ice melts and water with specific isotope composition drip to river. So, at the beginning of summer creeks in upper reaches of Naryn river has light isotopic composition, which is shifted to right from GMWL (on $\delta^2\text{H}$ vs. $\delta^{18}\text{O}$ diagram).

In Issyk-Kul lake catchment (on altitude about 1700–2200 m, where main part of observations were done) monitoring of isotopes detects strong influence of evaporation on water balance in the summer. It is evident from very heavy and fractionated isotopic composition of precipitation and some surface water $\delta^{18}\text{O} > -8.5$ and $\delta^2\text{H} > -60$ ‰. Naturally, as closed pond, Issyk-Kul Lake (1609 m above sea level) has most evaporated $\delta^{18}\text{O} \approx -0.6$ and $\delta^2\text{H} \approx -15$ ‰ and salty (6 g/l) surface water.

The average isotope composition of streams and reservoirs in Naryn river catchment on altitude from 900 to 1800 m above sea level, which was fixed by monitoring and periodic sampling outside monitoring points about 2–3 times in year, is:

- Naryn River before Toktogul reservoir has $\delta^{18}\text{O} = -13.0$ and $\delta^2\text{H} = -93.2$ ‰;
- water in the Toktogul reservoir has $\delta^{18}\text{O} = -13.0$ и $\delta^2\text{H} = -94.4$ ‰ (close to average annual precipitations);
- minor rivers have $\delta^{18}\text{O} = -13.1$ and $\delta^2\text{H} = -94.1$ ‰;
- underground water has $\delta^{18}\text{O} = -14.3$ and $\delta^2\text{H} = -105$ ‰

Interesting that isotope composition of water in Naryn River before Toktogul reservoir is not like to glacier ice in any season and became isotopically heavier in summer. It might not be possible, if ice-melt water gives significant contribution in Naryn river run-off. Therefore, current opinion, that Naryn River has melt-water from glacier, as main source of run-off in summer, apparently, are not correct.

Hydrological model was built to describe Naryn river run-off taking into account follow data and auxiliary constructions. (1) Simulated area has significant altitude scale (mark of water in reservoir is about 900 m, whereas ridges in heads of Naryn river reach 4800 m). Temperature, precipitation and evaporation, which are major factors influencing runoff, in turn are functions of elevation and were calculated in (Kuzmichenok, 2008). (2) Digital model of relief for Naryn catchment area has been created on Shuttle Radar Topography Mission data. These data were verified for errors by original software. (3) Tracing of thalwegs and watersheds was conducted with digital relief model in automatic mode and subsequent manual checking. (4) Naryn River catchment was divided on 500×500 m counting cells, and basins of small rivers were divided on 250×250 m cells.

Hydrological model was designed by using "R" language and Snow-melt Run-off Model paradigm. During computation, type of precipitation was determined for each counting cell and time step. Liquid precipitations (temperature is above 0°C) immediately flow into rivers (not considering time of flat surface run-off). If temperature was below 0°C , then precipitations were "solid" (snow) and they are accumulated in cell. Solid precipitation was thawed in time of positive temperatures. Melting rates were calibrated by actual meteorological, hydrological and remote sensing data. Retardation factor should be used in simulation for describing delay between snow-melt and fall-out maximum in spring, and summer maximum of Naryn river run-off. Time series of data for Toktogul reservoir filling and model GRACE were compared. High correlation between the observed and calculated values was found, assuming lag near 3 months between moment of precipitation fall-out and buildup of water in reservoir.

Joint analysis of isotope data and mathematical simulation shows, that Naryn River run-off has peculiarities, which are interfaced with hydrological conditions and hydrogeological structure of catchment. Naryn River catchment is composed of crystalline and very low permeable rocks, but there are several micro-artesian basins along stream channel (likes string of beads), which are filled with porous sediments. These basins play role of natural reservoirs, which delay water flow and redistribute river run-off in time from April-May on June-July. This creates illusion of growth river run-off from melting glacier.

Thus, on base of isotope and other data analysis conceptual and mathematical model of Naryn river catchment were constructed. It was shown that ice-melt water from glaciers take negligible part in river run-off. Consequently, degradation of glaciers due to climate variation (including completely theirs disappearing) will not influence on run-off, if amount of precipitations stays invariable, that follows from regional climate simulation. Using of GRACE

model allows to create prediction model for run-off for vegetative season and gives preconditions for equitable apportioning of water resources.

REFERENCES

- [1] V.V. Kuzmichenok, *Characteristics and digital models of West Tien-Shan humidification*. Bishkek, 2008, 196 p.
- [2] V.B. Aizen, *Ice-coring, climatic and environmental change research in Tien-Shan, Central Asia*, Ann. Rep. 2000/2001, DOE/INEEL contract BBWI 00000073 R10, U.S. Dep. of Energy, Washington, D.C. 2001, 40 p.

Analysis of 4-Nitrophenol Reduction over Gold Catalysts: Effect of Catalyst Surface

Brenda Acosta¹, Viridiana Evangelista¹, Serguei Miridonov², Andrey Simakov³

¹Posgrado en Física de Materiales, Centro de Investigación Científica y de Educación Superior de Ensenada, C.P. 22860, Ensenada, Baja California, México, ²Departamento de Óptica, Centro de Investigación Científica y de Educación Superior de Ensenada. Carretera Ensenada-Tijuana 3918, Zona Playitas, C.P. 22860 Ensenada, Baja California, México, ³Universidad Nacional Autónoma de México, Centro de Nanociencias y Nanotecnología, Km. 107 Carretera Tijuana a Ensenada, C.P. 22860, Ensenada, Baja California, México.
bracosta@cny.unam.mx

INTRODUCTION

The reduction of 4-nitrophenol into 4-aminophenol becomes one of the most popular reactions to test the catalytic effectiveness of gold catalysts for the reduction of aromatic nitro compounds [1] due to the well-detectable signal of both reagent and product in the UV-Visible spectrum, which makes easier the monitoring of the reaction course via UV-Vis spectroscopy. There is a well-acceptable mechanism for the reduction of aromatic nitro compounds: 1) direct route proceeds via the fast reduction of nitro compound to corresponding nitroso and then to the hydroxylamine compound which is finally reduced to amine compound; 2) second route involves the condensation of the nitroso compound with hydroxylamine compound to azoxy intermediate which is consequently reduced to azo intermediate and to final amine compound [2, 3]. Commonly, activity of catalysts is characterized by the decrease of signal intensity of nitrophenolate ion formed by the reaction of nitrophenol with NaBH₄ [4]. However, the complete analysis of the spectra collected during the reaction is required.

The present paper is devoted to the study of 4-nitrophenol reduction to 4-aminophenol over gold catalysts with different structure of support by a complete analysis of the all experimental spectra collected during the reaction. In order to clarify the evolution of the UV-Vis spectra, the principal component analysis (PCA) [5] method was applied.

EXPERIMENTAL

The catalytic reduction of 4-nitrophenol was carried out in an optical quartz cuvette with 1 cm of pathlength under constant magnetic stirring of reaction media. UV-Vis spectra were recorded in the transmittance mode every 2 seconds using a lab-made set-up including light source (AvaLight- DHS), UV-Visible spectrometer (AVANTES Ava- Spec-2048) and a home-made dark chamber. Before injection of aqueous catalyst suspension (100 μ L, 1.4 mg/mL) the reaction mixture of 4-nitrophenol (300 μ L, 1 mM) and NaBH₄ (3.7 mL, 0.1 M) was stirred during 15 min. To confirm the reproducibility of the activity level the experiments were repeated 3 times. The individual spectral components were resolved by the PCA method from the experimental UV-Vis spectra collected during the reaction.

RESULTS AND DISCUSSION

Typical experimental UV-Vis spectra for Au/CeO₂ catalysts with low and high surface area are presented in Fig. 1. In case of catalyst with low surface area in the course of the reaction the peak at 400 nm attributed to the 4-nitrophenolate ion decreased while the peak at 300 nm attributed to the 4-aminophenol raised (See Fig. 1-left). The intensity of the last peak correspond to the final concentration of 4-aminophenol. Reaction was well-described by a first-order rate law with respect to 4-nitrophenolate ion consumption. However, in case of catalyst with high surface area consumption of 4-nitrophenolate ion at the start of the reaction was accompanied with the appearance of a new intensive peak at 310 nm which decreased in intensity during the reaction. At the end, peak at 300 nm of 4-aminophenol was finally observed (See Fig. 1-right).

A new spectrum characterized by two intensive peaks at 265 and 310 nm and by less intensive peak at 485 nm was revealed by PCA from the experimental spectra (see insertion in Fig. 1-middle). This spectrum cannot be attributed to the 4-aminophenol formation for two main reasons: 1) spectrum of 4-aminophenol is characterized with one peak centered at 300 nm; and, 2) according to molar extinction coefficient for 4-aminophenol ($\epsilon = 125 \text{ M}^{-1} \text{ cm}^{-1}$),

intensity of spectrum should be at least 10 times less intensive compared to that for 4-nitrophenolate ion, as was shown for catalysts with low surface area.

The appearance of this new spectrum for catalysts with high surface area could be related with the formation of some intermediary compound to be stabilized on the catalyst surface. The adsorption of 4-nitrophenol and 4-aminophenol on the catalysts did not result in the appearance of a new spectrum, while adsorbed 4-nitrophenolate ion showed a new spectrum similar to the spectrum of 4-aminophenol at 300 nm but with a ϵ equal to $10,000 \text{ M}^{-1} \text{ cm}^{-1}$. Based on the literature, it was found that this new spectrum revealed by PCA is similar in shape and position to the spectrum for an azo compound in its *trans* and *cis* forms [6].

The appearance of azo intermediary compound corresponds to the condensation route of aromatic nitro compounds reduction. High surface area of Au catalysts seems to promote the accumulation of intermediaries (nitroso and hydroxylamine compounds) and their mutual interactions with formation of the condensation products.

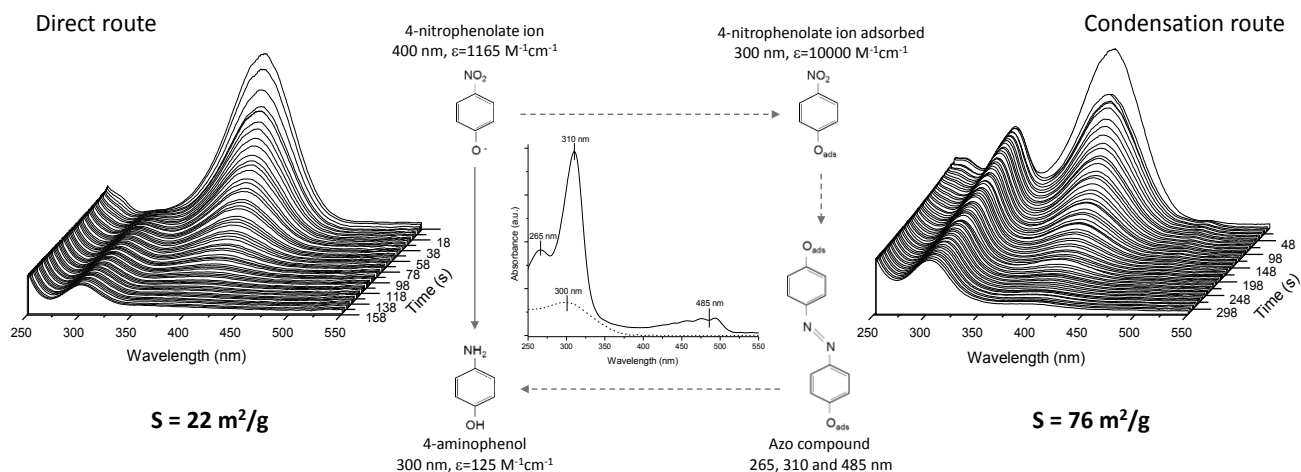


Fig. 1. UV-Vis absorption spectra collected *in situ* during the reduction of 4-nitrophenol over Au/CeO₂ catalysts with different surface area: low surface area (left) and high surface area (right). The routes of 4-nitrophenol reduction to 4-aminophenol are shown in the middle (direct route is marked with straight arrow while condensation route is marked with dotted arrows). Insert presents the UV-Vis spectrum found for 4-nitrophenolate ion adsorbed (dotted line) and for the intermediary azo compound revealed by PCA method (straight line).

CONCLUSIONS

Remarkable effect of the support structure on the catalytic performance of Au catalysts in the reduction of 4-nitrophenol was found. The preferable formation of 4-aminophenol via condensation route was induced by the high efficiency of catalyst support to adsorb reaction components.

ACKNOWLEDGMENT

The authors would like to thank O. Callejas, M. Vega, E. Flores, F. Ruiz, J. Peralta and M. Sainz for technical assistance. This research project was supported partly by CONACyT (Mexico) and PAPIIT-UNAM (Mexico) through grants 179619 and 203813, respectively.

REFERENCES

- [1] K. Kuroda, T. Ishida, M. Haruta, *J. Mol. Catal. A: Chem.* 298, 7–11 (2009).
- [2] F. Haber, *Z. Elektrochem.* 22, 506 (1898).
- [3] A. Corma, P. Concepción, P. Serna, *Angew. Chem.* 119, 7404-7407 (2007)
- [4] P. Veerakumar, M. Velayudham, K.-L. Lu, S. Rajagopal, *Appl. Catal. A. Gen.* 439-440, 197-205 (2012).
- [5] F. G. Halaka, G. T. Babcock, J. L. Dye, *Biophys. J.* 48, 209-219 (1985).
- [6] T. Ide, Y. Ozama, K. Matsui, *J. Non-Cryst. Sol.* 357, 100-104 (2011).

Synthesis of Plant-Derived Virus-Like Particles and his Potential Use as Vector

Rubén Darío Cadena-Nava
Centro de Nanociencias y Nanotecnología
Universidad Nacional Autónoma de México
rcadenacnyn.unam.mxt

ABSTRACT

The Cowpea Chlorotic Mosaic Virus (CCMV) is a nanoparticle of 28 nm of diameter; it consists of a capsid made up of 180 identical proteins that protects the genome (ssRNA of 3000 nts). Virus-like particles (VLPs) can be synthesized by self-assembly of capsid protein (CP) of CCMV around heterologous RNA molecules of different lengths from 100 to 12,000 nts, as well as from anionic polymers, quantum dots, and enzymes. This capacity to package a wide variety of cargoes can be used for deliver DNA, interfering RNA and metallic nanoparticles. Besides, the VLPs can be used as nanocontainers and nanoreactors when an enzyme is encapsidated. Our recent experiments show that the plant virus capsid can be used like vector for transfection of mammalian cells.

Kinetic study of water absorption in plant germination while using MWCNT as a growth promoter

D. K. Tiwari¹, N. Dasgupta-Schubert², L. M. Villaseñor Cendejas³

¹Centro de Nanociencias y Nanotecnología, Universidad Nacional Autónoma de México, Apdo. Postal 356, Ensenada, B.C. 22800, México, ²Instituto de Física y Matemáticas, ³Instituto de Investigaciones Químico-Biológicas, Universidad Michoacana de San Nicolás de Hidalgo, Cd. Universitaria, C. P. 58040 Morelia, Michoacán, México
dktpy@cyn.unam.mx

ABSTRACT

Water is one of the most important substances on earth. All plants and animals must have water to survive. Water molecule plays an important role in the life of Plants. Water helps to; germination of seeds, photosynthesis, the transport of nutrients and the maintenance of plant structure by providing the appropriate pressure to the plant tissue. It also affects the strength, permeability, and thermal stability of all plants. In the life of Plants, the water content should also be controlled at a proper level. Therefore, study on the interaction between water and plant cells is of great importance both in theory and in application. The absorption of water into the grains during germination is influenced by the soaking of water from the mediums. From an engineering point of view, one is interested not only in knowing how fast the absorption of water can be accomplished, but how it will be affected by processing variables such as supporting medium, temperature and also how to predict the soaking time under given conditions. In 1988, Peleg proposed a two parameter based sorption equation to calculate the water Adsorption of food products. The equation is shown below (Eq. 1);

$$M_t = M_0 + \frac{t}{K_1 + K_2 t}$$

$$\frac{1}{(M_t - M_0)} = K_1 \left(\frac{1}{t} \right) + K_2 \dots\dots\dots (\text{eq 1})$$

K₁=Peleg Rate Constant (t⁻¹), K₂= Peleg Capacity Constant (%⁻¹), M_t= Moisture Content at time t (%), M₀=Initial Moisture Constant (%), T= Time (Day)

In the present work, the kinetics of the water absorption has been studied during germination and the mathematical modeling is important to design and optimize the process during germination time. We studied the germination of maize plant with different growth mediums (control and MWCNT 20 mg/l) and the water absorption kinetics has been analyzed during time period of 7 days. The water content had been calculated physically by extraction of fresh and dry weight measurement of the growth systems (Figure 1). Peleg’s model was successfully applied to experimental data and the corresponding parameters were obtained and correlated with germinating medium. Peleg’s equation is based on non-exponential model and its parameters are in hydration kinetics that applied to weight gain during rehydration. The results shows that MWCNT germinated plants MWCNT not only promotes the water supply but also a continuous supply of water in plants during germination while for control system it is random.

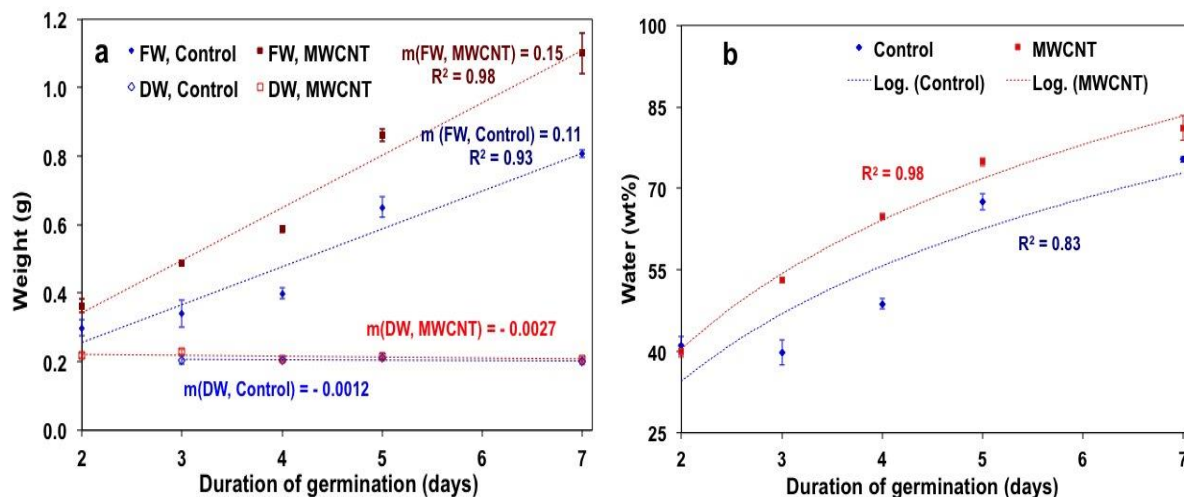


Figure 1: Variation of growth indices with duration of germination of maize seedlings grown in BA with/without 20 mg/l MWCNT. (a) Fresh weight (FW) and dry weight (DW). The dotted lines are the linear regression fits with the slopes (m) and correlation coefficient (R²) values as shown. (b) % Water intake. The dotted lines are the logarithmic fits.

Study of nanoparticles size distribution by acoustic method

Kalashnikov Sergei, Nomoev Andrei, Romanov Nikolai, Damdinov Bair
Buryat State University, Ulan-Ude, Russia
betch_kail@mail.ru

ABSTRACT

In recent years strengthening of interest to positioning micro and nanoparticles on surfaces, to their use for modifying of known materials and creation of the new is observed.

Modern methods of division of particles are based on density and size difference (the size-selective sedimentation, Brownian diffusion and use of a vibration segregation), on a difference of superficial properties (a highly effective liquid chromatography), on a charge difference depending on the size (gel electrophoresis), on a difference of a dielectric constant in connection with the size of particles, and as on an acoustic impedance (ultrasonic division).

As for acoustic division, it is a new and perspective method; however, use of this way for nanodimensional systems is still insufficiently studied. The first mentions of use of microfigures of Chladni for division of nanodisperse materials contain in [1]. Encouraging results on division of nanopowder of dioxide of silicon by an acoustic method are received in [2].

Classical way of visualization of standing fluctuations – putting any powder (usually sand) on a surface of the plate making cross fluctuations under the influence of, for example, bow of a violin. Thus powder forms the picture known under the name of figures of Chladni, which were open for them in 1787. Now this technique became standard school experiment [3]. Is much less known that very small powder accumulates in the antinodes surface fluctuations?

Formation of figures on flexible plate – the main example of influence of two forces – forces of Newton and Stokes's strength: Newtonian forces tend to form Chladni's classical figures, while Stokes's strengths tend to form Chladni's return figures.

Property of figures of Chladni spatially to divide particles into two fractions, various by the size, and is used in an acoustic method of division of particles. The main results of direct numerical modeling (are taken from [4]) are given in this article.

Results of modeling are the following. If modeling is executed with gold particles, their movement Newtonian forces operate. Because of fluctuations of a plate of a particle start jumping up and consecutive jumps tend to increase kinetic energy of particles. However, in nodal lines at a plate zero speed and collisions with it reduce kinetic energy of particles. As a result, since all 80000 particles which have been uniformly distributed on a plate in modelled system, within several seconds the majority of them accumulated in nodal lines, forming Chladni's standard figures.

Now we reduce density of particles to 20 kg/m³, holding constant diameter. It leads to Stokes's strength, which almost in thirty times more, than the gravitational force operating on a particle. These easy particles move in antinodes and form Chladni's forming division of particles by the sizes the inverse figures as the mass of particles depends on their size

REFERENCES

- [1] Acikalin T., Bietsch A., Dorrestijn M., Gerber Ch., Hegner M., Meyer E., Raman A. Phys. Rev. Let. **98**. 26102 (2007).
- [2] Kalashnikov S., Lygdenov V., Nomoev A., Romanov N. Actual problems of the Humanities and Natural Sciences. **8**. 21 (2012).
- [3] Stockmann H.-J. Ein Nomade der Wissenschaft // Physik Journal. **5**. 47 (2006).
- [4] Van Gerner H.J. Newton vs Stokes: competing forces in granular matter. – Enschede, 2009.

Reactions of Protonated Layered Titanates for Synthesis of Nanomaterials

Liliia D. Abdulaeva, Irina A. Zvereva
 Institute of Chemistry, Saint Petersburg State University,
 26 Universitetskiy pr., Petrodvorets, Saint Petersburg, 198504, Russia
 Lilian_chem@mail.ru

ABSTRACT

Layered perovskite-like oxides from the time of their discovery have attracted great attention due to their unique physicochemical properties, such as high ionic conductivity, catalytic and photocatalytic activity. There is increasing demand of development methods for obtaining such compounds with specified composition and structure by reason of the growing role of these compounds in technology and industry. Using the methods of “soft chemistry” we can create materials with different particle morphology by a sequence of low-temperature topochemical synthesis.

In this work, layered perovskite-like oxides $ALnTiO_4$ и $A_2Ln_2Ti_3O_{10}$ ($A = H, Na, K; Ln = La, Nd$) were used as precursors for the “soft chemistry” synthesis to create compounds with improved photocatalytic properties. Characterization by SEM, powder XRD, powder thermal XRD, TGA and STA have been performed for the determination of the structure, content and stability of synthesized oxides.

The thermal stability range of the protonic compounds $HLnTiO_4$ ($Ln = La, Nd$), thermal effects accompanying the decomposition processes were determined and were characterized all areas of mass loss on the TGA curves. It was found that due to the loss of stability of the protonic forms $HLnTiO_4$ can be obtained following perovskite-like compounds:

- Cation-deficient perovskites $Ln_{2/3}TiO_3$ ($Ln = La, Nd$) for the first time have been obtained by leaching of Ln^{3+} ions in acid solution. Obtained samples did not save the morphology of the initial layered oxides $HLnTiO_4$ and consist of irregularly shaped particles of intergrown crystals with sizes less than 100 nm.
- Hydrated metastable compounds $Ln_2 \square Ti_2 O_7 \cdot y H_2 O$ and defective layered compounds $Ln_2 \square Ti_2 O_7$ have been obtained by topochemical dehydration without change of morphology.

It was discovered exfoliation process of protonic form $HLnTiO_4$ и $H_2Ln_2Ti_3O_{10}$ ($Ln = La, Nd$) by treatment in $VOSO_4$ solution. The morphology of exfoliated nanostructured $(VO)_x H_{1-2x} LnTiO_4 \cdot y H_2 O$ и $(VO)_x H_{2-2x} Ln_2Ti_3O_{10} \cdot y H_2 O$ significantly changes compared with the morphology of the initial compounds. $VOSO_4$ causes exfoliation and reassembling of initial protonic oxides. Exfoliated particles are made up of interconnected flat crystallites with thickness below 10 nm. If $NaLnTiO_4$ и $K_2Ln_2Ti_3O_{10}$ were treated by vanadyl sulfate under same conditions, it was obtained partially exfoliated compounds where some of the particles with layered structure while other part of particles undergoes exfoliation and self-assembly.

Opportunity of using layered perovskite-like titanates for “soft chemistry” synthesis by topochemical reactions are discussed in comparison with results of sol-gel and hydrothermal method.

ACKNOWLEDGMENTS

Powder X-ray study was carried out in the X-ray Diffraction Centre, SEM study – in the Interdisciplinary Resource Center for Nanotechnology, TGA and STA – in Center for Thermogravimetry and Calorimetry of Saint Petersburg State University. This work has been supported by the RFBR (Grant 12-03-00761) and SPbSU grant № 12.0.105.2010.1.

Protonation and hydration of layered perovskite-like titanates and niobates

I.A. Rodionov, A.A. Burovikhina, T.D. Utkina, E.V. Mechtaeva, M.V. Chislov, I.A. Zvereva
Institute of Chemistry, Saint Petersburg State University,
26 Universitetskiy pr., Peterhof, Saint Petersburg, 198504, Russia
i.rodionov@chem.spbu.ru

ABSTRACT

Layered perovskite-like oxides are crystalline compounds in which two-dimensional perovskite slabs are interleaved with layers of other structure. Complex oxides $A_2Ln_2Ti_3O_{10}$ and $ANdNb_2O_7$ ($A = Li, Na, K, Rb, Cs$) belong to the three-layer Ruddlesden-Popper phases and the two-layer Dion-Jacobson phases, respectively. Such materials are interesting because of their high ionic conductivity and photocatalytic activity, particularly in the reaction of water splitting with hydrogen production. Alkaline forms of layered perovskite oxides are able to undergo protonation (substitution of cations to protons) and hydration (introduction of water molecules into the interlayer space) when exposed to aqueous solution or humid atmosphere [1]. These processes can significantly influence the physico-chemical properties, and should not be neglected when investigating them.

Complex oxides $A_2Ln_2Ti_3O_{10}$ ($A = Li, Na, K, Rb; Ln = La, Nd$) were prepared by solid state synthesis in the temperature range of 1100 – 1200°C in air at atmospheric pressure, according to following reaction:



For the niobates $ANdNb_2O_7$, only the Rb- and Cs-containing compounds could be obtained in this way. Other members of the series ($A = Li, Na, K$) were prepared by ion-exchange in a melt of alkali metal nitrate, because of their instability at high temperature. Suspensions of obtained compounds were prepared by adding the powdered samples to distilled water. These suspensions were kept under constantly stirring for certain periods of time, then the samples were centrifuged and dried. The summary protonation/hydration process occurring under contact with aqueous medium in the case of titanates can be described as:



The phase composition and structural parameters of the raw materials and the obtained samples were monitored by XRD analysis. To determine the degree of protonation and the amount of intercalated water thermogravimetric analysis (Netzsch TG 209 F1 Iris) was used [2].

As a result, the interaction characteristics of layered oxides with water were determined. The composition and structure of the hydrated and protonated forms were calculated. Among titanates the only relatively stable oxides under these conditions were found to be $Li_2Ln_2Ti_3O_{10}$. Sodium, potassium and rubidium-containing forms undergo partially substitution of interlayer alkali metal cations for protons. This process is accompanied by the introduction of water molecules in the interlayer space. Thus, these materials exist in aqueous solution in the form of compounds with general formula $H_xA_{2-x}Ln_2Ti_3O_{10} \cdot yH_2O$. In the case of niobates the presence of intercalated water was found only in the structure of Na-containing oxides. XRD and TGA showed the existence of stable forms of intercalated $NaNdNb_2O_7$ compounds in different temperature ranges and determined the content of water in each form. The protonation process of niobates takes place only in acidic solution.

ACKNOWLEDGMENT

The results were obtained with the support of SPbU resource centers "Research Centre for X-ray Diffraction Studies" and "Research Center of Thermal Analysis and Calorimetry". The authors acknowledge Saint Petersburg State University for a research grant 12.0.105.2010, and Russian Foundation for Basic Research (grant 14-03-31968).

REFERENCES

- [1] I. A. Rodionov, O. I. Silyukov, T. D. Utkina, M. V. Chislov, Yu. P. Sokolova, I. A. Zvereva, Russian Journal of General Chemistry, **82**, 1191-1196 (2012).
- [2] Silyukov O., Chislov M., Burovikhina A., Utkina T., Zvereva I., Journal of Thermal Analysis and Calorimetry, **110**, 187-192 (2012).

Zirconia nanoparticles with different composition, size and morphology, synthesized under hydrothermal conditions, and their properties

Bugrov A.N.^{1,2}, Rodionov I.A.¹, Smyslov R.Yu.², Almjasheva O.V.^{3,4}, Zvereva I.A.¹

¹Institute of Chemistry, Saint Petersburg State University; ²Institute of Macromolecular Compounds of RAS; ³Ioffe Physical-Technical Institute RAS; ⁴Saint Petersburg Electrotechnical University "LETI".
alexander.n.bugrov@gmail.com

ABSTRACT

On the one hand, zirconia is a very promising basis for the creation of modern functional materials, thanks to a set of unique characteristics. On the other hand, it is known that the properties of the substances in the nanoscale state change appreciably, and new effects often occur. Moreover, the particle size, their structure and morphology are very sensitive to the methods and conditions of synthesis. Therein, method of hydrothermal synthesis is of interest because the possibility of varying the large number of parameters (temperature, pressure, duration of isothermal exposure and composition of hydrothermal media) allows obtaining nanomaterials with desired structural characteristics. In this regard, the aim of the work was an integrated study of the influence of hydrothermal synthesis conditions on the size and morphology of nanoparticles based on ZrO_2 , as well as the definition of the functional characteristics of the nanoobjects obtained.

In this work, the spherical nanoparticles based on zirconia and its solid solutions with oxides of rare-earth elements were obtained by precipitating of $ZrO(OH)_2$ and mixtures $ZrO(OH)_2-ReOOH$ ($Re=Y, Eu, Tb, Sm$) from solutions of the corresponding chlorides followed by their dehydration in the hydrothermal treatment process. According to X-ray diffraction and electron microscopy of ZrO_2 nanoparticles and of its solid solutions with lanthanides, the zirconia-based crystallites are a mixture of tetragonal and monoclinic polymorphous modifications in a ratio 80:20, the average diameter of particles is $15\div 20$ nm. Introduction of 3 mol.% Y_2O_3 leads to stabilization of *t*- ZrO_2 nanoparticles and size reduction to 10 ± 2 nm, besides the specific surface area increased from 87 to 107 m^2/g .

Variation of the pH value of the hydrothermal solution and an increase in the synthesis temperature leads to the crystallization only ZrO_2 monoclinic polymorphous modification and change shape of nanoobjects formed during the synthesis. It was found that hydrolysis of $ZrOCl_2\cdot 8H_2O$ in the acid-alcohol mixture at pH=3 leads to the formation of hollow spheres with size of $300\div 700$ nm, wall thickness of 50 ± 10 nm and a specific surface area of 140 m^2/g . Using the 1M NaOH (pH=14) solution as hydrothermal media allows to obtain ZrO_2 nanorods with a diameter of 50 ± 5 nm and a length of 200 ± 40 nm at the synthesis temperature of 200°C. The specific surface area thus significantly reduced to 17 m^2/g . Hydrothermal treatment of $ZrOCl_2\cdot 8H_2O$ at 240°C and pH=2 in the presence of sodium acetate (CH_3COONa), leads to the formation of ZrO_2 star-like nanostructures with size ~80 nm and the specific surface area of 121 m^2/g .

According to electron microscopy and X-ray analysis, it was found that mesoporous hollow microspheres, star-like and rice-grain-like zirconia nanostructures are the agglomerates composed of *m*- ZrO_2 crystallites with an average size of 1 ± 5 nm.

The obtained nanoparticles based on ZrO_2 investigated as photocatalysts for the process of hydrogen evolution from aqueous suspensions irradiated with UV light. Investigation of the kinetics of hydrogen evolution was performed on the original installation comprising a photocatalytic cell equipped with a radiation source, a magnetic stirrer and a gas circulation system with access to the chromatograph [1]. Optical band gap of ZrO_2 nanoparticles with different composition, size and morphology were determined based on diffuse reflection spectra. It was shown that the photocatalytic activity of zirconia nanoparticles depends on the crystallite size and specific surface area; at the same time, the change of a band gap by introducing lanthanide ions (Eu^{3+} , Tb^{3+} , Sm^{3+}) into the ZrO_2 crystal lattice [2] practically does not affect on the amount of hydrogen generated (Fig. 1).

Nanoparticle dispersions of ZrO_2 (1 mol.% Eu_2O_3), ZrO_2 (1 mol.% Tb_2O_3) and ZrO_2 (1 mol.% Sm_2O_3) solid solutions in ethanol were investigated by fluorescent spectroscopy. It was shown that nanoparticles of ZrO_2 solid

solutions with lanthanides in the luminescence bands have the narrow lines located in different regions of the visible spectrum (Tb – green area, Eu and Sm – red ones), which are splitting in the crystal field on the energy levels of the Tb^{3+} , Eu^{3+} , Sm^{3+} ion in the zirconia matrix (fig 2). Lanthanide complexes can acquire unique magnetic and spectroscopic properties due to ligand field splitting of the multiplets.

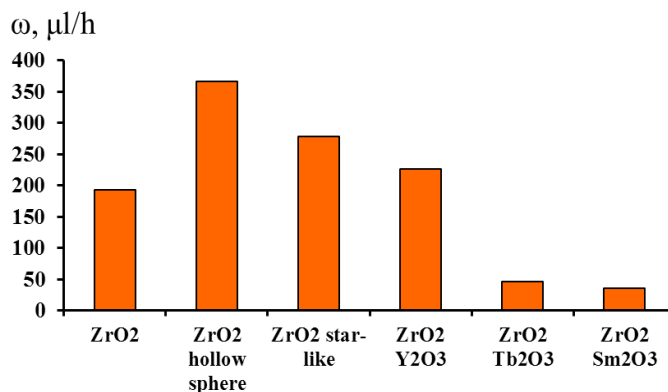


Fig. 1. Rate of hydrogen evolution from aqueous suspensions of ZrO_2 -based photocatalyst under UV-irradiation.

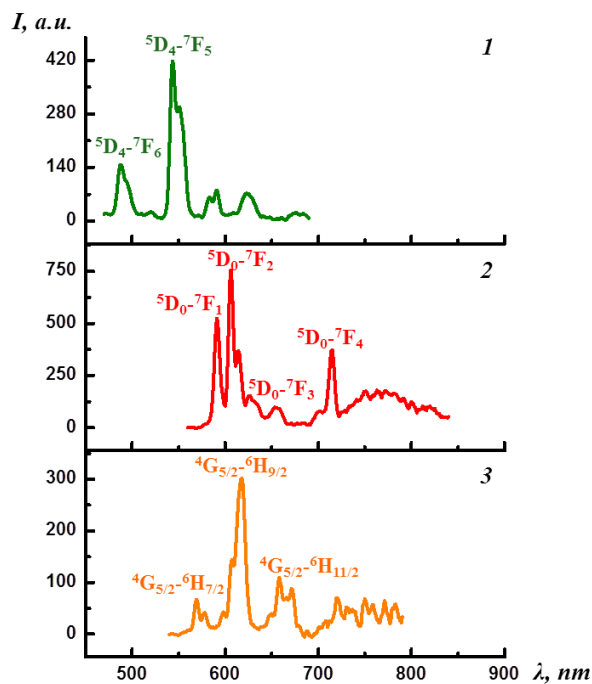


Fig. 2. The luminescence spectra of the nanoparticle dispersions of ZrO_2 solid solutions with lanthanides in ethanol at $\lambda_{excitation} = 228$ nm: 1 - ZrO_2 (1 mol.% Tb_2O_3), 2 - ZrO_2 (1 mol.% Eu_2O_3), 3 - ZrO_2 (1 mol.% Sm_2O_3).

ACKNOWLEDGMENTS

This work was supported by the Russian Foundation for Basic Research (grant № 14-03-31722) and grant SPbSU 12.38.257.2014

REFERENCES

- [1] A.I. Gavrilov, I.A. Rodionov, D.Yu. Gavrilova, I.A. Zvereva, B.R. Churagulov, Yu.D. Tret'yakov, Doklady Chemistry. V. 444. 2012. № 2. P. 133-136.
- [2] W. Du, Z. Zhu, X. Zhang, D. Wang, D. Liu, X. Qian, J. Du, Materials Research Bulletin. V. 48. 2013. P. 3735–3742.

KKR-CPA study of hydrogen induced phase transitions in disordered Ti-V-Cr alloys

O.O. Bavrina, M.G. Shelyapina

Department of Nuclear-Physics Research Methods, St. Petersburg State University,
198504, Ulyanovskaya 3, Peterhof, Russia
st036188@student.spbu.ru

INTRUDUCTION

Materials for hydrogen storage and transportation have been extensively studied lately in the view of the growing interest for hydrogen energetics, and derivative problems concerning corresponding infrastructure. In search of acceptable hydrogen storage compounds, many criteria should be taken into account, namely stability, hydrogen absorption capacity, synthesis complexity and more. It has been experimentally shown, that some transition metals (Ti, V, Cr) alloys tend to have considerable hydrogen absorption capacity and stability at wide range of temperatures. Moreover, Ti-V-Cr nanoparticles added to Mg essentially accelerate its hydrogen sorption kinetics.

Recent *in situ* neutron diffraction experiments [1] have shown that upon hydrogenation a bcc-to-fcc structural transition occurs. Thus, the process observed requires theoretical and numerical substantiation. However, any theoretical or modelling approach to disordered alloys is very complex compared to that to ordinary hydride structures, as the crystalline structure of said compounds contains chaotically positioned dislocations, and the bulk potential, periodic for ordinary structures, can be thought of as periodic only to a certain extent when it comes to disordered alloys.

As many, *ab initio* methods for material structural study imply knowing the exact structure of the primitive, or some super-cell of the crystalline lattice, there are very few methods allowing evaluation of the crystal total energy. Korringa-Kohn-Rostoker method combined with coherent potential approximation (KKR-CPA) as implemented in SPR-KKR framework has been used for calculations [2]. Here we report on the results of our theoretical study of hydrogen distribution over interstitial sites of the metallic lattice and hydrogen induced phase transitions in disordered Ti-V-Cr alloys.

CALCULATION PROCEDURE

The KKR-CPA procedure was common for all types of experiments. The total energy was calculated using the spin-polarised Korringa-Kohn-Rostoker method combined with coherent potential approximation within the SPRKKR framework. The electron charge density and the crystal potential are assumed to be spherically symmetrical within muffin-tin spheres and constant in the interstitial region. The radii of muffin-tin spheres were chosen in such a manner that, on the one hand not to overlap and on the other to improve the fitting of the Wigner-Seitz volume. The s-, p- and d-valence states were taken into account.

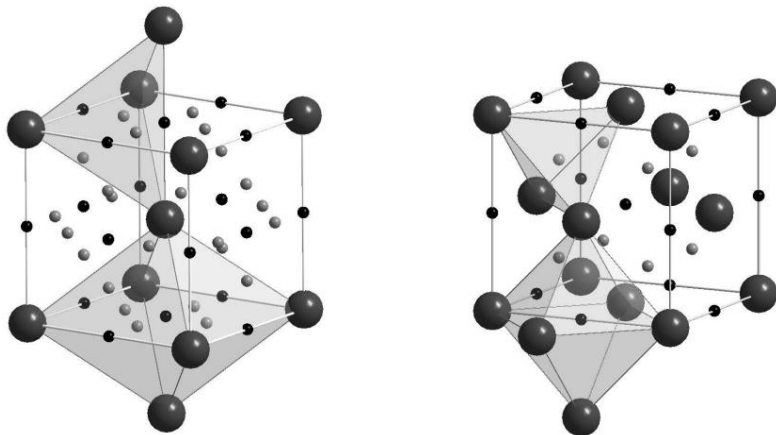


Fig.1 Octahedral and tetrahedral interstices in bcc (left) and fcc (right) lattice.

RESULTS AND DISCUSSION

It was earlier showed, that Ti-V-Cr alloys can be found in bcc or fcc crystalline structure depending on conditions [1,3]. For both structures, two types of interstitial hydrogen locations are possible- octahedral and tetrahedral sites (see Fig. 1). In the first part of the study, the KKR-CPA method was applied to find out which interstitial sites are preferable. In the second part, the MH_x crystals (arranged based on the obtained results) the total energies were compared, and the conclusion about phase transformation was made, where x is in the range from 0 to 2.

First of all for each of bcc and fcc structures, where the crystalline state is defined by a single structural parameter, the total energy of alloys was computed versus the lattice constant a . In order to determine the equilibrium lattice constant, up to 9 data points were fitted using fourth-order polynomial relations. An example of such data set along with fitting curve is shown in Fig. 2.

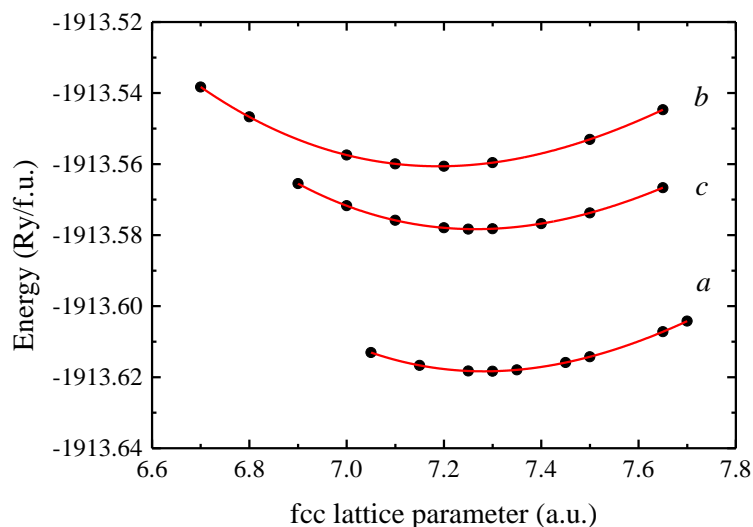


Fig. 2. Comparison of total energy for fcc $TiV_{0.8}Cr_{1.2}$ hydride with H/M ratio equal to 0.5. Hydrogen occupies tetrahedral sites (a), octahedral sites (b), equally distributed between octahedral and tetrahedral sites (c).

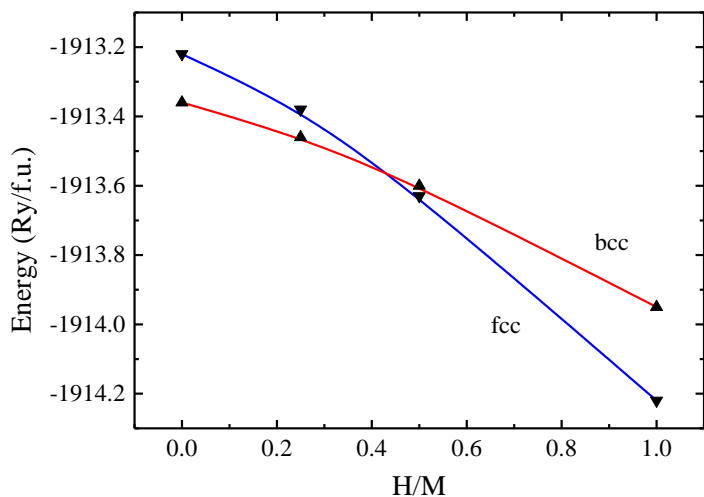


Fig.3. Total energy of $TiV_{0.8}Cr_{1.2}H_x$ versus hydrogen to metal atom ratio for fcc lattice with hydrogen in tetrahedral sites and bcc lattice with hydrogen in octahedral sites.

A number of hydrogen concentrations have been studied in order to find out the preferable hydrogen localization, so that the total hydride formulae were $MH_{0.5}$, MH_1 and MH_2 . In each case different cases were studied: H totally localized in tetrahedral sites, H totally localized in octahedral sites, and a 50/50 case.

In the second part of the study, the total energy was computed depending on H concentration for fcc and bcc hydride lattices, so that the phase transition was detected, based on the results of the first part.

The structural study of the first part was conducted in the range of H concentration from 0 to 2 for fcc lattice, and from 0 to 0.5 for bcc lattice. Further increase of hydrogen concentration in bcc hydride results in KKR method convergence deterioration, which causes namely severe increase of computational experiment time. This is supposed to be an additional evidence of such hydrides instability.

First of all, a conclusion can be made, that tetrahedral hydrogen pores are most preferable for FCC hydride structure, and octahedral pores are preferable for BCC structure (highlighted data corresponds to the lower energy case). This result corresponds to one earlier obtained, and is valid also for other metal compositions [1]. This could be due to excess of tetrahedral H positions in BCC lattice (12 for 1 primitive unit cell), so that at high concentration the hydrogen atoms are located too close to each other for the matter to be stable

The other conclusion is that the bcc-to-fcc phase transition takes place at rather low hydrogen concentrations, less than ratio $H/M = \frac{1}{2}$. Fig.3 shows the total energy traces for fcc and bcc hydrides plotted versus hydrogen concentration for a selected alloy.

REFERENCES

- [1] S. Miraglia, D. Fruchart, N. Skryabina, M. Shelyapina, B. Ouladiaf, E.K. Hlil, P. de Rango and J. Charbonnier. Hydrogen-induced structural transformation in $TiV_{0.8}Cr_{1.2}$ studied by in situ neutron diffraction. *J. All. Compd.* 442 (2007) 49–54.
- [2] The Munich SPR-KKR package, version 6.3, H. Ebert et al, <http://ebert.cup.uni-muenchen.de/SPRKKR>; H. Ebert, D. Ködderitzsch, J. Minár. Calculating condensed matter properties using the KKR-Green's function method—recent developments and applications. *Rep. Prog. Phys.* 74 (2011) 096501-1-48.
- [3] M.G. Shelyapina, V.S. Kasperovich, N.E. Skryabina, D. Fruchart. Ab initio calculations of the stability of disordered Ti-V-Cr solid solutions and their hydrides. *Phys.Sol. State* 49 (2007) 399–402.

First-principles estimation of hydrogen diffusion coefficient in magnesium

Konstantin Klyukin¹, Marina G. Shelyapina¹ and Daniel Fruchart²

¹Faculty of Physics, St. Petersburg State University, Ulyanovskaya 1, Petrodvorets, St. Petersburg, 198504 Russia

²Institut Néel, CNRS, 25 avenue des Martyrs, BP 166, 38042 Grenoble Cedex 9, France
konstantin.klyukin@gmail.com

INTRODUCTION

Hydrogen diffusion in solids is a topic of great scientific interests. This topic has a fundamental importance for understanding the properties of metal-hydrogen systems and practical application for the development of hydrogen storage materials. Due to high hydrogen capacity and low cost one of the most attractive material for hydrogen storage is magnesium. However, applications of pure MgH₂ are limited by a high temperature of hydrogen release and slow sorption kinetics. It was found that a limited dissociation rate of hydrogen on the magnesium surface may be improved by additions of transition metals catalyst. Investigations by means of in situ X-ray [1] and neutron [2] diffraction of Mg/Nb thin films and nanocrystallites have shown that hydrogen penetrates within Mg through Nb “gates”. Nevertheless, the role of the interface border between Mg and TM remains unclear. In our previous theoretical investigations [3] of Mg/Nb thin films we have found that Nb additives stabilize the Mg bcc structure on interface border. In addition, we have studied H-induced [4] transitions in Mg upon the hydrogenation.

In this contribution, we are focused on studying of hydrogen mobility in magnesium. Hydrogen diffusion rate through magnesium metal determines the rate of sorption kinetics. Thus, the investigations of interstitial hydrogen diffusion may explain the catalytic effect of transitional metals additions. The aim of this work is to present the results of ab initio calculations of hydrogen diffusion in different structures of magnesium, which may occurs near the Mg/Nb interface border upon the hydrogenation.

METHODS

The calculations were performed within the framework of periodic density functional theory (DFT) using the plane-wave pseudo-potential method and the Perdew–Burke–Ernzerhof GGA exchange and correlation potential as implemented in Quantum Espresso package [5]. For all calculated structures, the lattice parameters and the atomic positions were optimized. The charge and the kinetic energy cut-off were equal to 70 Ry and 260 Ry, respectively. For all investigated structures a total number of 12 x 12 x 12 k-points in irreducible Brillouin zone, was used for.

Following ref [6], the interstitial diffusion coefficient can be written as

$$D = nL^2\Gamma \quad (1)$$

where n is the numerical coefficient whose value depends on the location of the interstitial positions, L is the length of a jump projected onto the diffusion direction, Γ denotes the jump rate between the neighbouring sites. We were interested to effective temperatures ranging in between room temperature and that of hydrogen release and there the phonon energy $h\nu$ is always larger than kT . Under this conditions the jump rate can be written as [7]

$$\Gamma = \frac{k_B T}{H} \exp\left[-\frac{\Delta E + \Delta ZPE}{k_B T}\right], \quad (2)$$

that leads to the following expression for the diffusion coefficient for one-step migration pathway:

$$D = nL^2 \frac{k_B T}{h} \exp\left[-\frac{\Delta E + \Delta ZPE}{k_B T}\right]. \quad (3)$$

Here ΔE is the activation barrier value and ΔZPE is the difference in zero-point energies (ZPE) between the ground and transition states. It worth noticed that all energy values are given per Mg atom.

In the case of not direct hydrogen migration with a local metastable minimum along the diffusion path H atom can equilibrate in metastable site before another jump occurs. We assume that the distribution of hydrogen atoms between adjacent stable and metastable interstitial sites is governed by a local thermodynamic equilibrium. Within

this assumption according to Ref. [8] we have obtain the following equation for hydrogen diffusion between two tetrahedral sites via metastable octahedral one in fcc-Mg lattice

$$D_1 = D \left(1 + \frac{1}{2} \exp \left[-\frac{\Delta E_{tet-oct}}{k_B T} \right] \right)^{-1} \quad (4)$$

Here D is the diffusion coefficient for direct transition between tetrahedral site in fcc-Mg lattice and $\Delta E_{tet-oct}$ is the difference in the total energy between hydrogen in tetrahedral and octahedral sites.

To locate the minimum energy path (MEP) for hydrogen where the forces perpendicular to the path vanish, the nudged elastic band (NEB) method was applied. The configuration with the maximal energy along the MEP was obtained via climbing image implementation of the NEB method. Then the activation barrier was found as the difference between the optimized transition state and the ground state. To determine the activation barrier more accurately, we took into account ZPE contributions, estimated by calculating the phonon frequencies within the framework of the linear-response method. The ZPE contributions were obtained by summing up the zero-point vibrational energies of normal modes.

RESULTS AND DISCUSSIONS

We considered three possible structures of MgH_x , which should occur at low hydrogen concentration [4]: hcp- MgH_x , bcc- MgH_x and fcc- MgH_x . First, for each structure the preferable hydrogen site – octahedral or tetrahedral – was determined (we considered a single H atom in the empty Mg lattice) and then the activation energy of hydrogen migration between two neighbouring sites and diffusion coefficient was determined. Since the energy difference between O-sites and T-site occupation in hcp Mg is only about 0.0126 meV per atom Mg we have supposed that hydrogen atoms could occupy both the T- and O-sites. It was found that there are two competitive pathways that leads to translational motion of H atoms, either direct jumps between two neighbouring O-site along the c-axis (O2-O3) or transfer between neighbouring T- and O-sites (O1-T1).

DFT calculations predict that hydrogen atoms occupy the T-sites in the bcc-Mg lattice: the energy difference between T- and O-sites is rather important (~ 0.095 eV). For bcc-Mg the optimal diffusion path corresponds to direct jumps between two nearest T-sites, but the pathway corresponding to MEP is bended towards the O-site.

Similarly, for fcc-Mg, the hydrogen atoms prefer occupying T-sites. The energy difference between T- and O-sites also appears significant (~ 0.093 eV). However, in fcc-Mg direct jumps between neighbouring T-sites are not favourable. H-atom more easy diffuse towards neighbouring T-site through metastable O-site.

Using the methods described above we have estimated diffusion coefficient for the most favorable hydrogen migration paths in each lattice of Mg. The temperature dependencies of the diffusion coefficient are presented in Fig.1.

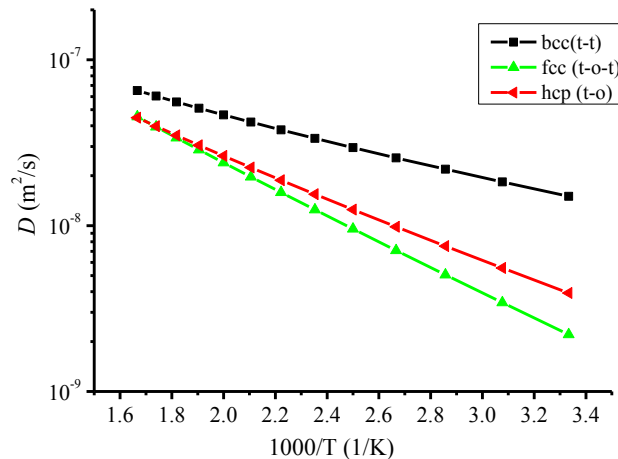


Fig. 1 Temperature dependence of the hydrogen diffusion coefficient calculated for the most probable diffusion paths in the hcp, bcc and fcc Mg lattices, respectively.

From the diffusion rates, it is found that the hydrogen is more likely to diffuse in bcc Mg. Keeping in mind that in bcc-Mg lattice hydrogen atoms tend to be randomly distributed over the interstitial sites [4], it is anticipated that the bcc-Mg could be considered as a promoter of hydrogen diffusion. From this point of view the so-called gate effect of transition metal additives, such as V, Nb, Fe etc, all metals that do not form any bulk alloy with Mg, can be explained by the following way. The presence of Nb layers or particles helps to stabilize locally the bcc-Mg arrangement in which hydrogen diffusion is faster due to (i) the lower activation energy and (ii) the homogeneous distribution of hydrogen atoms over T-sites.

REFERENCES

- [1] J.F. Pelletier et al., Phys. Rev. B, 63 (2001) 052103
- [2] P. de Rango et al., J. Alloys Compd., 445-447 (2007) 52
- [3] K. Klyukin, M.G. Shelyapina, D. Fruchart, Solid State Phenom., 170 (2011) 298-301
- [4] K. Klyukin, MG Shelyapina, D Fruchart, J. Alloys Compd. 580 (2013) S10-S12
- [5] P. Giannozzi, et al., J. of Physics: Cond. Matter, 21-39 (2009) 395502
- [6] C. Wert, C. Zener, Phys. Rev., 76 (1949) 1169
- [7] K.W. Kehr, in Hydrogen in Metals I, edited by G. Alefeld and J. Völkl (Springer, Berlin, 1978) 197
- [8] E. Wimmer et al., Physical Review B 77.13 (2008): 134305

DFT calculation of Cu(II) aqua complexes embedded in mordenite matrix

A.N. Kovalev¹, M.G. Shelyapina¹, V.P. Petranovskii²

¹St. Petersburg State University, 198504, Ulyanovskaya 3, Peterhof, Russia, ²Centro de Ciencias de la Materia Condensada, Universidad Nacional Autónoma de México, Apdo. Postal 2681, C.P. 22800, Ensenada, Baja California, México
kovalyov.lex@gmail.com

ABSTRACT

Zeolites due to their outstanding properties are applied in various areas, including heterogeneous catalysis. Copper exchanged zeolites act as catalysts in de-NO_x reactions [1,2]. Despite a considerable amount of both experimental and theoretical works, a fundamental and comprehensive understanding of intrinsic mechanisms that govern the catalytic processes in these materials still merit complementary investigations. Electronic paramagnetic resonance (EPR) is a powerful tool to study the copper ion (Cu²⁺) state in zeolites [3-6]. However, pure EPR experiment does not provide geometrical data of investigated complexes. So we tried to cause quantum-chemistry computing for provide geometric data of studied complexes.

According to the researchers [3,4,6] copper exchanged zeolites has a few paramagnetic centers of Cu(II). Ratio of these centers depends on ratio of Silica/Alumina in zeolite structure and temperature. Authors of article [4] have shown that in copper exchanged ZSM-5 mainly formed aqua complexes with Cu²⁺ ion and 6 atoms of water in octahedral symmetry. Authors of another article [7] have computed many free copper complexes with amount of water molecules changing from 4 to 6. They found that more energetically efficient complex is octahedral. Considering that we computed octahedral copper aqua complex embedded in the mordenite matrix.

In our calculations we use density functional theory (DFT) approach with basis set of 6-311++G** and B3LYP functional. All computations were performed in program software Gaussian. Firstly geometry of octahedral complex was obtained without surroundings. Result is presented in Fig. 1. After that mordenite matrix was constructed based on data presented in table-book [8]. The modelling part of matrix has shown on Fig. 2 where black centers are atoms of aluminum and location of aqua complex shown with arrow. While optimization was performing all positions of atoms of mordenite matrix was frozen and only atoms of aqua complex has optimized.

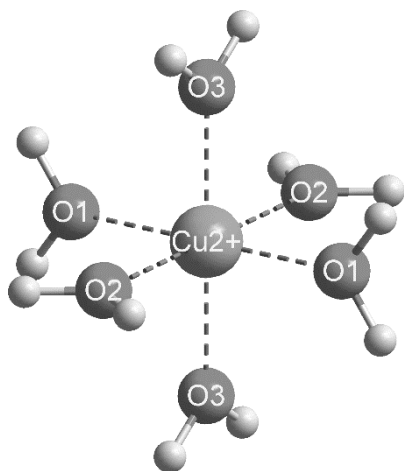


Fig. 1. Initial geometry of copper aqua complex.

Distances:

Cu-O1 = 1.9953 Å

Cu-O2 = 1.9971 Å

Cu-O3 = 2.2508 Å

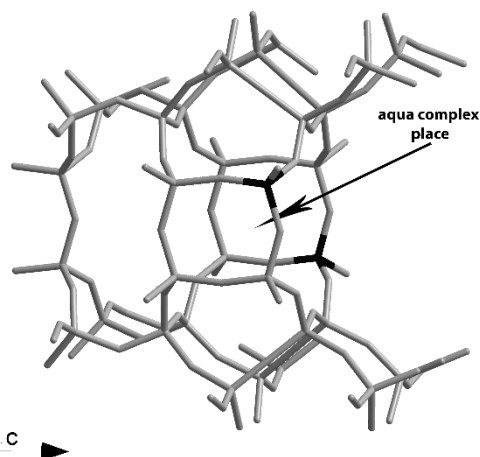


Fig. 2. Modelling part of silica-alumina mordenite matrix. Black centers are atoms of aluminum.

Geometry of aqua complex has obtained and presented at Fig. 3, 4. Geometry of obtained complex have changed from octahedral to distorted 5-angle pyramidal. We obtained that two hydrogen atoms of molecules of water attracts with aluminum atoms. That behavior explained as aspiration of positively charged aqua complex be a closely with negatively charged aluminum atoms of mordenite matrix. As result of this attraction sixth molecule of water remains outside the first coordination sphere.

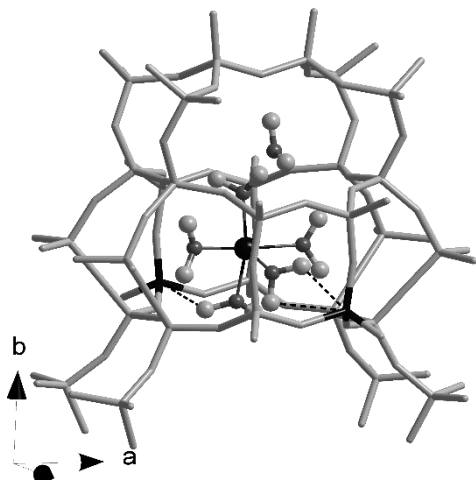


Fig. 3. Geometry of optimized complex.

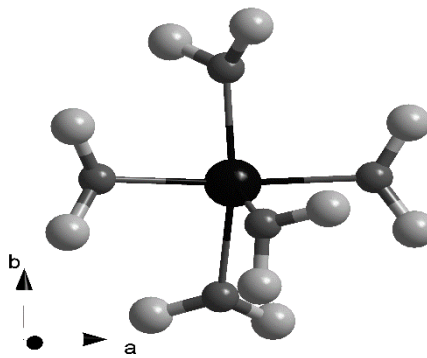


Fig. 4. Obtained aqua complex.

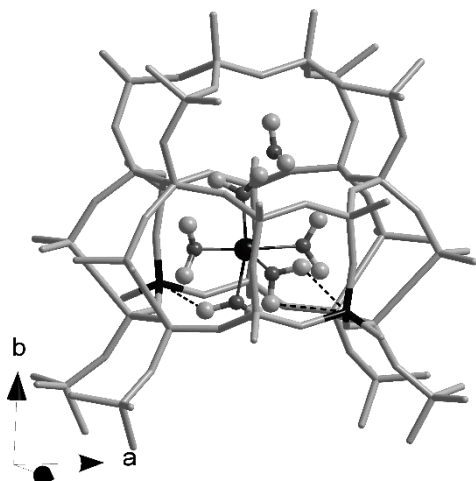


Fig. 3. Geometry of optimized complex.

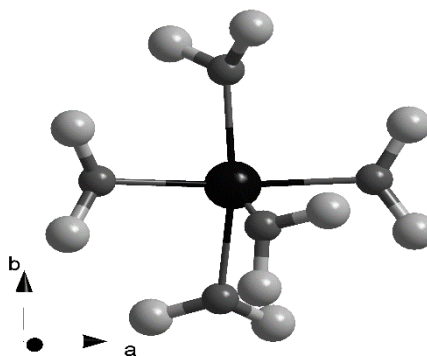


Fig. 4. Obtained aqua complex.

ACKNOWLEDGMENT

Research was carried out using computational resources provided by Resource Center "Computer Center of SPbU" (<http://cc.spbu.ru/en>).

REFERENCES

- [1] H. Yahiro, and M. Iwamoto, *Appl. Catal. A* 222 (2001) 163.
- [2] C. Torre-Abreu, C. Henriques, F.R. Ribeiro, G. Delahay, and M.F. Ribeiro, *Catal. Today* 54 (1999) 407.
- [3] M. Groothaert, K. Pierloot, A. Delabie, R.A. Schoonheydt, *Phys. Chem. Chem. Phys.*, 2003, 5, 2135–2144.

- [4] D. Biglino, H. Li, R. Erickson, A. Lund, H. Yahiro, M. Shiotani, *Phys. Chem. Chem. Phys.*, 1999, 1, 2887–2896
- [5] J. Dedecek, Z. Sobalik, Z. Tvaruzkova, D. Kaucky, B. Wichterlova, *J. Phys. Chem.* 1995, 99, 16327-16337
- [6] V. Petranovskii, E. Stoyanov, V. Gurin, N. Katada, M.-A. Hernandez, M. Avalos, A. Pestryakov, F. Chavez Rivas, R.Z. Ulloa and R. Portillo, *Revista Mexicana de Física* 59 (2013) 170–185.
- [7] M. Pavelka, J.V. Burda, *Chemical Physics* 312 (2005) 193–204.
- [8] M.M.J. Treacy and J.B. Higgins, *Collection of Simulated XRD Powder Patterns for Zeolites*, Elsevier 2001.

Chemical bonding in MoS₂: bulk, nanoparticles, MoS₂-G, and MoS₂-GO

E.P. Mikheenko¹, M.G. Shelyapina¹, D. H. Galvan Martinez²

¹Department of Nuclear-Physics Research Methods, St. Petersburg State University, 198504, Ulyanovskaya 3, Peterhof, Russia, ²Centro de Nanociencias y Nanotecnología, Universidad Nacional Autónoma de México, Apdo. Postal 2681, C.P. 22800, Ensenada, Baja California, México
evg-fgh@ya.ru

ABSTRACT

Molybdenum disulfide exhibits similar properties as noble metals and excellent catalytic behavior in several reactions, especially for hydrodesulfurization (HDS) and hydrogenation (HYD). Earlier research suggested that HDS reactions of sulfur-containing compounds occur at characteristic brim sites at the edges of MoS₂ nanoclusters and that HDS can take place following two different pathways: the HYD pathway, in which several hydrogenation steps precede sulfur extrusion, and the direct desulfurization pathway [1]. The role of carbon in MoS₂-based HDS catalysts has recently been reviewed by Chianelli and co-workers in [2-4]. In these studies, the importance of studying the catalyst in its stabilized state is highlighted, and it is emphasized that carbon substitution is a surface phenomenon occurring only on the surface of the particles. From this perspective deeper knowledge on the MoS₂ cluster geometry and their electronic structure, as well as the chemical bonding between Mo and S atoms, as well as between MoS₂ and graphene (G) and graphene oxide (GO) are required.

Here we report on the results of the theoretical study of the following systems:

- bulk MoS₂;
- small (MoS₂)_n clusters (with n = 1, ..., 5);
- MoS₂ interaction with graphene;
- MoS₂ interaction with graphene oxide.

The calculations have been carried out within the framework of the density functional theory (DFT) method applying the B3LYP hybrid exchange-correlation functional and 3-21G basis set using the GAMESS program package. Self-consistency of calculations is considered achieved when the total energies have converged by 0.1 mRy. The results of cluster calculations in case of MoS₂ have been compared with the bulk one calculated using the Full-Potential Linearized Augmented Plane Wave method using the Wien2k program package.

ACKNOWLEDGMENT

The work has been performed using the equipment of "Saint Petersburg State University Computer Center".

REFERENCES

- [1] H. Topsøe, B.S. Clausen, F.E. Massoth, *Hydrotreating Catalysis*, Springer Verlag, Berlin, 1996.
- [2] R.R. Chianelli, G. Berhault, B. Torres, *Catal. Today* 147 (2009) 275–286.
- [3] S.P. Kelty, G. Berhault, R.R. Chianelli, *Appl. Catal. A – Gen.* 322 (2007) 9–15.
- [4] R.R. Chianelli, M.H. Siadati, M.P. De la Rosa, G. Berhault, J.P. Wilcoxon, R. Bearden, B.L. Abrams, *Catal. Rev.* 48 (2006) 1–41.

Unsupported Ni(Co)Niobium sulfides as catalysts for HDS of Dibenzothofene

L. Pérez¹, C. Suresh², J. N. Díaz De León³, T. A. Zepeda¹, G. Alonso¹, D. H. Galván¹, S. Fuentes¹.

¹Centro de Nanociencias y Nanotecnología-U.N.A.M., Ensenada B. C. México, ²Central Electro Chemical Research Institute, Karaikudi, India.
pecluis@hotmail.com

INTRODUCTION

Niobium sulfide has characteristics of interest on the elimination of refractory sulfur compounds presents in hydrocarbon fuels. Due to their catalytic properties, NbS₂ represent an alternative for improving hydrodesulphurization processes (HDS) [1-2]. It has been reported that the addition of dopants as Ni improve the catalytic activity [1].

The Nb-S system is complex and different phases may be observed [1-3]. Traditional solid-state reactions (between Nb and S) need high temperature, e.g., above 900°C, and annealing for 1 or 2 days at 950 °C were sufficient to produce NbS₂ samples at equilibrium, it is hard to prepare NbS₂ catalysts [3]. Allali et al. [2] applied carbon and γ -alumina as supports for niobium sulfide and depending on the preparation and activation methods identified various phases: NbS₃, NbS₂, and Nb_{1-y}S. More recently, thio-sol-gel reactions have been used for the synthesis of NbS₂ powders [4].

EXPERIMENTAL

In our present work, we successfully obtained the fine NiNb nanocrystal powders by sol-gel method, using NbCl₅ as niobium source and NiAC.4H₂O as Nickel source. Samples were prepared with r = 0.3 (r = Ni (Co)/ (Ni (Co) + Nb)), atomic ratio. In final step, the Ni(Co)NbS nanocatalysts were obtained by sulfidation at 400 °C in gas flow of 15 % H₂S/H₂.

RESULTS

Unsupported Ni(Co)NbS catalysts were characterized with N₂ Physisorption and transmission electron microscopy (TEM). In order to evaluate the catalytic activity of niobium sulfides we used DBT as model molecule. TEM pictures only showed the presence of lamellar particles, characteristics of MS₂ layered sulfides. EDX coupled with TEM analysis demonstrated the homogeneous distribution of the transition metal elements (Ni(Co), Nb) (figure 1). NiNbS catalysts demonstrate higher activities than CoNbS sulfide ones (table I). An unsupported RuS₂ catalyst was used as a reference catalyst.

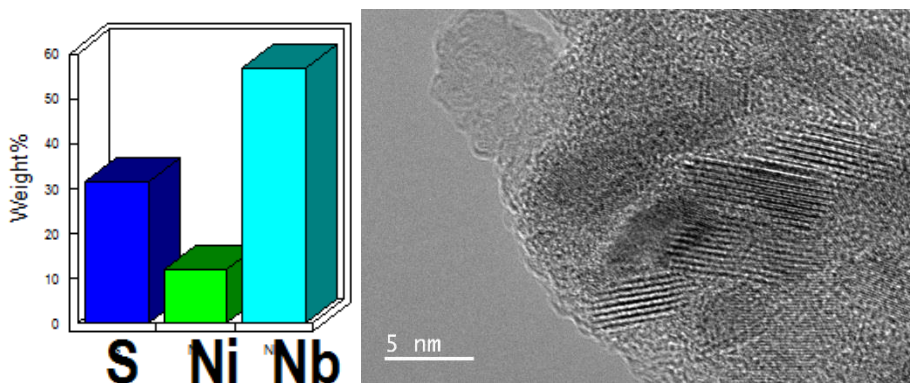


Fig. 1. TEM coupled to EDX characterizations for NiNb-S catalyst.

Table I. Catalytic properties of Ni(Co)NbS

Catalyst	Catalytic activity -rDBT (mol/g*s)	Selectivity HYD/DDS	Area (BET) m ² /g
^a RuS ₂	107.3	0.58	92
^a Ni-Ru-S	85.2	1.15	28
Ni-Nb-S	10.9	0.12	19
Co-Nb-S	4.3	0.16	18

^a L. Pérez, J. N. Díaz De León, T. A. Zepeda, S. Fuentes, C. Suresh, G. Alonso. "RuS₂ and Ni/RuS₂ nanocatalysts for sulfur removal", International Symposium on Nanoscience and Nanomaterials 2013.

ACKNOWLEDGEMENTS

The authors acknowledge SENER-CONACYT for financial support (Project 117373) and the valuable technical assistance to J. Peralta, M. Sainz, F. Ruíz, E. Flores, I. Gradilla, and E. Aparicio.

REFERENCES

- [1] C. Geantet, J. Afonso, M. Breyse, N. Allali, M. Danot, *Catalysis Today* 28 (1996) 23-30.
- [2] V. Gaborit, N. Allali, C. Geantet, M. Breyse, M. Vrinat, M. Danot, *Catalysis Today* 57(2000)267-273.
- [3] W. G. Fisher, M. J. Sienko, *Inorganic Chemistry* 19(1980)39-43.
- [4] M. A. Sriram, P. N. Kumta. *J. Mater. Chemistry* 8(1998)2441-2451.

Ti content effect in CoMo/alumina-titania catalysts to dibenzothiophene HDS activity

René Obeso-Estrella¹, Eder Lugo-Medina², Sergio Fuentes¹, Noe Diaz de Leon¹, Trino Zepeda¹

¹Centro de Nanociencias y Nanotecnología de la UNAM, ²Instituto Tecnológico de Los Mochis
mroem19@hotmail.com

ABSTRACT

In the actuality the solid catalysts are the most used materials in different chemical areas. The petrochemical process is a principal catalysts area where solid catalysts are used to reduce undesirable compounds content in the crude oil. The objective of the catalysts application in the petrochemical industry is removed the S compounds presents in diesel fractions. To achieve the objective to reduce the undesirable compounds we must study and elucidate the catalysis process to create more active catalysts.

In the present work we studied the Ti effect in the CoMo/Al₂O₃-TiO₂ catalysts using the hydrodesulfurization of dibenzothiophene as model molecule. The Alumina-titania mixed oxide supports were synthesized using modified Sol-Gel method reported by Yun Quan et.al. [1] and the titanium content in the supports was varied from 4% wt. to 12% wt. Cobalt and Molybdenum metals was incorporated using incipient wetness co-impregnation method with citric acid as chelating agent. In every samples was agree the Co amount around 3% wt., whereas to Mo was around 13.5% wt. Materials was activated with H₂S/H₂ mixed gas at 400 °C and maintaining for 1 h this conditions. Samples characterization was by diffuse reflectance spectroscopy; X-ray diffraction (XRD); N₂ adsorption; and the activity tests were performed in dibenzothiophene (DBT) HDS reaction in a batch reactor at 320 °C and 800 psi to temperature and pressure conditions.

The DRS results showed that the titanium presence increase the Mo species in octahedral symmetry after materials impregnation. In other hand, a superficial area reduction around 20 percent of the impregnate samples and mesoporous type isotherms were observed in the textural measurements. The catalyst with alumina as support was the more active to DBT HDS. In the reaction tests the selective route was to Direct Desulfurization (DDS) to alumina pure support and that materials with 4 and 12 % wt. of Ti content in the supports, whereas 8 % wt. Ti content sample showed a selective increased to Hydrogenation route (HYD), both behaviors were observed at low conversions (see Fig. 1).

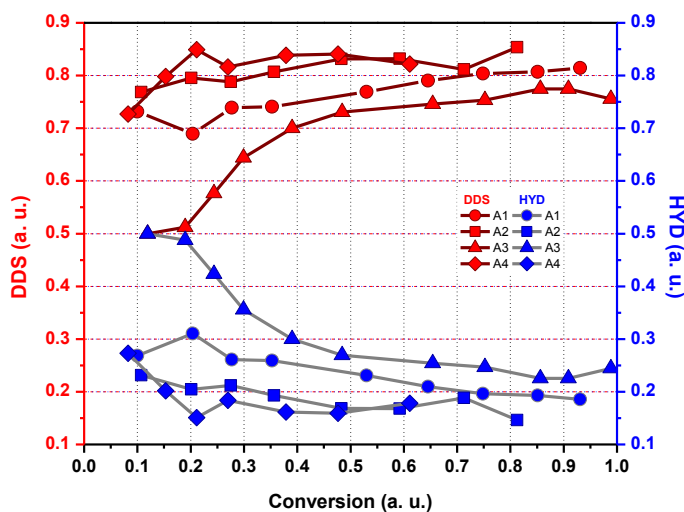


Fig. 1. Materials selective routes (DDS and HYD) versus conversion.

ACKNOWLEDGMENTS

The authors are grateful to Eric Flores, Eloisa Aparicio, David Dominguez, Jose Antonio Díaz, Francisco Ruiz and Israel Gradilla for their technical assistances and CONACYT projects 152012, 155388 and 117373 for the financial supports.

REFERENCES

[1] Quan Yuan An-Xiang Yin, Chen Luo, Ling-Dong Sun, Ya-Wen Zhang, Wen-Tao Duan, Hai-Chao Liu, and Chun-Hua Yan, A. Chem. Soc. Vol. **130**, (2008) 3465-3472.

Study of the support effects in ultra-deep hydrodesulfurization W catalysts

J. N. Díaz de León^{1,*}, G. Torres-Otañez¹, L.A. Zavala-Sánchez¹, T. A. Zepeda¹, S. Fuentes¹, J. A. de los Reyes²

¹Universidad Nacional Autónoma de México, Centro de Nanociencias y Nanotecnología, Carretera Tijuana-Ensenada Km. 107, 22800 Ensenada B.C., México, ²Departamento de Ciencias Básicas e Ingeniería, UAM-Iztapalapa, San Rafael Atlixco 186, Col. Vicentina, Iztapalapa, 09340, D. F. México
noejd@cyn.unam.mx (J.N. Díaz de León Ph.D)

ABSTRACT

The use of γ -Al₂O₃ as a support of hydrodesulfurization catalysts has to be ascribed to its mechanical properties, to a relatively low cost and to its ability to provide high dispersion of the active metal phase. Improvements in the preparation of this oxide as well as the use of additives such as fluorine and phosphate led to the last generation of commercialized hydrotreating catalysts. However, other supports, such as oxides, carbon and zeolites have been also used, at least at the laboratory scale, as supports for conventional CoMoS and NiMoS active phases. Some results have been earlier exhibited for CoMo and NiMo based systems supported on supported on SiO₂, TiO₂, ZrO₂ and Al₂O₃ [1,2]. Recently other support systems have been studied like amorphous silica aluminas (ASAs), zeolites, Al-MCM-41, Al-SBA-15 and mixed oxides like Al₂O₃-TiO₂, ZrO₂-TiO₂, MgO-Al₂O₃ [3-6]. Some of these materials when used as supports can impart four to five folds higher activities in NiMo systems. Nowadays, 95% of the entire research about HDS catalysts has been done over the CoMo and NiMo systems and this acquired knowledge is extended to NiW system [7]. Nevertheless, direct information of this system is scarce despite the fact that NiW catalysts has shown different catalytic activity trend, different selectivity and yield, better nitrogenated compounds poisoning resistance and several specific chemical differences than typical systems. In this work we want to get insight on the support effects for the ultra-deep hydrodesulfurization W and NiW catalysts. Typical pure oxides as □-Al₂O₃(A), SiO₂(S), TiO₂ (T) and ZrO₂ (Z) and Al₂O₃-TiO₂ (AT), ZrO₂-TiO₂ (ZT) mixed oxides where synthesized and calcined at 500°C. Then W and NiW catalysts where prepared by incipient wetness impregnation with a surface density of 2.8 W atoms per square nanometer (W nm⁻²) and maintaining fixed the Ni/(Ni+W) atomic ratio to 0.41 in the respective case. Once impregnated and dried at 120°C materials where calcined at 450°C. Catalysts and supports were characterized by XRD, N₂ isotherms, UV-vis, ICP. Primary catalytic activity evaluation of sulphided NiW catalysts were carried out in a gas phase reactor with dibenzothiophene (DBT) as model molecule. Selected catalysts were evaluated as well in a batch reactor using 4,6-dimethyl-DBT (300 ppm S) which is wide recognized as a more refractory compound.

ACKNOWLEDGMENTS

To CONACyT for master and Ph. D scholarships and to PEMEX project SENER 117373.

REFERENCES

- [1] Catalysis Today **86**, (2003), 31–43
- [2] Catalysis Today **130**, (2008), 3–13
- [3] Comptes Rendus Chimie **12**, (2009), 6–7,
- [4] Applied Catalysis A: General, **253** (2003) 151–163
- [5] Catalysis Today **98**, (2004) 131–139
- [6] Catalysis Today **72-1**, (2011), 203–208
- [7] H. Topsøe, B.S. Clausen, F.E. Massoth, in “Hydrotreating Catalysis—Science and Technology” (J.R. Anderson, M. Boudart, Eds.), Vol. 11, Springer Verlag, Berlin, **1996**.

Experience of geothermal exploration on the Kamchatka Peninsula using the audiomagnetotelluric sounding method

Ksenia Antaschuk, Alexander Saraev, Igor Tokarev
St. Petersburg State University
tokarevigor@gmail.com

INTRODUCTION

There is quite a big world experience of the magnetotelluric (MT) and audiomagnetotelluric (AMT) soundings application for the geothermal exploration. These researches are usually focused on the structural investigations, allocation of conductive anomalies and discovering geothermal deposits. Results of AMT soundings for the geothermal exploration in the Palana area (north-western part of the Kamchatka Peninsula) are considered in this abstract.

FEATURES OF INVESTIGATED AREA

The Palana area is located in the north-western part of the Kamchatka Peninsula. Two structural horizons are allocated here. The lower one is represented by volcanogenic (basalts, andesites), volcanogenic-sedimentary (tuffs, tuff-sandstones, diabases, porphyrites) and sedimentary (sandstones, argillites, siltstones) rocks of the cretaceous age. These rocks are metamorphized and broken by intrusions. The largest faults with the vertical displacements reaching 0.5-1 km limit horsts of rocks in the lower horizon. The upper horizon by thickness up to 1 km contains volcanogenic (basalts, andesite-basalts, andesites) and sedimentary (sandstones, conglomerates, argillites and siltstones) palaeogene and volcanogenic-sedimentary (tuff-sandstones) neogene rocks. In the upper horizon numerous faults with vertical displacements from tens up to first hundreds meters are also presented.

The main tasks of AMT investigations were the study of area structural features, faults mapping and allocation of local conductive anomalies which are promising for geothermal deposits discovering. Researches have been focused on the search of relatively shallow (up to 2 km), low and mid temperature (up to 150 °C) geothermal deposits.

AMT SOUNDINGS

AMT soundings are based on measurements of natural electromagnetic fields in frequency range from units to several thousands hertz. The horizontal and mutually orthogonal components of electric and magnetic fields are measured, and the impedance amplitude (or apparent resistivity - ρ_a) and impedance phase (φ_z) are determined. The amplitude and phase curves are used in inversion software tools for the geoelectric sections deriving. At the AMT investigations the ACF-4M system developed by the St. Petersburg State University and MicroKOR Ltd. (Saraev et al., 2011) has been used. The equipment includes a digital recorder with four synchronous channels and 24-bit ADC in each channel, two magnetic coils, two electric lines, preamplifier of electric signals and four electrodes. The frequency range of the equipment is 0.1-1000 Hz (including AMT and part of MT ranges), sampling frequencies are 160, 1600 and 3200 Hz. The remote reference technique and robust data processing have been used in the described investigations for the data quality improvement. For 2D inversion the REEBOC algorithm (Siripunavaraporn and Egbert, 2000) has been used.

RESULTS

An area in the vicinity of the Palana settlement with the square about 9 km² has been selected, and AMT investigations have been fulfilled there. Separation between profiles was 250 m and between sounding stations - 125-250 m. On results of the primary data analysis and taking into account available geological information the 2D structure of geoelectrical sections has been ascertained. In this area ρ_a and φ_z curves for the azimuth 150° correspond to TM mode, and for the azimuth 60° - TE mode. Area distributions of ρ_a and φ_z for frequency 80 Hz is shown in Fig. 1. The orientation of linear conductive anomalies in the north-eastern direction both for TM and for TE modes shows, that the determinative in this site are 2D structures. Last years for the AMT data inversion in geothermal areas and the selection of places for verifying wells the 3D inversion has been often applied. At the same time, at the confidently determined 2D structure of a site more authentic and detail data can be obtained from the 2D inversion.

After 2D bimodal inversion the three layers geoelectric structure of the Palana area has been derived up to the depth of 3 km. As examples, five sections are presented in Fig. 2. The reliability of the geoelectric structure reflection in results of the 2D inversion of AMT data is proved by the similar behavior of the sections. The use of 2D inversion has also allowed us to reduce an influence of AMT curves static distortions.

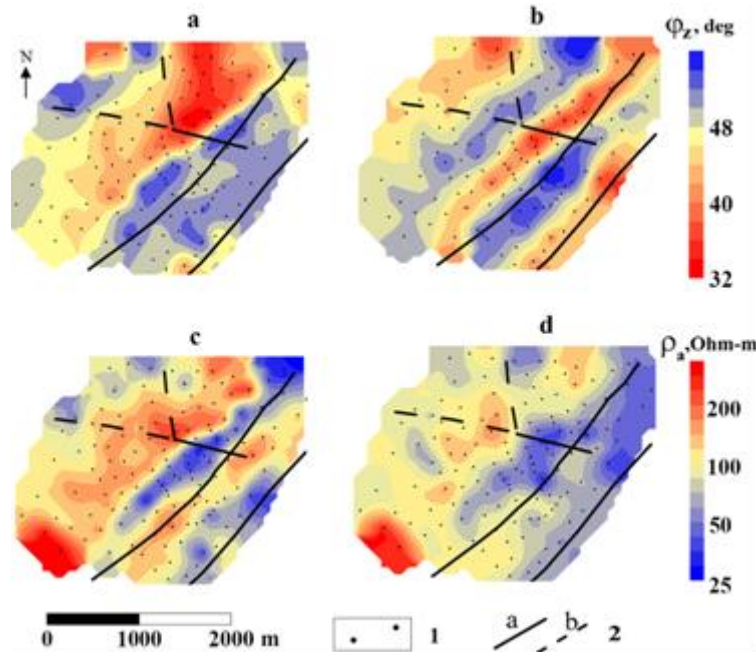


Fig. 1. Area distributions of ϕ_z (a,b) and ρ_a (c,d) for frequency 80 Hz for TM (a,c) and TE (b,d) modes. 1 – sounding stations; 2 – faults from data of previous investigations (a – confidently mapped, b – supposed).

The obtained geoelectric sections in general have three layers. The first (upper) layer about 1500 m thickness of high resistivity (first thousands Ohm-m) is connected with volcanic and volcano-sedimentary rocks. The second layer about 500 m thickness of low resistivity (30-50 Ohm-m) is represented by sedimentary rocks. The third layer of higher resistivity (60-100 Ohm-m) is connected with volcanic rocks. Faults are observed in north-western and south-eastern parts of the profiles. Characteristic feature of these sections is the presence in their south-eastern parts a deep low resistive zone with an inclined conductive channel from this zone up to the earth surface, which can be considered as a drainage system for the thermal water circulation. The position of the considered deep zone coincides with two faults (Fig. 1).

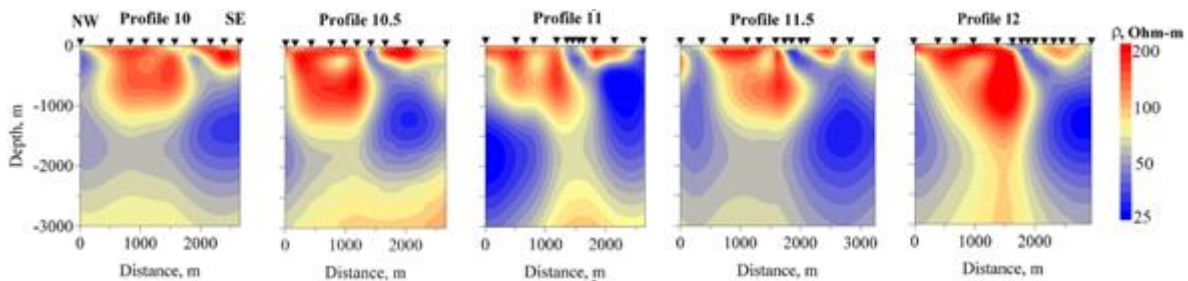


Fig. 1. Geoelectric sections according to results of the 2D inversion of AMT soundings data

The results of AMT soundings have been used for the selection of the most perspective zone for the revealing of a geothermal source. The conductive anomaly in the south-eastern part of the site can be considered as a perspective zone for further supplementary investigations and the subsequent checking by drilling.

ACKNOWLEDGMENT

The work was fulfilled with the support of the Core stock center “Geomodel” of St. Petersburg State University.

REFERENCES

- [1] Saraev A.K., Antaschuk K.M., Pertel M.I., Eremin I.S., Golovenko V.B., Larionov K.A. *Hardware-software complex of audiomagnetotelluric soundings ACF-4M*, Papers of the 5th school-seminar of M.N. Berdichevsky and L.L. Vanyan on EM soundings of the Earth – EMS-2011. Book 2, SPb, SPbSU, 2011, 475-478.
- [2] Siripunavaraporn W. and Egbert G. *An efficient data-subspace inversion method for 2-D magnetotelluric data*. Geophysics, 2000, Vol. 65, No. 3, 791-803.

Application of the radiomagnetotelluric sounding method for the solution of engineering and environmental tasks

Alexander Saraev, Alexander Simakov, Igor Tokarev
St. Petersburg State University
tokarevigor@gmail.com

INTRODUCTION

The radiomagnetotelluric (RMT) sounding method is a very promising tool for the solution of a wide range of engineering and environmental tasks. It operates usually without own source, permits tensor measurements and can be applied on local areas because of using of a small array (10-20 m). The distance between the stations can be chosen relatively small so that a high resolution of the subsurface can be achieved. Foot, mobile and controlled source modifications of the RMT method are described and examples of their application are considered in this abstract.

FOOT, MOBILE AND CONTROLLED-SOURCE MODIFICATIONS OF THE RMT METHOD

The RMT method is based on the measurement of electromagnetic fields of remote radio transmitters: VLF (10-30 kHz), LF (30-300 kHz) and MF (300-1000 kHz) [2]. It has been actively developed last years. Electromagnetic waves from radio transmitters diffuse in the conductive earth and induce current systems which excite alternating electric and magnetic fields. In the far-field zone of a source (several skin depths away) the electromagnetic field can be considered as a plane wave. Surface impedance can be estimated using measurements of mutually orthogonal horizontal components of electric and magnetic fields. The RMT transfer functions are derived by spectral analysis from time series, thus enabling a multidimensional inversion of data. The impedance is usually converted into the apparent resistivity and impedance phase. This transformation allows us to relate the measurements data more easily to the subsurface geology. Well-developed and tested magnetotelluric software tools can be directly applied to the RMT data interpretation. The inversion techniques are routinely used to derive the subsurface resistivity distribution.

Five channel RMT instrument for foot survey (RMT-F) has been developed by the St. Petersburg State University, MicroKOR Ltd. and University of Cologne [3]. There is an experience of successful application of the RMT-F instrument for the solution of different near-surface geophysics tasks. Then mobile and controlled-source RMT instruments (RMT-M and RMT-C) have been developed [1]. Realization of fast RMT surveys using mobile RMT-M system is the very important for the survey of large-area territories. The RMT-C system is intended for the application in remote territories where there are not enough radio transmitters. Its using is also necessary to obtain of RMT transfer functions in frequency range 1-10 kHz, where there are no radio transmitter's signals. The decreasing of the lowest frequency up to 1 kHz allows us to increase the investigation depth in approximately three times. By using ungrounded (capacitive) electric lines the measurements can be realized in different grounding conditions in the summer time (on asphalt, concrete, gravel) and in the winter time (on frozen soils, snow and ice).

EXAMPLES OF THE RMT METHOD APPLICATION

The landfill of the coal ashes from power plants is located in the northern part of Spain. Wastes fill in a V-shaped valley of a stream. After the RMT foot survey it was found that the landfill is distinguished well from host rocks. The area resistivity distributions for several depths are presented in Fig. 1. We can see a good correlation of the landfill's contour with the RMT results. The main amount of ashes is localized in the depth interval up to several first meters. The deep conductive zone in the northern part of the landfill is located in the interval 14-22 m. Geoelectric section for the profile 1 is shown in Fig. 2 and it illustrates internal heterogeneity of the landfill.

Results of application of the controlled source modification of the RMT method for the solution of engineering tasks in Chukotka region (far North-East of Russia) is presented in Fig. 3. In this region there is a possibility to measure only VLF radio transmitter's signals, which can be used for realization the VLF-R profiling. Application of the controlled source modification has allowed us to get full sounding curves. Results of the RMT method have been confirmed by drilling.

The RMT method is 10 times faster than the DC vertical electric sounding (VES) one. The RMT measurements are carried out and RMT surveys are realized at bad grounding conditions in the summer time (asphalt, concrete, gravel) and in the winter time (frozen soils, snow and ice) using ungrounded (capacitive) electric antennae.

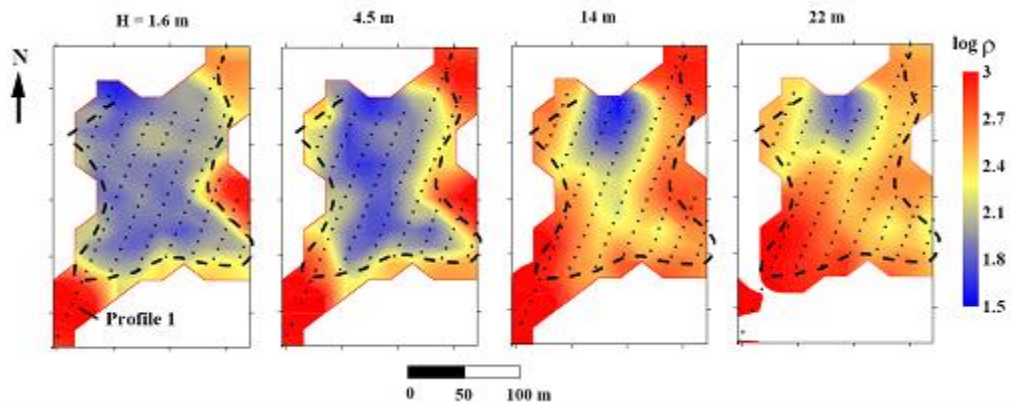


Fig. 1. Distribution of rocks resistivity at several depths at the landfill of coal ashes, Spain (foot survey).

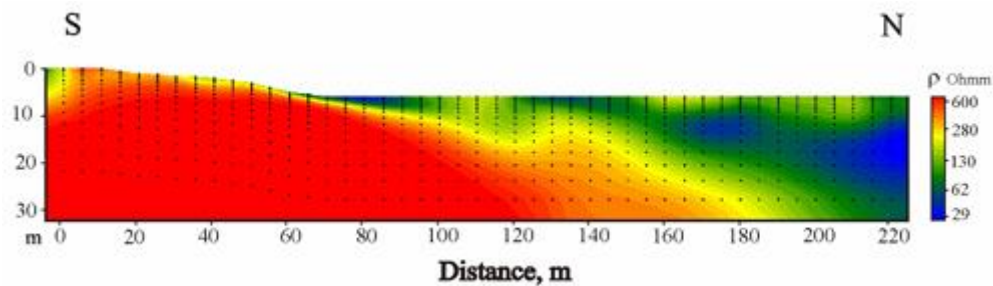


Fig. 2. Geoelectric section along the profile 1 at the landfill of coal ashes, Spain (foot survey).

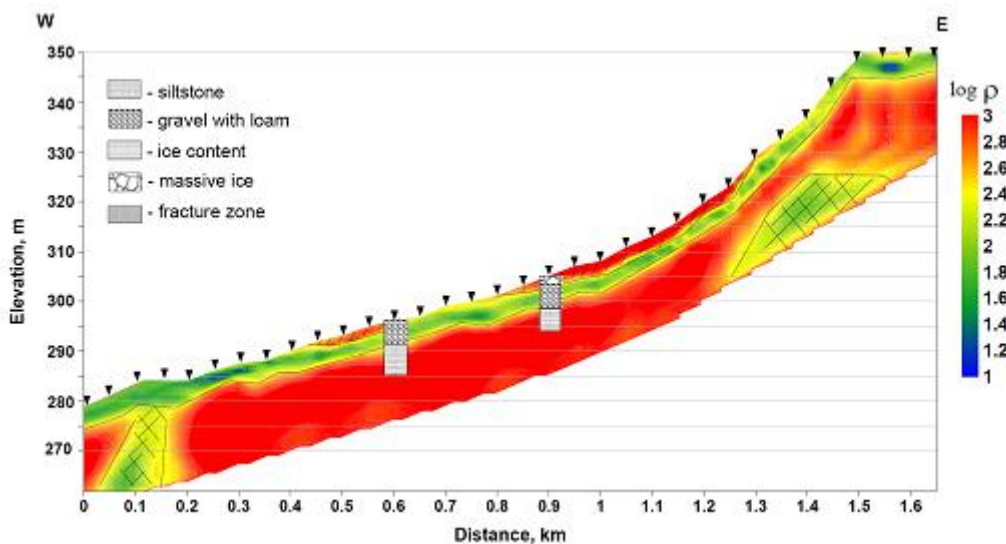


Fig. 3. Geoelectric section and its comparison with boreholes data, Chukotka (controlled source survey). Horizontal and vertical scales ratio is 10:1

ACKNOWLEDGMENT

The work was fulfilled with the support of the Core stock center “Geomodel” of St. Petersburg State University.

REFERENCES

- [1] Saraev A.K., Simakov A.E., and Tezkan B. *Foot, Mobile and Controlled Source Modifications of the Radiomagnetotelluric Method*. Near Surface 2011 – 17th European Meeting of Environmental and Engineering Geophysics, Leicester, UK, 12-14 September 2011.
- [2] Tezkan B. *Radiomagnetotellurics*. Groundwater Geophysics: A Tool for Hydrogeology. (2008), P. 295-317.
- [3] Tezkan B., and Saraev A. *A new broadband radiomagnetotelluric instrument: application to near surface investigations*. Near Surface Geophysics, Vol. 6, No 4. (2008), P. 245-252.

Characterization of Zirconium Oxide Films Deposited by Using the Atomic Layer Deposition Method

J.R. Martínez-Castelo^a, H. Tiznado^b and M.H. Farias^c

Centro de Nanociencias y Nanotecnología, Universidad Nacional Autónoma de México, Apdo. Postal 14, C.P. 22800, Ensenada, Mexico

^ajesusmtz@cryn.unam.mx, ^btiznado@yahoo.com, ^cmario@cryn.unam.mx

ABSTRACT

Zirconium oxide (ZrO₂), is considered a very attractive material for application as dielectric gate as it exhibits good thermodynamic stability in contact with silicon, has a relatively high dielectric constant (25 ~ 30), a large gap (5.8 eV), and high compatibility with current manufacturing process of integrated circuits. The above properties are desirable for the gate dielectric of the field-effect transistor (FET) and other electronic devices. In order to obtain thin films with specific values of dielectric constant and bandwidth, a deposition technique that allows controlling the thickness at the atomic level and coat any surface uniformly, is required.

Atomic Layer Deposition (ALD) is the technique that best fits these requirements; it is self-limited which ensures that the amount of deposited material is highly controlled; is able to cover porous surfaces; and does not limit the design of dielectric systems, as it can be applied to a wide variety of materials.

In this work, ZrO₂ thin films were deposited by ALD, using Cp₂ZrCl₂ (Cp = Ciclopentadienyl) as a zirconium precursors and water as an oxidizing agent. The films were deposited on silicon substrates while the temperature used during the deposition process was adjusted to 300°C. Under such conditions, a deposition rate of ~ 0.3Å(cycle) was obtained. Deposited films were characterized by ellipsometry, and electronic spectroscopy techniques, for example X-ray photoelectron spectroscopy (XPS). The materials proposed in this work have high potential for application as MOS capacitors.

ACKNOWLEDGMENT

The authors would like to thank Dr. Jesus Antonio Diaz and M.C. David Dominguez for the XPS and Auger characterization, Dr. Roberto Machorro to facilitate the ellipsometry characterization and CONACYT for the support.

Synthesis of PVP stabilized Co and Ni nanoparticles for APR reaction

I. Simakova¹, Yu. Demidova¹, D.Yu. Murzin², A. Simakov³

¹Boreshkov Institute of Catalysis, Novosibirsk (Russia) simakova@catalysis.ru ²Process Chemistry Centre, Abo Akademi University, FI-20500, Turku/Abo (Finland), ³Universidad Nacional Autonoma de Mexico, Centro de Nanociencias y Nanotecnologia, C.P. 22860, Ensenada, B. C., (Mexico), andrey@cny.unam.mx
simakova@catalysis.ru

INTRODUCTION

Catalysts on the basis of the VIII group metals demonstrate a high potential to be used in catalytic aqueous phase reforming (APR) of biomass resources resulting in a mixture of hydrogen and alkanes. APR is thus a promising route for sustainable fuel production. However, high amounts of expensive noble metals (Pt, PtRe) [1] are required for APR and structure-activity relationship is still needed to be revealed. In the current work different controlled methods of base metal nanoparticles (NPs) synthesis with controllable size have been studied, being applicable for a wide range of catalytic reactions.

RESULTS

Ni NPs were prepared by the microemulsion method. The cationic surfactant cetyltrimethyl bromide (CTAB), n-octane, n-butanol, nickel chloride, hydrazine hydrate (64% wt.) mixed with sodium hydroxide (20% wt.) were used without purification [2]. The formation process for Ni-CTAB synthesized in CTAB and hydrazine was monitored by UV-vis spectroscopy as a representative example. The original NiCl₂ solution (before heating) exhibited peaks at 400, 650, and 725 nm in UV-vis spectrum. As the heating time was increased, these peaks totally disappeared after 2 min indicating that NiCl₂ has been completely converted and that Ni colloids were formed. UV-vis spectra indicated formation of metallic Ni nanoclusters at the beginning of the reduction but thereafter they formed complex compounds in the absence of reducing agents that was quite stable with time. According to TEM analysis Ni clusters of Ni-CTAB-A system are characterized by an uniform particle distribution with an average size 2.6 nm and a standard deviation 0.8 nm. Ni NPs have a rather round shape (Figure 1).

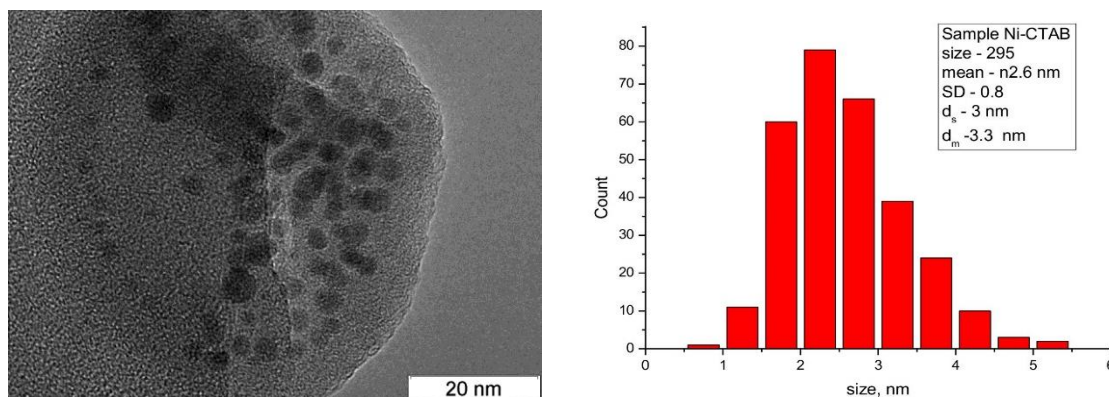


Figure 1. TEM image (left) and histogram of particle size distribution (right) of as-prepared Ni colloids Ni-CTAB-A1.

Co(NO₃)₂ was used to synthesize Co NPs according to [2]. However, CoCl₂ used as a Co NPs precursor provided a narrower particle size distribution. Polyol synthesis of Co NPs by hydrazine reduction of CoCl₂ in ethylene glycol at 80°C and a high pH resulted in Co black instead of 4.5 nm NPs [3].

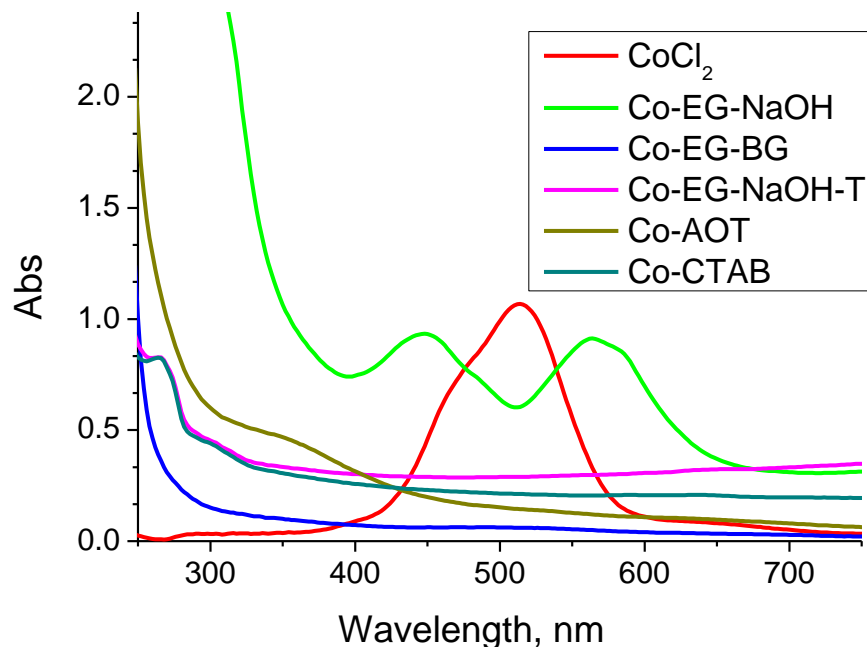


Figure 2. UV-Vis absorption spectra of Co colloids.

Utilization of the microemulsion method by stabilization with cetyltrimethyl bromide (CTAB) (oil - n-octane and n-butanol) and reduction by hydrazine hydrate (64% wt.) in a basic media afforded formation of Co bearing NPs while stabilization with sodium dodecylsulphosuccinate (AOT) exhibited formation of cobalt hydroxide instead of metallic Co NPs. UV-vis spectra indicated formation of metallic Co nanoclusters for all samples except those heated below 80°C probably resulting in formation of Co complexes (Figure 2).

ACKNOWLEDGMENT

The SusFuelCat project has received funding from the European Union's Seventh Framework Programme for research, technological development and demonstration under grant agreement No 310490 (www.susfuelcat.eu).

REFERENCES

- [1] A.V. Kirilin, A.V. Tokarev, H.Manyar, C. Hardacre, T. Salmi, J.-P. Mikkola, D.Yu. Murzin. *Cat. Tod.* 223 (2014) 97.
- [2] Martinez A., Prieto G. *Catalysis Communications.* 8 (2007) 1479.
- [3] Balela M. D. L., Lockman Z., Azizan A., Matsubara E., Amoroso A. V. *AIP Conference Proceedings* 1217 (2010) 113.

Preparation of PVP stabilized Ru nanoparticles for sugar alcohol APR

I. Simakova¹, Yu. Demidova¹, D.Yu. Murzin², A. Simakov³

¹Boreskov Institute of Catalysis, Novosibirsk (Russia), ²Process Chemistry Centre, Abo Akademi University, FI-20500, Turku/Abo (Finland), ³Universidad Nacional Autónoma de México, Centro de Nanociencias y Nanotecnología, C.P. 22860, Ensenada, B. C., (Mexico).
simakova@catalysis.ru

INTRODUCTION

Aqueous phase reforming (APR) of bioderived sugar and sugar alcohols results in production of hydrocarbons and hydrogen - potential fuel components from renewable resources [1]. Xylitol is the second most abundant sugar alcohol produced industrially by catalytic hydrogenation of xylose monomers which in turn originate from hemicelluloses being one of the main constituents of wood [2]. In this work colloidal approaches have been applied to synthesis PVP stabilized Ru nanoparticles (NPs) with controllable size for APR application.

RESULTS

Microemulsion method with AOT was initially applied in this work to synthesize small Ru NPs [3]. Contrary to the data reported in [3] it was found that this method did not provide formation of expected small Ru NPs and thus the polyol method was applied. Typically, $\text{RuCl}_3 \cdot n\text{H}_2\text{O}$ was dissolved in ethylene glycol (EG) and stabilized by polyvinylpyrrolidone (PVP, $12\,600 \pm 2700$, Vekton) with the ratio range from 1:1 to 1:50 under stirring to form a dark red solution (Figure 1), which was thereafter heated under vigorous stirring to reflux. UV-Vis spectra were recorded to monitor NPs formation (Unicam SP1750 UV-vis spectrophotometer). The mean particle diameter and the standard deviation of Ru NPs were characterized by transmission electron microscopy (TEM) (Hitachi-9000 NAR) by counting at least 250 NPs. Although the standard reduction potential of RuCl_3 to $\text{Ru}(0)$ is relatively high ($E_o \approx 0.3862\text{ V}$), we have not been able to obtain polymer-stabilized ruthenium clusters by simply refluxing RuCl_3 solution contrary to the literature [4]. This experiment indicated that Ru (III) reduction was sensitive to air. During the reduction under Ar the color of the solution changed from dark red to light yellow then turned to dark green and finally a transparent dark brown colloidal solution of Ru NPs was obtained without any precipitate (Figure 1).



Figure 1. Change of color during reduction of the sample Ru-EG-5 under reflux conditions.

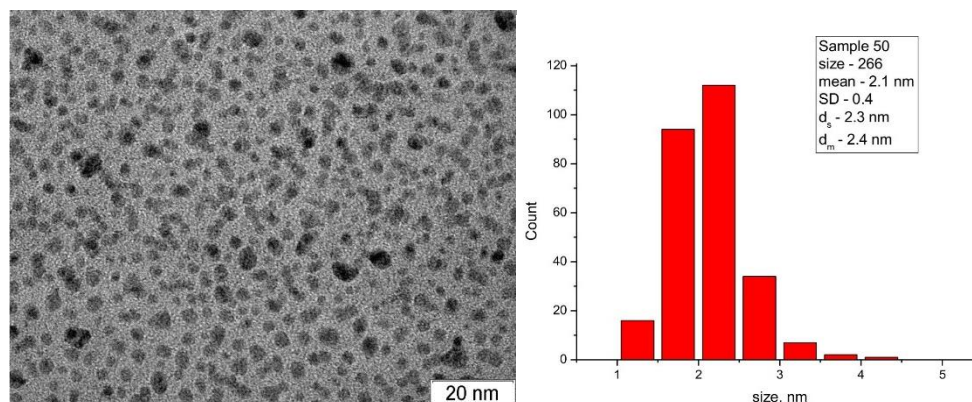


Figure 2. TEM image (left), and the corresponding particle size distribution (right) of PVP-stabilized ruthenium Ru:EG=1:5 (mol/mol).

Ru NPs synthesized by the polyol method exhibited a relatively narrow range of sizes with the average size 2.1 nm (or 1.7 nm depending on the reduction temperature) (Figure 2). Ru NPs were quite stable for 4 months, only a slight increase of mean size up to 2.4 nm was observed.

ACKNOWLEDGMENT

The SusFuelCat project has received funding from the European Union's Seventh Framework Programme for research, technological development and demonstration under grant agreement No 310490 (www.susfuelcat.eu).

REFERENCES

- [1] A.V. Kirilin, A.V. Tokarev, H.Manyar, C. Hardacre, T. Salmi, J.-P. Mikkola, D.Yu. Murzin. *Cat. Tod.* 223 (2014) 97.
- [2] E. Sjostrom, *Wood Chemistry – Fundamental and Applications*, Academic, London, 1993.
- [3] S.U. Nandanwar, M. Chakraborty, Z.V.P. Murthy. *Ind. Eng. Chem. Res.* 50 (2011) 11445.
- [4] Hirai H., Toshima N., in *Tailored Metal Catalysis*, ed. Y. Iwasawa, Reidel, Dordrecht, 1986, p. 121.

The reduction of 4-nitrophenol over Au@ZrO₂ and Au-Ce@ZrO₂ nanoreactors

Viridiana Evangelista¹, Brenda Acosta¹, Serguei Miridonov², Andrey Simakov³

¹Posgrado en Física de Materiales, Centro de Investigación Científica y de Educación Superior de Ensenada, C.P. 22860, Ensenada, Baja California, México, ²Departamento de Óptica, Centro de Investigación Científica y de Educación Superior de Ensenada, C.P. 22860 Ensenada, Baja California, México, ³Universidad Nacional Autónoma de México, Centro de Nanociencias y Nanotecnología, C.P. 22860, Ensenada, Baja California, México.
vevangel@cnyun.unam.mx

INTRODUCTION

The reduction of 4-nitrophenol to 4-aminophenol by NaBH₄ has often been used as a model reaction to test the catalytic activity of metal nanoparticles in aqueous solution at room temperature. The progress of the reaction can be easily monitored via UV-Vis spectroscopy [1, 2]. It is found that the decoration of supported gold nanoparticles with oxides strongly affects their catalytic activity in CO oxidation due to formation of highly active Au-oxide interface [3, 4]. The aim of this work is the analysis of the effect of the nucleus decoration with ceria in Au@ZrO₂ nanoreactors on the catalytic reduction of 4-Nitrophenol.

EXPERIMENTAL

The decoration of Au core was carried out via injection of ceria precursor into a void space of nanoreactors with its consequent hydrolysis and thermal treatment. TEM data of the obtained Au-Ce@ZrO₂ nanoreactors are presented in Fig. 1. The obtained nanoreactors were tested in the reduction of 4-nitrophenol with an excess of NaBH₄ as reducing agent at room temperature. In a typical experiment 0.3 mL of nitrophenol and 3.7 mL of NaBH₄ solutions were mixed in a quartz cell (1 cm of pathlength) for 15 minutes. Then, the 0.1 mL aqueous suspension of nanoreactors was injected by micro pipette under constant magnetic stirring of the reaction mixture. The progress of the reaction was monitored on line by UV-Vis spectroscopy in a transmittance mode using the AVANTES Ava-Spec-2048 UV-Visible spectrometer equipped with an AvaLight-DHS light source. The spectra were collected every 2 seconds up to the complete consumption of nitrophenol. To confirm the reproducibility of the activity level experiments were repeated 3 times.

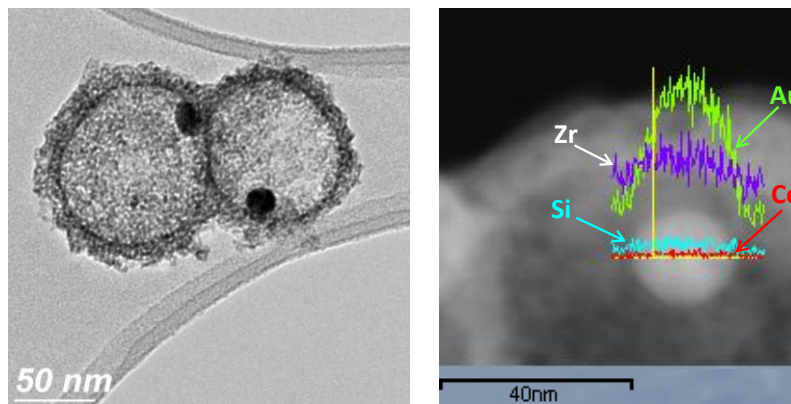


Fig. 1. Typical TEM image for Au-Ce@ZrO₂ nanoreactors (left). Profiles of Au, Zr, Ce and Si elemental distribution across an Au-Ce@ZrO₂ nanoreactor according to STEM-EDS line-scanning technique (right).

RESULTS

Typical evolution of UV-Vis spectra collected during the reduction of 4-nitrophenol by NaBH₄ in the presence of the Au-Ce@ZrO₂ nanoreactors at room temperature is presented in Fig. 2 (left). Usually, activity of catalyst is estimated by the change of peak at 400 nm related to the nitrophenolate ions formed via the reaction of nitrophenol with NaBH₄. In an excess of NaBH₄ reaction of nitrophenol reduction is considered to be described by a first-order rate law with respect to 4-nitrophenolate ion concentration. Commonly, the value of the apparent reaction rate constant is estimated from a linear slope of the relative nitrophenolate ion content (A/A_0) in logarithmic form.

However, in case of nanoreactors obtained in the present work, nonlinear relationship between $\ln(A/A_0)$ and the reaction time was found (see in Fig.2 (right)). In addition, consumption of nitrophenolate ion at the start of the reaction was accompanied with the appearance of a new intensive peak at 310 nm. Then, intensity of this peak decreased and peak at 299 nm was observed.

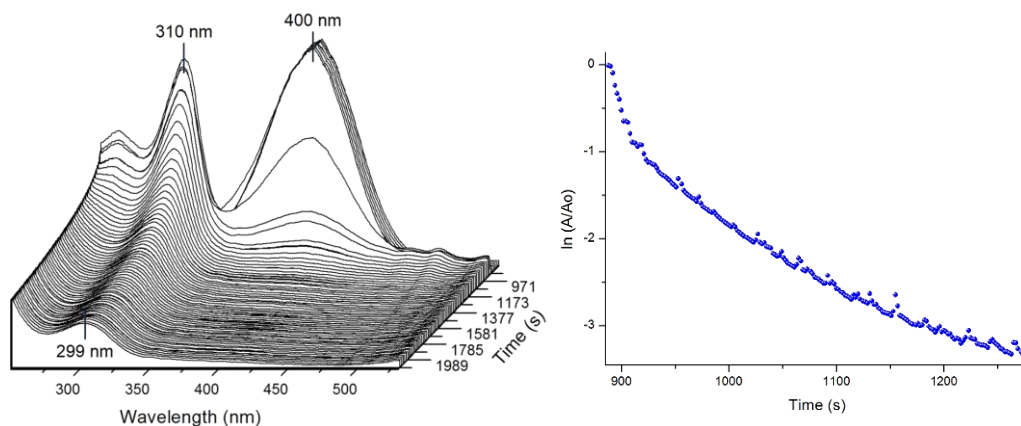


Fig. 2. Kinetic analysis of catalytic reduction of 4-Nitrophenol on Au-Ce@ZrO₂ nanoreactors. UV-Vis absorption spectra collected during the reaction (left). The change in the absorbance at 400 nm in logarithmic form versus the reaction time (right).

The method of principal component analysis (PCA) was applied to the absorption-wavelength-time surfaces generated by UV-Vis spectroscopy *in situ* during the reduction of nitrophenol on Au@ZrO₂ or Au-Ce@ZrO₂ nanoreactors in order to resolve individual spectral components and their time courses. Based on PCA analysis it was revealed a new spectrum related with the formation of some azo intermediate compound adsorbed on the shell surface of nanoreactors. These results are consistent with a condensation route in which one molecule of the nitroso compound interacts with a molecule of the hydroxylamine to give the azoxy compound, which is reduced in a series of consecutive steps to the azo, hydrazo, and finally amine compounds [5]. The estimated values of the reaction rate constants indicated that decorated nanoreactor is much more active than none decorated one.

CONCLUSION

The decoration of nuclei in Au@ZrO₂ nanoreactors with ceria strongly improves catalytic activity in the reduction of 4-nitrophenol due to formation of highly active Au-oxide interface and the promotion of the condensation route.

ACKNOWLEDGMENT

The authors would like to thank E. Flores, F. Ruiz, J. Peralta, M. Sainz and O. Callejas for their technical assistance. This research project was partly supported by CONACyT (Mexico) and PAPIIT-UNAM (Mexico) through grants 179619 and 203813, respectively.

REFERENCES

- [1] K. Kuroda, T. Ishida, M. Haruta, J. Mol. Catal. A: Chem. 298 (2009) 7–11.
- [2] P. Veerakumar, M. Velayudham, K. Lu, S. Rajagopala, Appl. Catal. A: Gen. 439–440 (2012) 197–205.
- [3] R. Guttel, M. Paul and F. Schuth, Catal. Sci. Technol. 1 (2011) 65–68
- [4] A. Horvath, A. Beck, G. Stefler, T. Benko, G. Safran, Z. Varga J. Gubicza, and L. Gucci, J. Phys. Chem. C 115 (2011) 20388–20398.
- [5] A. Corma, P. Concepción, P. Serna, Angew. Chem. 119, 7404–7407 (2007).

Modifier effect of metal oxides in CO oxidation over gold supported on silica

Y. Kotolevich¹, O. Martynyuk^{1,2}, J.E. Cabrera Ortega¹, V. Maturano Rojas³, A. Aguilar Tapia³, H.J. Tiznado¹,
N. Bogdanchikova¹, A. Pestryakov², R. Zanella Spesia³

¹ Centro de Nanociencias y Nanotecnología (CNYN), Universidad Nacional Autónoma de México (UNAM), 22860 Ensenada, México, ² Tomsk Polytechnic University, Tomsk 634050, Russia, ³ Centro de Ciencias Aplicadas y Desarrollo Tecnológico (UNAM), Circuito Exterior S/N, Ciudad Universitaria, CP 04510, México, DF, México
Julia.Kotolevich@gmail.com.

ABSTRACT

It should be recognized that there is a great deal of excitement in the realization that gold has previously unrecognized properties. Indeed the field of catalysis by gold is just beginning to open up. In fact gold has been demonstrated to be the element of choice for some catalytic reactions, which has a surprisingly high activity and is not replicated by other metals. There are several processes, such as low-temperature oxidation or PROX CO, for which there are no alternatives deserving gold catalysts. There is, therefore, a rich redox chemistry of gold that we are currently exploring, and we can expect new exciting discoveries in the coming years. It was studied the influence of support nature on activity of CO oxidation reaction which is now being used by many researchers as a standard test reaction. After many years of research of gold catalysts essential requirements for their high oxidation activity were formulated: small particle size, use of "reactive" support, and a preparative method that achieves in intimate contact of Au particle with the support.

We were studied SiO₂-based supports which were modified with Ce, La, Fe or Mg oxides by co-precipitation of HMS with FTIR CO, TEM, TGA and in CO oxidation after different pretreatment. It was found that FTIR spectra of CO adsorbed on gold catalysts are correlate with their catalytic activity. Thus, FTIR measurements showed that Au/CeHMS, Au/MgHMS and Au/HMS catalysts in the presence of oxygen can be oxidized much easily as compared with Au/FeHMS and Au/LaHMS samples and can form catalytically active sites.

ACKNOWLEDGMENTS

This work is funded by CONACYT projects 79062, 83275 and 130407 and PAPIIT-UNAM projects 103513, IN114209, IT200311-3 and IT200114 (Mexico); CSIC, project 201180E104 and MICINN, project ENE2009-14522-C05, (Spain); Russian Science Foundation. We thank E. Flores, Sh. Sandoval, I. Gradilla, J. Mendoza, E. M. Aparicio, J. Peralta, M. Sainz and R. Velez for technical assistance.

Semiconductor/MOR nanostructured composites: characterizations and photocatalysis

O. E. Jaime-Acuña^{1,a}, H. Villavicencio², V. Petranovskii³, and O. Raymond³

¹Posgrado en Física de Materiales, Centro de Investigación Científica y de Educación superior de Ensenada-Centro de Nanociencias y Nanotecnología- Universidad Nacional Autónoma de México, Ensenada 22890, Baja California México, ²Dirección Nacional de Informática Educativa, Ministerio de Educación de Cuba, La Habana, Cuba,

³Centro de Nanociencias y Nanotecnología, Universidad Nacional Autónoma de México, AP 14, Ensenada 22890, Baja California México.
o.jaime.acuna@gmail.com

ABSTRACT

The synthesis of porous materials is important for the chemical industry because of the various potential uses that they may have. Furthermore, the inclusion of transition metals and/or semiconductors nanoparticles in these matrices change their properties (optical and structural) allowing the design and development of new application-convenient materials. Several Si and Al precursors (including waste solid materials derived from geothermal energy conversion process) were used in this work following the MX/a/2012/013218 patent route to synthesize semiconductor/mordenite composites, demonstrating the capability to governing the morphology and chemical composition of obtained materials. By varying the synthesis conditions is possible to tune the whole system including the optic-spectral responses, which permits to design the materials for a specific final application.

Variations of morphology, chemical composition and crystalline structure of nanostructured mordenite-based composites due the different synthesis conditions were characterized using XRD, HRTEM, SEM, EDS, ED, UV-Vis, IR, and PL spectroscopic techniques. Results of samples probing as photocatalysts were discussed.

ACKNOWLEDGMENTS

This work was partially supported by CONACYT (Grants 127633 and 102907) and DGAPA-UNAM (Grants IN113312 and IN110713). The authors thank E. Aparicio, I. Gradilla and F. Ruiz for technical assistance.

Natural Iron-Exchanged Mordenite: UV-Vis Diffuse Reflectance and Mössbauer Characterization.

D. Tito Ferro^{1,a}, I. Rodríguez Iznaga^{2,b}, B. Concepción Rosabal², F. Chávez Rivas³, V. Petranovskii⁴, F. F. Castellón Barraza⁴ and A. Penton Madrigal⁵

¹Centro Nacional de Electromagnetismo Aplicado, Universidad de Oriente, Cuba. ²Instituto de Ciencia y Tecnología de Materiales (IMRE) - Universidad de La Habana, Cuba. ³Departamento de Física, ESFM-IPN, México. ⁴Centro de Nanociencias y Nanotecnología – UNAM. Ensenada, B.C. México. ⁵Facultad de Física - Universidad de La Habana. La Habana, Cuba.

^adaria@cnea.uo.edu.cu, ^binocente@imre.oc.uh.cu

ABSTRACT

Natural zeolites, such as mordenite, are attractive because of their ion-exchange properties, thermal stability, availability and low price. Their modification with Fe is stimulated by their possible applications in environmental catalysis for the selective catalytic reduction of nitrogen oxides (SCR-NO_x) in the exhaust gases, as well as their use for elimination of contaminants in water, such as nitrates and chromate anions, etc.

The aim of present work was to prepare natural mordenite (ZP) from Palmarito de Cauto deposit, Cuba, with particle size +0.038-0.074 mm, purify it, modify it via Fe²⁺ and Fe³⁺ ion-exchange in acid medium at 80°C, and characterize starting and modified materials by UV-Vis diffuse reflectance and Mössbauer spectroscopies.

The UV-Vis diffuse reflectance spectra of ZP itself demonstrate significant and complex optical absorption; that is typical for natural zeolites. Samples modified by Fe²⁺ and Fe³⁺ ion-exchange, Fe²⁺ZP and Fe³⁺ZP respectively show an additional absorption at ~ 275 nm. In addition, for Fe³⁺ZP very wide increased absorption is observed in the range from 300 to 700 nm (see Fig. 1). Broad and, most likely, multicomponent absorption band at ~275 nm, according to the reported in [1] was associated to an oxygen-to-iron charge-transfer complex dispersed iron species in zeolitic channels. Note, the starting ZP material also have this band, due to inherent iron admixture. The wide adsorption observed in the Fe³⁺ZP sample in the range 300-700 nm was associated with agglomerate particles of iron oxide on external surface of zeolite crystals.

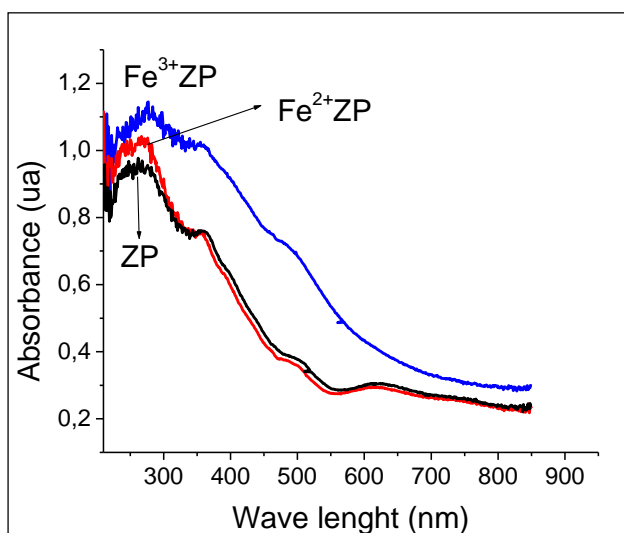


Fig. 1. UV-Vis diffuse reflectance spectra of ZP and iron-modified Fe²⁺ZP and Fe³⁺ZP zeolites.

The Fig. 2 shows Mössbauer spectra, at room temperature, of ZP and iron-exchanged Fe²⁺ZP and Fe³⁺ZP samples. Three doublets for all exchanged samples were used for determination of Mössbauer spectra resolution and

parameters (Table I). Two doublets are associated to Fe^{3+} and one to Fe^{2+} . The analysis of the values of the Mössbauer parameters and the reported studies [2-4] lead to conclusion that all Fe^{2+} is found in octahedral coordination, while Fe^{3+} is present both in octahedral and tetrahedral coordination.

All previously mentioned lead to conclusion that in the Fe^{2+}ZP sample all Fe^{2+} incorporated by ion exchange should be mainly in cationic extra-framework positions inside of mordenite channels as a charge compensating cations. In the case of the Fe^{3+}ZP sample, the incorporated Fe^{3+} can be both in cationic extra-frameworks positions as a charge compensating cation and in form of oxy-hydroxides originated by Fe^{3+} hydrolysis.

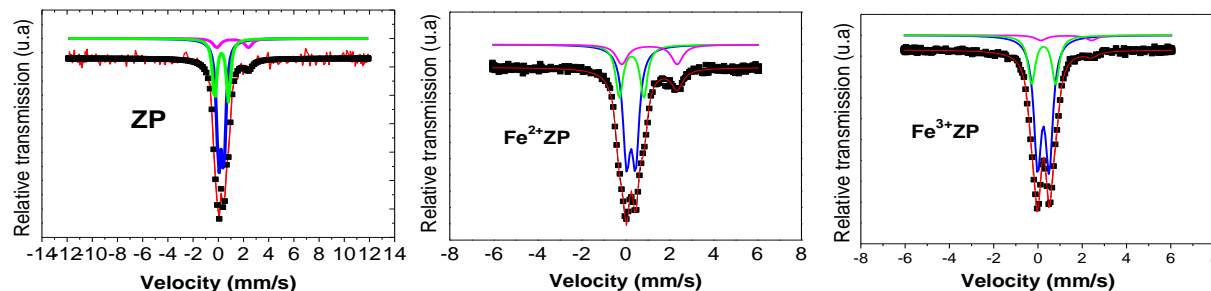


Fig. 2 Mössbauer spectra at room temperature for ZP and iron modified zeolites.

Table I. Mössbauer parameters for ZP and iron modified Fe^{2+}ZP and Fe^{3+}ZP zeolites.

Sample	Doublet (1) Fe^{3+} tetrahedral			Doublet (2) Fe^{3+} octahedral			Doublet (3) Fe^{2+} octahedral		
	IS mm/s	QS mm/s	A %	IS mm/s	QS mm/s	A %	IS mm/s	QS mm/s	A %
ZP	0,35	0,41	59,0	0,38	1,09	32,0	1,25	2,51	8,0
Fe^{2+}ZP	0,36	0,41	54,0	0,39	1,11	29,0	1,20	2,52	17,0
Fe^{3+}ZP	0,36	0,53	69,0	0,37	1,08	27,0	1,39	2,29	4,0

IS: isomer shifts QS: quadrupole splitting A: relative area

ACKNOWLEDGMENT

Thanks are given to E. Aparicio, I. Gradilla, J. Peralta and E. Flores for the technical assistance. This research was supported by CONACYT, México, through grant 102907 and UNAM-PAPIIT through the grants IN207511, IN110713 and IA200914-2. F. Chavez Rivas acknowledge support from COFAA-IPN-Mexico.

REFERENCES

- [1] F. Chávez-Rivas, G. Rodríguez-Fuentes, G. Berlier, I. Rodríguez-Iznaga, V. Petranovskii, R. Zamorano-Ulloa and S. Coluccia. *Micropor. Mesopor. Mater.* 167, 76 (2013).
- [2] A. Tuel, I. Arcon and J. M. M. Millar. *J. Chem. Soc., Faraday Trans.* 94, 3501 (1998)
- [3] R. Roque-Malherbe, C. Díaz-Aguila and M. Hernández-Vélez, *Zeolites* 10, 685 (1990)
- [4] G. Rodriguez-Fuentes, L.C. de Ménorval, E. Reguera and F. Chávez Rivas, *Micropor. Mesopor. Mater.* 111, 577 (2008)

A theoretical study of Cu_2O and Cu_x clusters hosting in MOR dealuminated zeolite

Joel Ant3nez-Garc3a^{1,2}, D. Homero Galv3n Mart3nez¹, Vitalii Petranovskii¹

¹Centro de Enseñanza T3cnica y Superior, CINAP, Av. CETYS Universidad No. 4, Fracc. El Lago, Apdo. Postal 1196, 22210 Tijuana, B. C. M3xico, ²CNyN-UNAM, Ensenada, Baja California, M3xico
donald@cnyunam.mx

INTRODUCTION

Mordenite (MOR), a high rich silica zeolite[1,2], possess a network of channels that interconnects a 12-membered-ring (12-MR) channels (6.5×7Å) with tortuous 8-MR channels [3] (2.6×5.7Å). Since 8-MR channels are considered too narrow to be accessed by molecules, just 12-MR channels are considered as molecular sieves. The interest on rich silica MOR zeolites, relays on that their catalytic properties can be manipulated and the thermal stability increased as the Si/Al ratio increases [4–6]. However, dealuminated MOR zeolite presents minor stability in comparison with synthetized rich silica [7]. The goal of the present work is to perform a systematic study of the configuration of different composites, obtained by the inclusion of different cooper-oxide clusters within 12-MR channel (main channel), and study how the electronic properties becomes affected as effect of those inclusions. On addition to this study, the effect of composites immerse on water were also studied. Is expected that the present work, serve as support for future theoretical studies on which not only wants to understand the effect of different inclusions in composite properties, but also the presence of other atomic species (Al,Na) within the frame of a MOR zeolite.

COMPUTATIONAL DETAILS

For our calculations, Cu_2O_x ($x=1,4$) and Cu_x ($x=2,5$) cluster configurations were considered. As starting point, the MOR unit cell at ground state was geometrically optimized by density functional theory (DFT) method, employing the Dmol³ [8–10] program package. For the exchange-correlation energy, was employed the Becke, Lee, Yang and Parr (BLYP) [11,12] gradient-corrected functional. For the expansion of wave functions of different atomic species under consideration, double numerical with d and p polarization (DNP) basis set (comparable to 6-31G, 6-31G(d) and 6-31G(d,p) Gaussian-type basis sets) [12] was used to take into account all core electrons interactions reasonably. After MOR unit cell was geometrically optimized, a cooper or cooper-oxide cluster was disposed at the center of the main channel of it, and then the composite was conducted to the minimal energy configuration under the parameterization early described. To investigate the effect on forbidden energy gap of dry and water immerse MOR- Cu_2O_x optimized configurations, was employed the conductor-like screening model (COSMO).

RESULTS AND DISCUSIONS

Our results shown that on all composites, different cluster were captured via electrostatic confinement. From analysis of structural configurations for distinct composites under study, we observe slightly structural changes in zeolite frame, while different clusters presents certain grade of reconfiguration as effect of charge redistribution on zeolite. A comparison of electrostatic potential surfaces, show that cooper-oxide clusters have stronger confinement that just pure cooper clusters. Particularly, the composite MOR- Cu_2O presented the highest confinement value ($\sim\pm 0.2$ Ha). [Cu]4s, [O]2p and [Cu]3d. However, while [O]2p contribution increases as x increases for Cu_2O_x inclusions, our results suggest that for odd x-value on Cu_x inclusions [Cu]3d orbital domains, contrarily for a pair value hybridized orbital [Cu]4s domains.

A comparison of different forbidden energy gap value is shown on Table 1, on it is observed that in comparison with pure zeolite (MOR), the different inclusions on composites conducts to a considerably decrease of this value. However, the observed energy behavior has not lineally dependency as the number of atomic species increases.

CONCLUSIONS

On addition to White *et al.* [13], our results shows that not only pure dealuminated MOR-zeolite is stable, but almost the composited discussed here are also stables. Our results show that both Cu_2O_x and Cu_x composites, are confined electrostatically within the main channel of zeolite. Although the number of atomic species (Cu, O) in

clusters is a factor to diminish the forbidden energy band gap, this effect is most pronounced for Cu clusters as effect of metallization of system, however their confinement is weaker.

ACNOWLEDGMENT

This research was supported by CONACyT (México) under the grant No. 102907.

Figure 2: Table 3: Forbidden gap energy for different composite configuration. Wet is referred to water immerse zeolite.

Hosting of Cu ₂ O _x Clusters			Hosting of Cu _x Clusters	
Configuration	Gap [eV]		Configuration	Gap [eV]
	Dry	Wet		Dry
MOR	6.4218	6.4491	MOR-Cu ₂	1.5238
MOR-Cu ₂ O	1.3061	1.6598	MOR-Cu ₃	0.6530
MOR-Cu ₂ O ⁻	1.1973	N/A	MOR-Cu ₄	0.6762
MOR-Cu ₂ O ⁺	1.4422	N/A	MOR-Cu ₅	0.0314
MOR-Cu ₂ O ₂	0.5714	0.6258		
MOR-Cu ₂ O ₃	0.2177	0.0381		
MOR-Cu ₂ O ₄	0.2449	0.2176		

REFERENCES

- [1] W. M. Meier, Z. Kristall. **115**, 439 (1961).
- [2] P. Joshi, A. Shaikh, and V. Chumbhale, J. Inclusion Phenom. Molec. Recogn. Chem. **13** (1992) 171-179.
- [3] A. Corma, F. Rey, S. Valencia, J. L. Jordá, and J. Rius, Nature Materials **2** (2003) 493-497 .
- [4] G. Ooms and R. A. van Santen, Recl.Trav. Chim. Pays-Bas **106** (1987) 69-71.
- [5] F. Goovaerts, E. F. Vansant, J. Philippaerts, P. De Hulsters, and J. Gelan, J. Chem. Soc., Faraday Trans. 1 **85** (1989) 3675.
- [6] N. Viswanadham and M. Kumar, Microporous Mesoporous Mater. **92** (2006) 31-37.
- [7] H. K. Beyer, I. M. Belenykaja, I. W. Mishin, and G. Borbely, *Structural Peculiarities and Stabilisation Phenomena of Aluminium Deficient Mordenites*, Elsevier, Budapest (1984).
- [8] Software from Accelrys Inc.: <http://www.accelrys.com>.
- [9] B. Delley, J. Chem. Phys. **92** (1990) 508-517.
- [10] B. Delley, J. Chem. Phys. **113** (2000) 7756-7764.
- [11] A. D. Becke, PRA **38** (1988) 3098-3100.
- [12] C. Lee, W. Yang, and R. G. Parr, PRB **37** (1988) 785-789.
- [13] J. C. White and A. C. Hess, J. Phys. Chem. **97** (1993) 6398-6404.

Natural mordenite as an ionic exchanger of Cr³⁺ from alkaline solutions

V. Córdova Rodríguez^{1,a}, I. Rodríguez Iznaga^{2,b}, R. M. Acosta Chávez³ and V. Petranovskii⁴.

¹Facultad de Ingeniería Química, Universidad de Oriente, Cuba. ²Instituto de Ciencia y Tecnología de Materiales (IMRE)-Universidad de La Habana, Cuba. ³Facultad de Ciencias, Universidad de Oriente, Cuba. ⁴Centro de Nanociencias y Nanotecnología – UNAM, Ensenada, B.C. México.

^aval@fiq.uo.edu.cu, ^binocente@imre.oc.uh.cu

ABSTRACT

The use of natural zeolites for the protection of the environment has stimulated by the excellent results obtained, as well as by the non-toxic nature of these materials, their availability and low cost. One of the most important properties of the zeolites is ion exchange, which allows their use for the removal and recovery processes of noxious metal cations from aqueous solutions and residual liquors. In practice, these processes tend to be cyclical, and therefore requires taking into account the possibility of regeneration for re-use of the zeolite [1]. The aim of the present work is to evaluate the capacity of the natural mordenite from Palmarito de Cauto (ZN) deposit, Cuba, [2] as an ion exchanger for removal of Cr³⁺ cations from aqueous solutions with alkalinity and different chrome concentration. The stability of the mordenite under cyclic processes of treatment with alkaline solutions and its capacity to descend the pH of the solutions is analyzed as well.

To study the chromium removal, ZN samples, with particle-size +0.09 -0.315 mm, were treated with CrCl₃ solutions of different concentration (1.06, 2.55 and 3.55 mg/L) and variable alkalinity (pH = 4.4, 6.1 and 8.3). To determine the neutralizing effect of this zeolite in the aqueous mediums, ZN samples of different particle-sizes were treated with NaOH solution with diverse pH values (11, 12 and 13). To evaluate the stability of the mordenite, the ZN sample with particle-size +0.09 -0.315 mm, was subject of twenty cycles of treatment with NaOH solution at pH = 12. All treatments were performed at room temperature and using 1g/20mL solid/solution ratio.

The X-ray diffraction patterns of ZN after twenty cycles of treatment with NaOH solution don't show significant change of the mordenite framework, which shows that this mordenite originated from Palmarito de Cauto deposit has high stability in alkaline mediums.

The results of treatment of NaOH solutions with ZN samples of different particle-sizes (Zp) showed that zeolite has an important neutralizing effect on this alkaline solution, expressed in a decrease of pH to a value next to seven (Fig. 1). Several factors can influence in this neutralization. Non-zeolitic phase, such as carbonates, and protons from surface OH-groups presents in this natural zeolite can react with hydroxyl anions from NaOH solution, which provoke a decrease to pH. Neutralizing effect is more prominent in the samples with lower particle-sizes, which is in line to higher contact surface. The results are consistent with the amphoteric character reported to the zeolites [3].

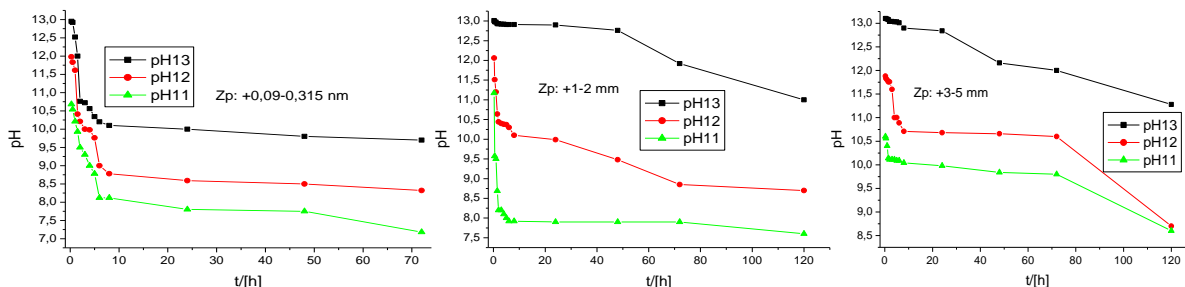


Fig. 1. Evolution of pH during treatment time in the alkaline solutions treated with ZN.

Ion-exchange of ions, such as Ca²⁺, Na⁺ and K⁺, presented in the natural mordenite with Cr³⁺ cations from the ion-exchanged solutions lead to the removal of chromium from liquid phase and its retention in a solid phase of zeolite (Fig. 2). As a results of the treatments, contain of chromium in solution is decreased to a value next to zero. This

behavior is independent of the starting chromium concentration and pH of exchanged solution used. However, a limited precipitation of chromium phase of low solubility at higher pH is not discarded. On the other hand, low amount of iron in the treated solution is observed. It can be explained by dissolution of non-zeolitic iron-containing impurity phase present in the mineral sample of natural zeolite ZN. The presence in ZN of iron associated phases, such as iron oxides, was shown in our previous work [4].

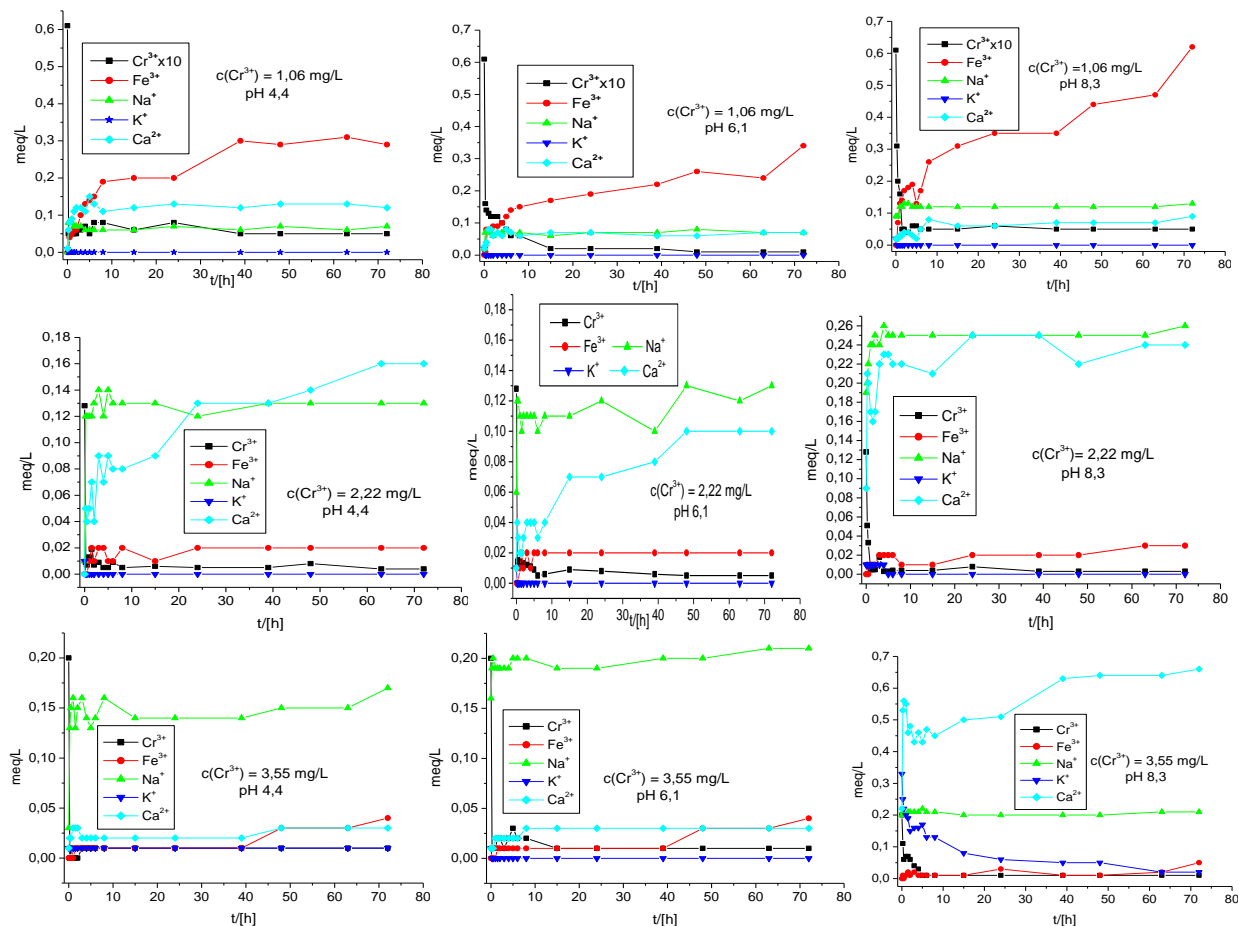


Fig. 2. Milliequivalents of Cr^{3+} and others cations in solution.

The obtained results lead to the conclusion that natural zeolite from Palmarito de Cauto deposit has an important neutralizing effect on alkaline solutions. The mordenite is stable in alkaline mediums and has capacity to remove Cr^{3+} ions from solution with wide range of pH.

ACKNOWLEDGMENTS

Thanks are given to E. Aparicio, I. Gradilla, J. Peralta and E. Flores for the technical assistance. This research was supported by CONACYT, México, through grant 102907 and UNAM-PAPIIT through the grants IN207511, IN110713 and IA200914-2.

REFERENCES

- [1] I. Rodríguez-Iznaga, A. Gómez, G. Rodríguez-Fuentes, A. Benítez and J. Serrano. *Micropor. Mesopor. Mater.* 53, 71 (2002).
- [2] M. C. Céspedes-Ortiz, I. Rodríguez-Iznaga, V. Petranovskii, R. Rizo-Beyra y L. Aguilera-Domínguez. *Rev. Cuba. Quím.*, XXIII, 80 (2011).
- [3] A. Rivera G. Rodríguez-fuentes and E. Altshuler. *Micropor. Mesopor. Mater.* 40, 173 (2000).
- [4] D. Tito Ferro, I. Rodríguez Iznaga, B. Concepción Rosabal, F. Chávez Ribas, V. Córdova Rodríguez y R. Rizo Beyra. *Rev. Min. y Geol.*, 27, 22 (2011).

Study of Ag nanoparticles growth over monometallic (Ag) and bimetallic (Fe/Ag) systems supported in mordenite

P. Sánchez-Lopez¹, R. Obeso-Estrella¹, S. Miridonov², S. Fuentes³, F. F. Castellón-Barraza³ and V. Petranovskii³

¹Posgrado en Ciencia e Ingeniería de Materiales de la Universidad Nacional Autónoma de México, CNYN-UNAM, Apdo. Postal 14, C.P. 22800, Ensenada, B. C., México, ²Departamento de óptica, Centro de Investigación Científica y de Educación Superior de Ensenada. C.P. 22860, Ensenada, B. C., México, ³Universidad Nacional Autónoma de México, Centro de Nanociencias y Nanotecnología, Apdo. Postal 14, C.P. 22800, Ensenada, B. C., México
perlaroe@cnyunam.mx

INTRODUCTION

The technique of ion exchange is frequently used to alter the properties of zeolites, e.g., to prepare acidic or basic catalysts [1]. In this work mordenite type zeolite with molar ratio $\text{SiO}_2/\text{Al}_2\text{O}_3$ of 13 was selected to prepare monometallic (Ag or Fe) and bimetallic (Fe/Ag) systems. Ag and Fe ions were introduced by ion exchange method from aqueous solutions of AgNO_3 and FeSO_4 at 0.03 N concentration. Samples treated with FeSO_4 solution were acidified with a several drops of H_2SO_4 solution, to adjust the pH to a value of 2.

EXPERIMENTAL

The materials were characterized by XRD to evaluate the crystallinity of the phases. Chemical composition of the samples was determined by EDS technique; the type of metal species was identified by UV-Vis spectroscopy. Surface area was calculated by BET method and the morphology was studied by TEM micrographs.

RESULTS

The patterns of X-Ray diffraction (Fig. 1) presented significant changes, such as variation of intensity of some peaks and appearance of other, for example corresponding to Ag_2O . However, crystalline structure of mordenite save intact. The surface characteristics of ion-exchanged bimetallic system showed very little variation with respect to the starting mordenite, which may indicate that the metal species occupy little space in the channels of the mordenite. The study by UV-Vis showed that the monometallic (Ag or Fe) and bimetallic (Fe/Ag) systems had absorbance in the UV range, which can be attributed to the charge transfer from oxygen to ions Fe^{3+} or Fe^{2+} or the electronic transition of the isolated ion Ag^+ .

The TEM micrographs revealed that the agglomeration of silver nanoparticles is very different with the presence of Fe, in the AgFeMOR sample, in comparison with monometallic AgMOR system. This difference is illustrated in Fig. 2 and Fig. 3. It should be noted that in the micrographs of bimetallic FeAgMOR sample are noticeable ordered groups of monosized nanoparticles. Their size matches to the diameter of the channel of the mordenite. Presumably, these domains correspond to clusters of silver, formed in the channels, so they have regular sizes limited by channel diameter, and orderly geometric arrangement imposed by mordenite crystal lattice.

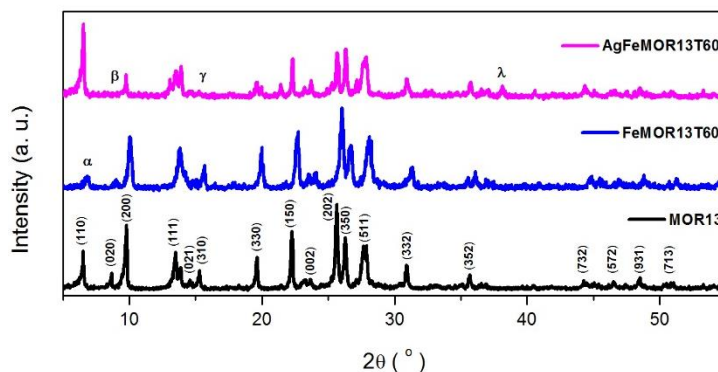


Fig. 1. XRD patterns of the MOR, FeMOR and AgFeMOR.

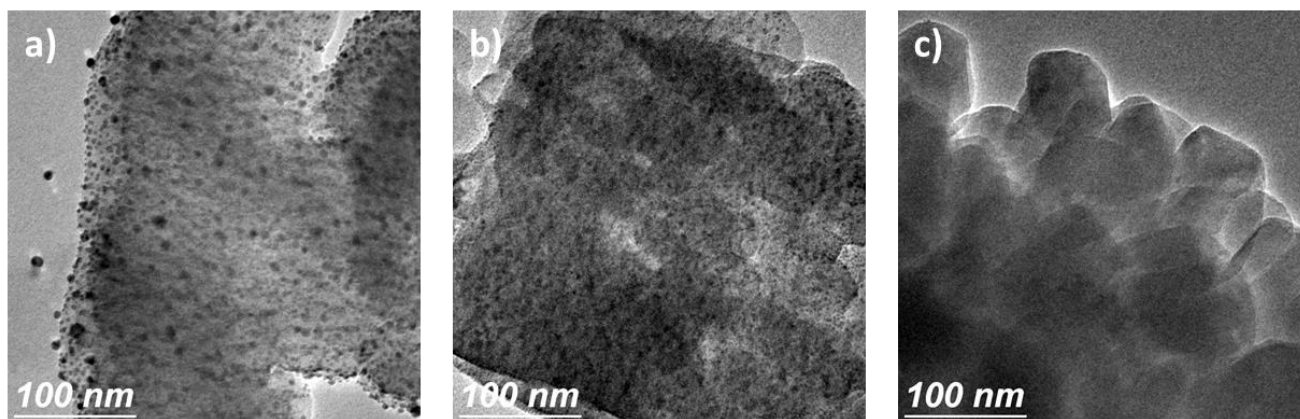


Fig. 2. Micrographs of the samples; a) AgMOR, b) FeAgMOR and c) FeMOR

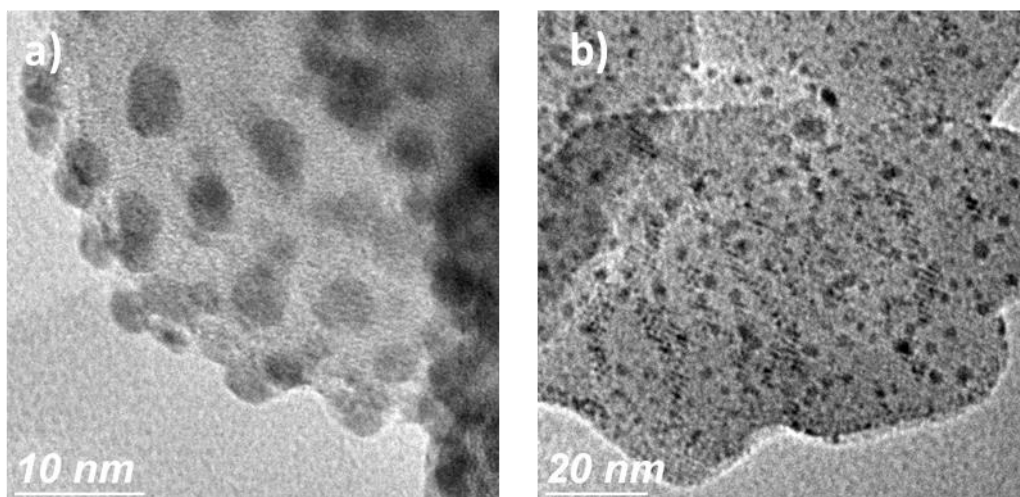


Fig. 3. Micrographs at higher resolution of the samples; a) AgMOR, and b) FeAgMOR.
Difference in the formation pattern of Ag nanoparticles is clearly seen.

ACKNOWLEDGMENTS

Authors acknowledge technical assistance of F. Ruiz, E. Aparicio, I. Gradilla, J. Peralta, and E. Flores, and financial support from CONACYT 102907, 179619 and DGAPA 203813 grants.

REFERENCES

[1] H. Van Bekkum, E. M. Flanigen, P. A. Jacobs and J. C. Jansen, *Studies in Surface Science and Catalysis*. Elsevier, Vol. 137, 1-57, (2001).

Insight of the silver influence to hidrothermal stability of Cu-mordenite catalysts for selective catalytic reduction of NOx.

R.E. Ramírez-Garza¹, F.F. Castellón-Barraza¹, I. Rodríguez-Iznaga², A. Simakov¹

¹Centro de Nanociencias y Nanotecnología – UNAM. Ensenada, B.C. México, ²Instituto de Ciencia y Tecnología de Materiales (IMRE)-Universidad de La Habana, Cuba.

rramirez@cnyunam.mx

ABSTRACT

Automobile exhaust gases and emission of combustion gases from the industries are the principal responsible of the NOx emissions at the atmosphere (Lloyd, 2011). The NOx emissions lead to several issues such as smog formation, acid rain and ozone layer abatement (Janssen and Santen, 1999; Lloyd, 2011).

Catalytic reaction is the most efficient method to eliminate the NOx emissions (Larese et al., 2003; Lloyd, 2011). At the earliest 90's, Iwamoto et al. (1991) reported that hydrocarbons, such as propene, are effective to the NOx reduction in zeolite-supported catalysts. From that time to nowadays, there have been a great number of articles related to the hydrocarbon selective catalytic reduction (HC-SCR) of NOx. Copper-catalysts for the HC-SCR presents the higher catalytic activities and are more economic compared with Pt, Pd and Rh catalysts (Gervasini, 1999; Maia et al., 2010). However, the deactivation of copper catalysts caused by water is a well known phenomenon. Hydrothermal aging is a process that occurs in automobile catalytic converters. The presence of water provokes that Cu⁺¹ species migrate from the zeolite structure and form CuO clusters (Kuroda et al., 2002). In addition, it is observed that the presence of water induces a dealumination of zeolite and phase transformation of copper (Park et al., 2001).

The addition of a second metal into a catalyst normally increases the activity and the chemical and thermal stability. Boix and Fierro (1999) found that cobalt only reduces at temperatures above 400 °C. Chajar et al. (1998) found that silver addition to copper catalysts, prepared by conventional ion exchange, leads to a partial hydrothermal stability of copper. However, little efforts have been done to elucidate the factors that influence to the improvement of the hydrothermal stability of copper-catalyst.

This study deals with the factors that influence the hydrothermal stability for the silver addition. Copper-silver catalysts were characterized by mean of TPR and UV-vis techniques. The results of NO conversion suggest that silver is located close to sites where copper was exchanged. A higher copper mass in the catalysts generates more stable copper species, which silver is not capable to remove. The rise in temperature reduction peak in TPR analysis for the copper-silver catalysts allow us to infer that silver is promoting the stability of Cu⁺ species.

REFERENCES

- [1] Lloyd, L. (2011). Environmental catalysts. In: Handbook of Industrial Catalysts, Fundamental and Applied Catalysis, pages 439–470. Springer US.
- [2] Janssen, F. and Santen, R. (1999). Environmental Catalysis. Imperial College Press, London.; Kim, M. H., Nam, I.-S., and Kim, Y. G. (1997). Water tolerance of mordenite-type zeolite catalysts for selective reduction of nitric oxide by hydrocarbons. Applied Catalysis B: Environmental, 12(2-3):125 – 145.
- [3] Larese, C., Galisteo, F., Granados, M., Mariscal, R., Fierro, J., Furi, M., and Ruiz, R. (2003). Deactivation of real three way catalysts by CePO4 formation. Applied Catalysis B: Environmental, 40(4):305 – 317.
- [4] Iwamoto, M., Yahiro, H., Tanda, K., Mizuno, N., Mine, Y., and Kagawa, S. (1991). Removal of nitrogen monoxide through a novel catalytic process. 1. Decomposition on excessively copper-ion-exchanged ZSM-5 zeolites. The Journal of Physical Chemistry, 95(9):3727–3730.
- [5] Gervasini, A. (1999). Characterization of the textural properties of metal loaded ZSM-5 zeolites. Applied Catalysis A: General, 180(1-2):71 – 82.
- [6] Maia, A., Louis, B., Lam, Y., and Pereira, M. (2010). Ni-ZSM-5 catalysts: Detailed characterization of metal sites for proper catalyst design. Journal of Catalysis, 269(1):103 –109.
- [7] Kuroda, Y., Kumashiro, R., and Nagao, M. (2002). Prominent redox feature of copper ion exchanged in ZSM-5-type zeolite. Applied Surface Science, 196(1-4):408 – 422.

- [8] Park, G. G., Chae, H. J., Nam, I.-S., Choung, J. W., and Choi, K. H. (2001). Deactivation of mordenite-type zeolite catalyst by HCl for the reduction of NO_x with NH₃. *Microporous and Mesoporous Materials*, 48(1-3):337 – 343.
- [9] Boix, A. and Fierro, J. L.G. (1999). X-ray photoelectron spectroscopy analysis of platinum and/or cobalt-loaded zeolites relevant for selective catalytic reduction of nox. *Surface and Interface Analysis*, 27(12):1107–1113.
- [10] Chajar, Z., Denton, P., Berthet de Bernard, F., Primet, M., and Praliaud, H. (1998). Influence of silver on the catalytic activity of Cu-ZSM-5 for no scr by propane. effect of the presence of water and hydrothermal agings. *Catalysis Letters*, 55(3-4):217–222.

Synthesis and characterization of mordenite (MOR) dispersed into silica

Z. Bedolla, J.N. Díaz, G. Alonso, V. Petranovskii

Centro de Nanociencias y Nanotecnología, UNAM, Km. 107 carretera Tijuana-Ensenada, Apdo. Postal 14, C.P. 22800, Ensenada, Baja California, México
zairabe@cryn.unam.mx

ABSTRACT

In the last years the interest to develop novel materials for reducing gas emission produced from incomplete fossil fuel burning was increased [1]. It was reported that zeolite catalysts containing transition metal ions within their structure often show activity as heterogeneous catalysts being able to reduce NO_x selectively. The catalytic activity of copper ion-exchanged in FAU and MFI zeolite for this purpose was for the first time reported in the 80's by M. Iwamoto *et. al.* [2], and later confirmed by Yuejin Li and W. Keith Hall [3]. These researches have led to studies focused on metal promoted zeolites, being iron and copper zeolites extensively studied.

Copper containing hybrid supports based on silica gel with different amounts of mordenite (MOR) additive (up to 50 wt %) were prepared by two different routes. In the first one, MOR was exchanged by Cu²⁺ before the sol-gel (SG) process, in the second one ion-exchange was realized after MOR-SiO₂ preparation. The presence of zeolite did not inhibit the silica gel formation, as well as the zeolite structure was not destroyed during sol-gel process. It is important that MOR pore volume was not sealed, its internal surface area was not closed by silica gel, and the ion-exchange was not obstructed. MOR-SiO₂ hybrid samples becomes thermally more stable in reference to pure silica gel.

In both cases, copper was concentrated in mordenite; at least, the presence of copper on the silica gel substrate was not observed. Analysis by UV-Vis spectra showed that the copper state in the samples significantly depends on the synthesis route. Temperature of appearance of copper plasmon is different for these sets of specimens. Also, it was observed that reducibility of copper was more evident for the samples where the amount of MOR was higher.

ACKNOWLEDGMENTS

The authors acknowledge technical support of this research by Eric Flores Aquino, Eloisa Aparicio, Israel Gradilla, and financial support by the projects PAPIIT-UNAM IN110713, CONACyT N°102907, and CONACyT N°155388.

REFERENCES

- [1] P. Granger, V. I. Parvulescu, *Chem. Rev.* 111 (2011) 3155-3207.
- [2] M. Iwamoto, H. Furukawa, Y. Mine, F. Uemura, S. Mikuriya, S. Kagawa, *J. Chem. Soc., Chem. Commun.* (1986) 1272-1273.
- [3] Y. Li, W. Keith Hall, *J. Catal.* 129 (1991) 202-215.

Mass to frequency change in frequency domain sensors coated with zeolites

Fabian N. Murrieta-Rico^{1,a}, Vitalii Petranovskii^{2,b}, and Oleg Yu. Sergiyenko^{3,c}

¹ Center for Scientific Research and Higher Education of Ensenada, Ensenada, Baja California, Mexico, ² CNYN-UNAM, Ensenada, Baja California, Mexico, ³ Engineering Institute of Autonomous University of Baja California, Mexicali, Baja California, Mexico

^afmurriet@cicese.edu.mx, ^bvitalii@cnyun.unam.mx, ^csrgnk@iing.mx1.uabc.mx

INTRODUCTION

One of the unique properties of zeolites is that they can selectively absorb molecules. As consequence a zeolite increases its mass when absorbs the molecules of a chemical compound, for this reason they are excellent materials for building selective sensors. Frequency domain sensors (FDS) convert a measurand into a frequency domain output. When a FDS is coated with zeolite, detection and concentration measurement of specific chemical compounds can be done. There are many kinds of zeolite coated FDS [1], with frequency output range from some MHz to GHz. Since a small change in the zeolite mass is proportional to a small frequency shift, frequency measurement system is critical for the sensor. According to the sensor and the zeolite there is a relationship between the absorbed mass in the zeolite and the sensor's frequency output. In this work it is explained how the mass changes in the zeolite depend from the dimensions of the coating and the crystal dimensions in a quartz crystal microbalance (QCM).

FDS COATED WITH ZEOLITES

A mass increment exists in a zeolite when it absorbs molecules of a specific chemical compound, and a decrement happens in desorption. If a FDS is coated with a zeolite, the mass change (increment or decrement) generates a modification in the pressure on the FDS surface. A FDS is made of a piezoelectric element that resonates when it is on a specific electronic circuit configuration; when the pressure applied on the crystal surface is varied, the resonance frequency changes. There are three kinds of FDS coated with zeolites: quartz crystal microbalances (QCM), devices based on surface acoustic wave (SAW), and microcantilevers [1].

MASS CHANGE MEASUREMENT FOR FDS

The relationship between mass change (Δm) and frequency change (Δf) in a QCM is expressed through the Sauerbrey equation [2]:

$$\frac{\Delta f}{\Delta m} = -\frac{2.3 \times 10^{-6} F^2}{A} \quad (1),$$

where Δf is the observed frequency change in Hz, F [Hz] is the fundamental resonant frequency of the crystal, A [cm^2] sensing surface area.

One particular case reported in the literature illustrates a QCM that was prepared for detection of gases [2]. In such device, zeolite-A was used for coating the QCM. The QCM device was composed of AT-cut quartz with dimension of $15mm \times 15mm \times 0.33$ mm. It has Au electrodes (200 nm in thickness) attached on both sides. Cr layers (50 nm) were formed as binding layers between the Au-electrodes and the quartz to improve the adhesion.

According to Eq. 1 and the QCM parameters, Δm can be easily calculated for the frequency shifts (Δf) reported on the literature [2]; for the crystal used on that experiments, Eq. 1 can be expressed as Eq. 2.

$$\gamma \Delta f = \Delta m \quad (2)$$

Eq. 2 indicates that using $\gamma = -10.9 \times 10^6 g/Hz$, a mass change equal to $\Delta m = 10.9 \times 10^{-6} g$ leads to frequency shift of $\Delta f = 1 Hz$. From Eq. 1, if the QCM fundamental resonance frequency (F) value is higher, we can detect smaller mass changes For a experiments in [2], can be easily shown that for $\Delta m = 10.9 \times 10^6 g$ is equal to

3.64×10^{17} H₂O molecules; for the maximum frequency shift reported $\Delta f = 50\text{Hz}$, we know that 1.82×10^{19} water molecules have been detected.

The experiments reported in [1] used a frequency counter Iwatsu SC-7201; in that frequency counter the reciprocal counting technique is used for measuring, this means that for a frequency measuring with 9 digits of exactitude are needed 10 seconds [3]. Frequency measurement using rational approximation allows to have a minimum error in measurements in a very short time [4]. For the sensor developed by Sasaki, minimum error is achieved in 1 ms, with a relative error of 11.39 Hz, this means that in a very short time it is possible to measure $\Delta m = 120.9 \times 10^{-6} g$ in $\Delta f = 12\text{ Hz}$ above the minimum relative error. Also is important to note that for frequency measurement using rational approximations, the frequency resolution can be improved if a reference frequency value closer to the frequency of the measurand is used.

CONCLUSIONS

A FDS coated with zeolite is able to detect very small mass changes. The Sauerbrey equation shows the relationship between a mass and a frequency change, due to physical dimensions of the crystal used, moreover the fundamental resonant frequency of the quartz crystal determines the resolution of the mass to frequency conversion. For being able to use such FDS it is required to have a fast and accurate frequency measuring system. This leads to a measuring system that is able to measure chemical compounds concentration with very small mass resolution.

ACKNOWLEDGMENT

This research was supported by CONACYT, Mexico, through the Project 102907 and UNAM-PAPIIT through the grant IN110713

REFERENCES

- [1] Zheng, Y.; Li, X.; Dutta, P.K. Exploitation of Unique Properties of Zeolites in the Development of Gas Sensors. *Sensors* 2012, *12*, 5170-5194.
- [2] Sasaki, I., Tsuchiya, H., Nishioka, M., Sadakata, M., & Okubo, T. Gas sensing with zeolite-coated quartz crystal microbalances—principal component analysis approach. *Sensors and Actuators B: Chemical*, 2002, *86*(1), 26-33.
- [3] Johansson, S. (2005). New frequency counting principle improves resolution. In *Frequency Control Symposium and Exposition, 2005. Proceedings of the 2005 IEEE International*, 638-635.
- [4] Daniel Hernández Balbuena, Oleg Sergiyenko, Vera Tyrsa, Larysa Burtseva, Moisés Rivas López, Signal frequency measurement by rational approximations, *Measurement*, 2009, *42*(1), 136-144.

Specific features of the spin echo signal in ferromagnetic $\text{Fe}_{100-x}\text{V}_x$

Elena Kurenkova¹, Marina G. Shelyapina²

¹Center for Magnetic Resonance, Saint-Petersburg State University, Russia, ²Department of Nuclear – Physics Research Methods, Saint-Petersburg State University, Russia
e.kurenkova@spbu.ru

INTRODUCTION

Currently pulse nuclear magnetic resonance (NMR) is widely used to study magnetic properties of magnetically ordered materials. NMR spectra provide information about magnetically nonequivalent nucleus sites in solids. Such information is especially valuable when one deals with disordered and amorphous bulk solids or magnetic nanoparticles, where polarized neutron diffraction can not provide exhaustive information.

In the past recent years, there was an increasing interest in the magnetic properties of bcc $\text{Fe}_{1-x}\text{V}_x$ disordered alloys and artificially structured systems such as Fe/V multilayers. The interest is caused by a number of exceptional magnetic properties of these materials. Bulk bcc V is often considered as a non-magnetic metal. But in $\text{Fe}_{1-x}\text{V}_x$ disordered alloys and for small vanadium concentrations x , the V atom can exhibit an induced magnetic moment up to about $1 \mu_B$. Furthermore, small V clusters and monolayers supported on the surface of nonmagnetic metal reveal localized magnetic moments.

There is a number of publications devoted to the study of $\text{Fe}_{1-x}\text{V}_x$ by X-ray magnetic circular dichroism (XMCD) [1], neutron scattering [2], and theoretically as well [3]. Both experiment and theory confirm the antiferromagnetic couplings between Fe and V atoms. However, all abovementioned methods provide information averaged over the lattice. Nevertheless, even in disordered alloys the distribution of atoms over the lattice is not absolutely homogeneous, and the knowing of local structure is very important, as it governs the magnetic properties of the alloy. From this perspective NMR is a unique tool that may provide such kind of information. But, to extract it correctly a deep understanding of how a magnetic system responds on an rf pulse is required. Here we report on the results of the NMR study of the $\text{Fe}_{0.92}\text{V}_{0.08}$ alloy.

EXPERIMENTAL DETAILS

All the experiment has been made using the universal NMR/NQR Tecmag Redstone spectrometer in the frequency range 20-81 MHz in zero magnetic field at $T = 77$ K. We used the Hahn echo method, which is based on the excitation of a nuclear spin system by two rf pulses of equal duration and amplitude. According to the theory the spin echo signal occurs in time 2τ after the action of the second rf pulse, where τ is the delay between two pulses. The appearance of the echo signal is determined by the spin relaxation processes. The resonance frequency is determined by the hyperfine field at the nucleus site. To reproduce the NMR spectrum one plots the echo signal amplitude versus the rf frequency.

RESULTS AND DISCUSSION

It has been found that the ^{57}Fe nuclear echo signal in $\text{Fe}_{0.92}\text{V}_{0.08}$ can not be explained within the framework of the Hahn echo approach, which is usually used in NMR, due to (1) an anomalous dependence of the echo amplitude on the delay between pulses and the delay between pulse trains; (2) presence of additional echo signals; (3) too large echo signal shift etc. Moreover, it was found that the echo shape strongly depends on the rf pulse duration (at fixed pulse amplitude), Fig. 1. If the pulses are sufficiently short, the echo has a Gaussian shape, however, with pulse duration increasing it becomes more and more complex and additional echo signals appear. In Ref. [5] similar phenomena were reported.

From our point of view there are several possible issues of the appearance of additional echo signals: (1) incomplete recovery of thermodynamic equilibrium of the spin system; (2) quadrupole interactions, leading to multi-quantum transitions (despite the ^{57}Fe nucleus has no quadrupole moment ($I = 1/2$), the signal from the ^{51}V nucleus, which is quadrupole ($I = 7/2$), may interfere); (3) dynamic effects caused by electron-nuclear interactions, that leads to the dynamic frequency shift. Due to the presence of a multidomain structure the enhancement factor (that is a ratio between the applied rf field and the rf field that “feel” the nucleus due to the screening by the electron shell) in the

domains and domain walls is significantly different in magnitude. It leads to the spread of the oscillation frequencies of the magnetic moments of nuclei during exposure to alternating field and induces the corresponding nonlinear effects.

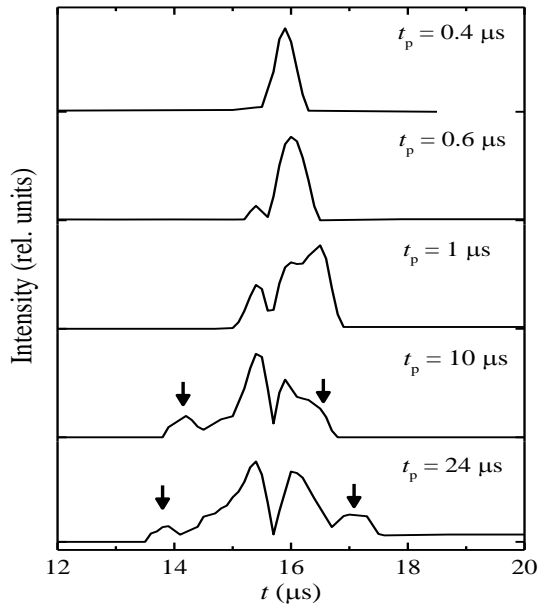


Fig.1. ^{57}Fe spin echo signal in $\text{Fe}_{0.92}\text{V}_{0.08}$ at different pulse duration t_p . Delay between pulses $\tau = 25\mu\text{s}$, delay between scans of pulses is 100 ms, number of scans = 8192. The additional signals are shown by arrows.

Another interesting result is that at continuous repetition of identical excitation conditions one observes jump changes in the spin echo amplitude. It may be caused by phenomena related to Barkhausen effect, which was observed in these alloys [6]. However, in our experiment the sample is in a zero external magnetic field, and the question, is it possible to observe such kind of phenomena under the action of an alternating rf pulse, is open. An alternative explanation is that such changes are caused by Foucault currents.

As it was mentioned above, in magnetically ordered compounds to reproduce NMR spectra one has to plot the echo amplitude versus the rf frequency. From this perspective the correct measurement of the echo amplitude value is extremely important. However, it has been found, that the echo amplitude in $\text{Fe}_{0.92}\text{V}_{0.08}$ is sensitive to the direction, in which we change the rf frequency when recording the spectrum, from low to high frequency or vice versa (the spectrum width is about 50 MHz). Possibly one deals with the effect of demagnetization of domains like in magnetic hysteresis.

Thus, the main conclusion is following. In $\text{Fe}_{0.92}\text{V}_{0.08}$ the excitation parameters and the distribution of the enhancement coefficient in the domains and domain walls are very important as they result in non-linear phenomena that affect the spin-echo signal and, consequently, the NMR spectrum.

ACKNOWLEDGEMENTS

The work was performed at the Center for Magnetic Resonance of Saint-Petersburg State University.

REFERENCES

- [1] M.M. Schwickert, et al. Phys. Rev. B 57 (1998) 13681.
- [2] I. Mirebeau, G. Parette, J. Appl. Phys. 53 (1982) 1960.
- [3] D.D. Johnson, F.J. Pinski, J.B. Staunton, J. Appl. Phys. 61 (1987) 3715.
- [4] A. Scherz et al. Phys. Rev. B64 (2001) 180407.
- [5] D.K. Fowler et al. Phys. Stat. Sol. (a) 92, 545 (1985)
- [6] D. Fruchart, N. Skryabina, L. Spivak. J. Alloys Compd. 383 (2004) 180-183

Unusual structures of aggregates of silica nanoparticles

N. Bogdanchikova¹, O. Martynyuk^{1,2}, A. Pestryakov², R. Luna Vázquez G.³, F. Ruiz Medina¹, A. Huerta-Saquero¹,
J.L. Calvario V.³

¹ Centro de Nanociencias y Nanotecnología-UNAM, Ensenada, México, ² Tomsk Polytechnic University, Tomsk, Russia, ³ Universidad Autónoma de Baja California, Ensenada, México
oxanam@cryn.unam.mx

ABSTRACT

A study of the different structures of silica nanoparticles obtained by high resolution transmission electron microscopy (HRTEM) is presented in this work. Silica nanoparticles was synthesized by neutral S⁰I⁰ templating route [1,2], modified with the aim of preparation of separated nanoparticles. The unusual structures were observed after one day with small amount of water that was added and after several months without water addition.

It was observed that majority of silica nanoparticles are chaotically distributed, but during their storage the formation of spontaneously self-assembled nanoparticles aggregates with great multiplicity of morphologies were revealed. Silica displays intricate patterns assembling from nanosize particles and form structures with different shapes and organization. It was found that silica nanoparticles have tendency to self-assemble in aggregates around empty circular spaces with diameter ~160 (Fig.1). It was also found that silica nanoparticles can form aggregates with different morphologies which include angle of approximately 90-120° as typical element. The present work consists in the discussion of morphologies of these silica nanoparticle aggregates.

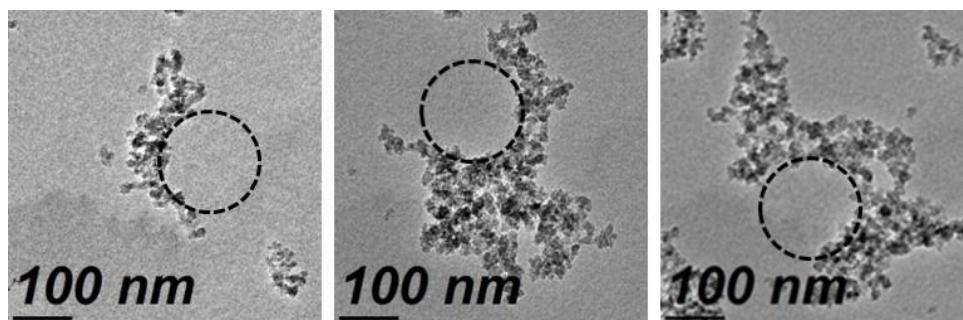


Fig.1. Example of complex structures of silica nanoparticles ensembles

ACKNOWLEDGMENTS

We are further grateful to E. Flores, J. Mendoza, J. Peralta and M. Sainz for technical assistance. Financial support by CONACYT Project No 79062, PAPIIT-UNAM Projects IT200311, IT200114 (Mexico) and Russian Science Foundation is greatly appreciated.

REFERENCES

- [1] Tanev, P., Pinnavaia, T.J. Science 267, 865-867 (1995).
- [2] B. Pawelec, P. Castano, T.A. Zepeda. Appl. Surf. Sci. 254, 4092–4102 (2008).

Au Seeds Stability

L. Avalos^{1,a}, J.M. Romo-Herrera^{2,b}, O.E. Contreras^{2,c}, E.I. Chaikina^{1,d}, E.R. Méndez^{1,e}

¹Depto. Optica, Div. Física Aplicada CICESE, Ensenada B.C., México, ²CNyN-UNAM, Ensenada B.C., México,

^aavalosm@cicese.edu.mx, ^bjmromo@cnyunam.mx, ^cedel@cnyunam.mx, ^dchaikina@cicese.mx,

^eemendez@cicese.mx

ABSTRACT

Gold metal nanoparticles (NPs) have attracted great attention due to their ability to support localized surface plasmon resonances (LSPRs). These Plasmon modes can be tailored by modifying the size and shape of the NPs. Such optical properties suggest them for sensing, imaging, diagnosis and biomedical therapeutic applications among others.

Colloidal techniques have become one of the most useful techniques to synthesize such Au NPs, with the ability to obtain a high degree of shape control by means of non-sophisticated equipment. Specifically, the seed-mediated approach [1] gives access into a wide range of morphology when adjusting the synthesis parameters. There, the basic idea is to use a strong reducing agent to prepare Au⁰ seeds (2-5nm sphere NPs) from gold salts in water as the first step; to subsequently use a weak reducing agent to reduce more gold salt onto the seed NPs as the second step. In the solution-phase synthesis, the shape displayed by the NPs is strongly dependent on the initial seeds.

We follow a common colloidal method to obtain the Au seeds (3-4nm sphere NPs) using NaBH₄ as the strong reducing agent and citrate, CTAB and CTAC as stabilizers (Figure 1).

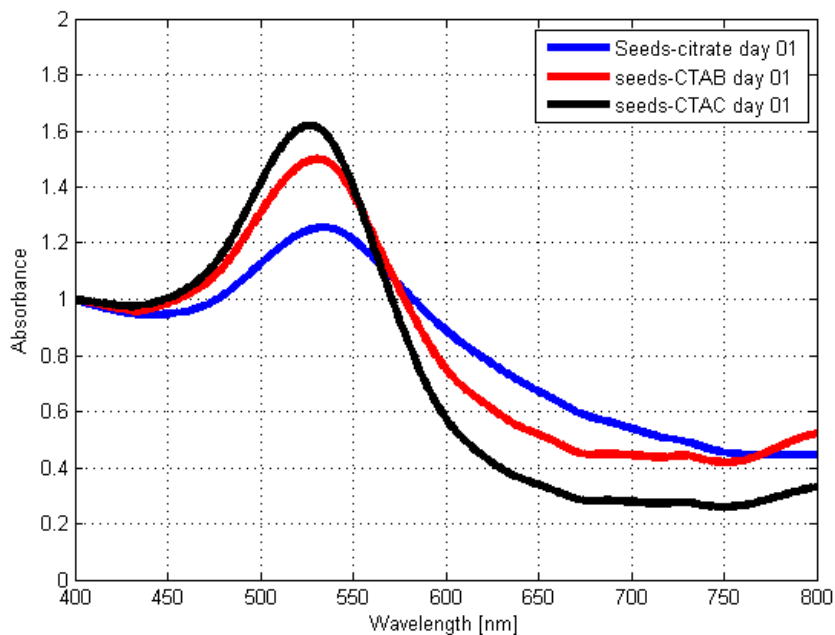


Figure 1. Absorbance of the seeds one day after synthesis and stabilized with citrate, CTAB or CTAC.

Once obtained, we have monitored the NPs stability when protected by different capping agents. Besides, we have been able to finely tune the seeds size increasing their diameter in steps of 1nm and analyzing the role of different capping agents into the size increment control. Finally, we explore the aging effect of the seeds for obtaining anisotropic NPs. The samples were characterized by UV-Vis spectroscopy and TEM.

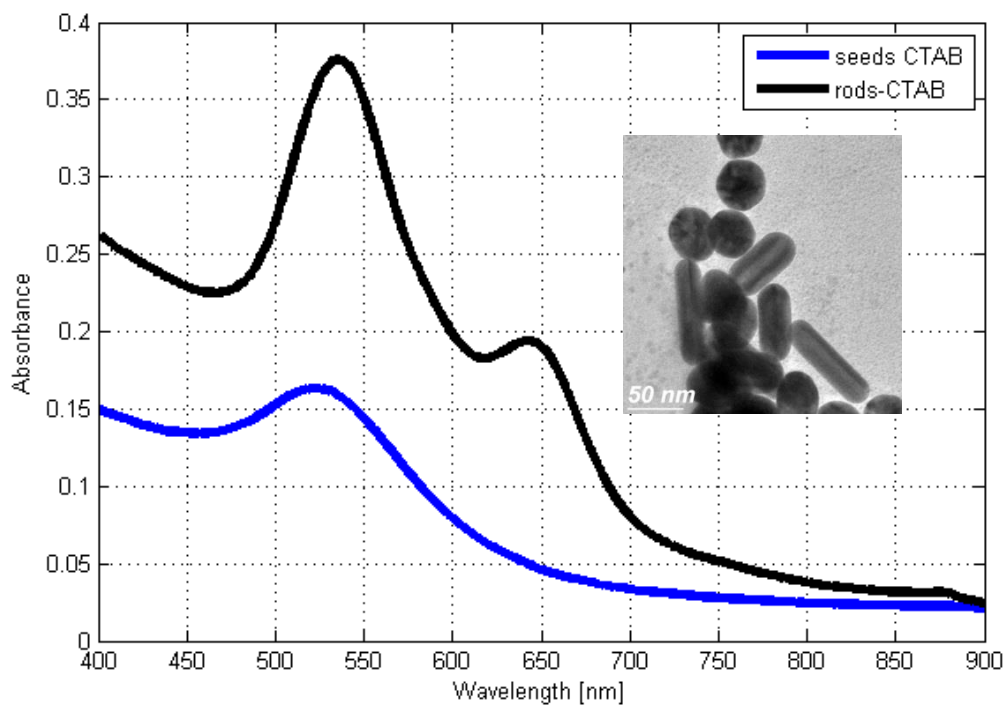


Figure 2. Absorbance of seeds and nanorods. The inset shows a TEM image of nanorods and spheres synthesized by the seed-mediated approach.

ACKNOWLEDGEMENTS

We thank J. Mendoza, F. Ruiz, E. Flores and H.F. Alonso for technical assistance.

REFERENCE

[1] N.R. Jana, L. Gearheart, C.J. Murphy. *J. Phys. Chem B* 105: 4065-4067 (2001).

Effect of laser pulses overlapping on the yield of silver nanoparticles

D.O. Oseguera-Galindo, M.A. Santana-Aranda, A. Martínez-Benítez,
G. Gómez-Rosas, A. Pérez-Centeno

Departamento de Física, CUCEI, Universidad de Guadalajara, Blvd. M. García Barragán 1421, Guadalajara, Jal.
44430, México

davidhor@cnyun.unam.mx

ABSTRACT

Chemical reduction method is the most commonly used for the synthesis of metal nanoparticles. However, from 1993 the year, the laser ablation method has been used as an alternative method to obtain these nanoparticles in a medium liquid [1]. Which consist at the irradiation with a laser on solid immersed in liquid and the nanoparticles were obtained thanks to the condensation of the laser generated plasma's ions in the liquid [2]. In addition, parameters laser as frequency, energy density, repetition rate, pulse duration, in combination with optical properties of the target, play a key role in the size and shape of nanoparticles. Nevertheless, other effect could influence on the yield nanoparticles is the pulse overlapping. There are works where overlap occurs totally in the pulses because of the target is not displaced during synthesis, while in other works are decreasing the overlapping using an X-Y or rotational driving mechanics which allows scanning laser irradiation on the target. Although, they used these mechanics to avoid craters in the target do not use to analyse the effect to obtain nanoparticles. In this work, we analyse the effect of the pulses overlapping on the yield of nanoparticles, for this purpose, silver nanoparticles were obtained for laser ablation of a silver target immersed in water. Besides, we employed the emission of a pulsed Nd:YAG laser at 532 nm, with an energy of 0.5 J/pulse, a pulse duration of 5 ns, a repetition rate of 10 Hz and a spot diameter of 1 mm. We used a XY driving mechanism which allows scanning laser irradiation on target's surface with different speeds. We could control the scanning density to 2500, 5000, 7500 and 10000 pulses/cm², combining scanning speed v_x and repetition rate of the laser R_{rep} as a shown in next equation

$$\rho = \left(\frac{R_{rep}}{v_x} \right)^2 \quad (\text{pulses} / \text{cm}^2)$$

where ρ is the pulses density or density scanning which involve the overlapping of a number of consecutive pulses. The obtained nanoparticles suspensions were analyzed by UV-Vis absorbance. We observed a clear decrease of peak absorption of nanoparticles suspensions as the scanning density increases. This means that increasing the amount of overlapping pulses decreases the production of nanoparticles by laser ablation.

ACKNOWLEDGEMENTS

Authors want to thank the technical assistance of Israel Ceja Andrade. This work was partially supported by U. de G. (under programs pro-SNI and PROCOFIN) and CONACyT (under grant CB156773). Actually, David Omar Oseguera Galindo thanks to CONACyT for posdoctoral fellowship and the Centro de Nanociencias y Nanotecnología Universidad Nacional Autónoma de México (CNYN-UNAM), Ensenada B.C México for allowing to continue with the posdoctoral position.

REFERENCES

- [1] Neddersen J, Chumanov G, Cotton TM, Applied Spectroscopy, 47, 1959 (1993)
[2] Oseguera- Galindo D, Martínez -Benítez A, Chávez- Chávez A, Gómez -Rosas G, Pérez- Centeno A, Santana – Aranda, J Nanopart Res , 14, 1133 (2012).

Synthesis of Cu₂O nanoparticles by pulsed laser ablation of a Cu target submerged in water

Juan J. Velarde¹, Roberto Machorro², Catalina López², Vitalii Petranovskii², Gabriel Alonso², Serguei Stepanov¹

¹Centro de Investigación Científica y de Educación Superior de Ensenada (CICESE), Ensenada, B.C., México,

²Centro de Nanociencias y Nanotecnología, Universidad Nacional Autónoma de México (CNyN-UNAM),

Ensenada, B.C., México

jjvelard@cnyn.unam.mx

INTRODUCTION

Pulsed laser ablation in liquid (PLAL) provides a technique to synthesize nanoparticles. Due to the high pressure and the high temperature reached within the plume of the ejected material, the formation of metastable phases is favored. Also, chemical interactions between the plume species and the surrounding liquid provide routes for the synthesis of new materials [1,2].

There are two types of copper oxides: cupric oxide (CuO) and cuprous oxide (Cu₂O). Both oxides are of interest due to their applications [3,4]. Laser ablation of a copper target submerged in water is a viable alternative for the synthesis of Cu_xO nanoparticles [5,6]: the interaction of laser light with the copper target provides the ionized copper species (Cu⁺ and Cu⁺²) that can interact with water molecules and diluted oxygen. However, to ensure that the stoichiometry of the desired product is obtained, the proportion of ionized species must be controlled. This control can be achieved by controlling the energy of the laser pulse [5,6,7].

EXPERIMENTAL

Nanoparticles were synthesized by laser ablation of a copper (5N purity, 99.999%) target submerged in a column of 10 mm of distilled water. The metal plate was placed on the bottom of a glass vessel and it was irradiated by the fundamental output ($\lambda = 1064$ nm) of a Q-switched Nd:YAG laser operating at 10 Hz with a pulse duration of 6 ± 1 ns. A converging lens having a focal length of 200 mm was used to focus the beam onto the target surface. The obtained diameter size of the obtained spot were of 0.9 mm. The energy of the pulse was measured to be 108 mJ/pulse and the computed fluence 18 J/cm². The target was exposed to ablation during 20 min. To ensure that the ablation occurred on a non-afore-ablated surface, the vessel containing the copper target was continuously displaced.

Upon irradiation, the color of the suspension turned to olive green. After exposure to ablation, the absorption spectrum of the obtained colloidal suspension was measured and a sample for observation by a TEM was prepared. A drop of the suspension was placed on a copper grid coated with carbon and was dried at ambient temperature and the process was repeated three times to ensure nanoparticle content on the grid. The distribution of the particle size was obtained by measuring the diameters of more than 600 particles in sight on 7 different micrographs of the same sample suspension.

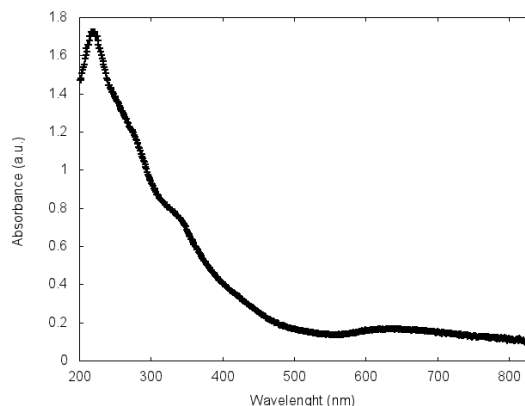


Fig. 1 Absorption spectrum of colloidal suspension of obtained nanoparticles.

RESULTS

Fig. 1 shows the obtained absorption spectrum. In the UV interval, the spectrum exhibits a peak at 216 nm and two shoulders, one at 270 nm and the other at 340 nm, whereas in the visible a broad absorption peak appears at 645 nm. The absorption spectrum is similar to the ones reported in the literature [5,6,8], which is an indication of the formation of Cu_xO nanoparticles. The peak at 216 nm indicates the presence of Cu^0 whereas both shoulders at 270 nm and 340 nm can be associated with the formation of Cu_2O . Also, the broad peak at 645 nm is typical of a displaced signal for the surface plasmon resonance mode due to an interface interaction of Cu^0 and Cu_xO .

A TEM micrograph and the computed histogram for the distribution of particle size are shown in Fig. 2. Average particle size was estimated to be 2.4 ± 1.1 nm, which is a small size and a narrow size distribution [5]. This small size is due to the small fluence of the laser beam. The available average energy for every superficial site of the target under the spot limits the depth (and, thus, the volume) of the ablated material and the temperature of the generated plume is low. Therefore, condensation of the plume occurs rapidly preventing the growth of the formed particles.

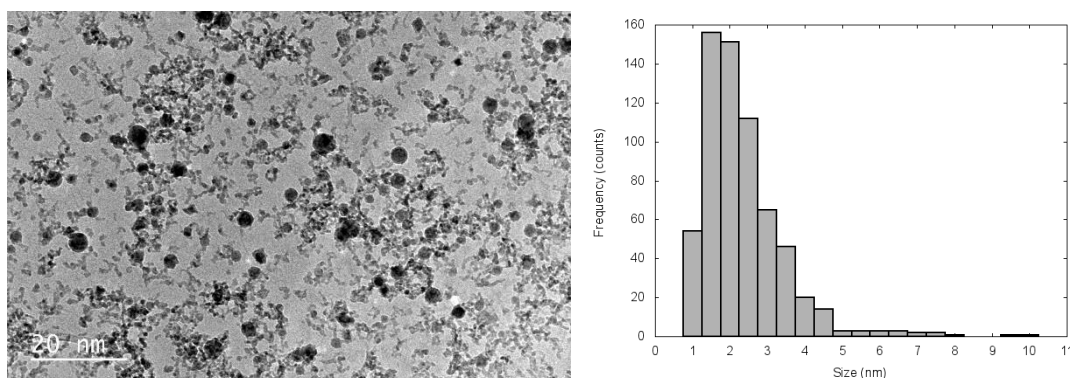


Fig. 2. A TEM micrograph of synthesized nanoparticles and a histogram depicting the particle size distribution.

The formation of $\text{Cu@Cu}_2\text{O}$ core-shell nanoparticles has been observed in similar experimental settings [8]. Some features of the nanoparticles on the recorded TEM micrographs are indication of the formation of a core-shell structure. This structures are in agreement with the displacement for the signal of the surface plasmon resonance for Cu, and the presences of peaks and shoulders for both Cu^0 and Cu_2O in the absorption spectrum.

CONCLUSIONS

PLA of a copper target under water resulted in the production of small nanoparticles. Absorption spectrum gave indication of the presence of metallic copper and the formation of copper oxide, preferably cuprous oxide. The average size of the obtained nanoparticles is in agreement with reported results indicating that at small fluences, nanoparticle size decreases [5]. Chemical composition of nanoparticles and the dependence between chemical composition and fluence must be further investigated.

ACKNOWLEDGMENTS

We acknowledge the support of the project PAPIIT-IN105914. We also acknowledge the valuable assistance of Eduardo Pérez-Tijerina and the use of the ablation facilities at CICFIM-UANL.

REFERENCES

- [1] G. W., Yang, P. *Mat. Sci.* **52**, 648 (2007).
- [2] L. Lin, M. Hong, M. Schmidt, *et al.*, *CIRP Annals* **60**, 735 (2011).
- [3] P. Korzhavyi and B. Johansson, *Literature review on the properties of cuprous oxide (Cu_2O) and the process of copper oxidation*, Technical Report (Swedish Nuclear Fuel and Waste Management Co., Stockholm, Sweden, 2011), pp. 41.
- [4] P. Tran, S. Batabyal, S. Pramana, *et al.*, *Nanoscale* **4**, 3875 (2012).
- [5] A. Nath and A. Khare, *J. Appl. Phys.* **110**, 043111 (2011).
- [6] T. Tsuji, K. Iryo, Y. Nishimura, *et al.*, *J. Photochem. and Photobio. A* **145**, 201 (2001)
- [7] A. Bogaerts, Z. Chen, R. Gijbels and A. Vertes, *Spectrochim. Acta B* **58**, 1867 (2003).
- [8] N. Haram and N. Ahmad, *Appl. Phys. A* **111**, 1131 (2013).

Nonlinear optical properties and light guiding in spherical and elongated Ag nanoparticles.

Bonifacio Can-Uc¹, Raúl Rangel-Rojo¹, Luis Rodríguez-Fernández² and Alicia Oliver²

¹Centro de Investigación Científica y de Educación Superior de Ensenada, Carretera Ensenada-Tijuana No. 3918, Zona Playitas, C.P. 22860, Ensenada, B. C. México, ²Instituto de Física, Universidad Nacional Autónoma de México, Circuito de la Investigación Científica S/N, Ciudad Universitaria, Distrito Federal, México.
bcan@cicese.edu.mx

ABSTRACT

We report the study of the nonlinear response and light guiding of a composite material and channel waveguide containing silver nanoparticles. The absorptive and refractive contributions to the nonlinearity of the sample were studied using the z-scan technique with 80 fs pulses at 825 nm. A large anisotropy was observed in both the refractive and absorptive contributions to the nonlinearity of a sample containing aligned elongated NPs. On the other hand, the channel waveguide propagation losses at 632 nm are also presented.

INTRODUCTION

Metallic nanoparticles (NPs) embedded in dielectric substrates have showed several interesting properties, such as large optical nonlinearities, with response times in the ps regime [1]. Thereby these materials have attracted a considerable amount of attention for their application in optical systems [2], in particular, glass matrices containing metal NPs, for their third-order optical susceptibility $\chi^{(3)}$, whose real part is related to the nonlinear refractive index n_2 [3]. For these materials, the size, shape, and composition of the NPs become design parameters to optimize $\chi^{(3)}$, including the relative contributions of nonlinear refraction and absorption (described by the twophoton absorption coefficient [4]). In particular, elongated, aligned NPs have shown interesting highly anisotropic linear, and nonlinear optical properties [1, 5]. The complete characterization of the nonlinear optical response is made by using the z-scan technique, which allows determination of both the n_2 and χ parameters, including their signs [6], using a fs laser source. In this work, we focus in the study of nonlinear absorption and refraction and the propagation of light of both spherical and elongated Ag NPs embedded in silica waveguides. The nonlinearities were done using the z-scan technique with light pulses from a Ti:Sapphire oscillator, whose wavelength is centered at 830nm, and a 88 fs pulse duration (FWHM), at 94 MHz repetition rate. The channel waveguide were obtained by a single implantation through an electroformed mask of nickel-cobalt alloy. The waveguide propagation is also presented with the 632 nm of a laser diode.

RESULTS

Figure 1a shows the absorption spectra of both spherical and elongated Ag NPs, where we used linearity light polarized at 0° and 90° with respect to the long axis of the elongated NPs. The samples were produced by ion-implantation techniques described elsewhere [7]. The top figure shows the typical spectrum for spherical NPs, while in the case of elongated NPs, show the usual surface plasmon resonance at 375 nm for the 0° , while the 90° data shows a second broader plasmon resonance, that are characteristic of elongated NPs. The open and closed aperture z-scan results are shown in Fig. 1b and Fig. 1c for spherical and elongated NPs respectively. The results show in 1b the typical behavior of the positive nonlinear refraction index (bottom) and no discernible contribution of the nonlinear absorption (top). In the case of elongated NPs, the figure show the clear presence of two photon absorption for 0° polarized light ($\chi > 0$), and no discernible nonlinear absorption for the 90° polarization in red color. In the case of the closed-aperture z-scan results, shown in black, the presence of a sizeable positive nonlinear refraction effect ($n_2 > 0$) for 0° polarization is observed, and no discernible response for the 90° polarization.

In order to characterize the propagation losses of the waveguides, a laser diode operating to 632 nm with a pigtail of single mode optical fiber was coupled to the waveguide entrance, and the transmitted light was measured through a microscope objective and directed to an optical detector. Figure 2a is the transmission image of the channel waveguides containing spherical NPs and the Fig. 2b and Fig. 2c show the transmission image of the output face of the waveguides and intensity distribution of waveguide output light respectively.

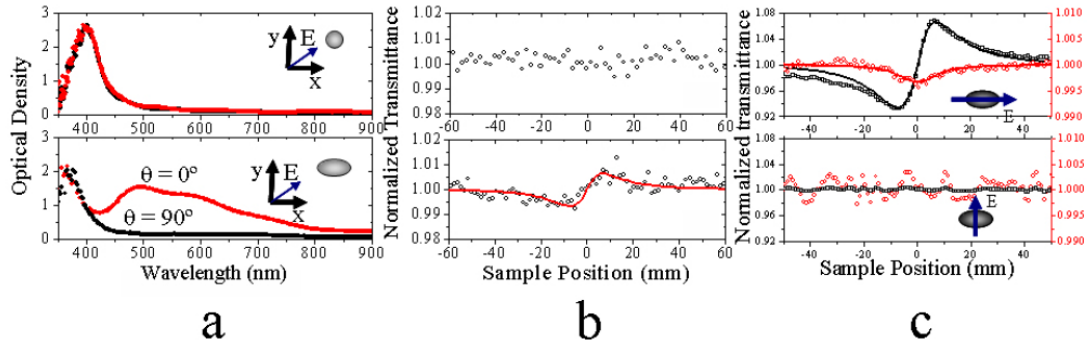


Fig. 1 The a are the absorption spectra for both spherical and elongated NPs. The b are the nonlinear absorptive (top) and refractive scans (bottom) for spherical NPs. The c are the nonlinear absorptive and refractive scans where the red data are the response to the absorptive contribution and the black are the refractive contribution. The continuous lines are the theoretical fits.

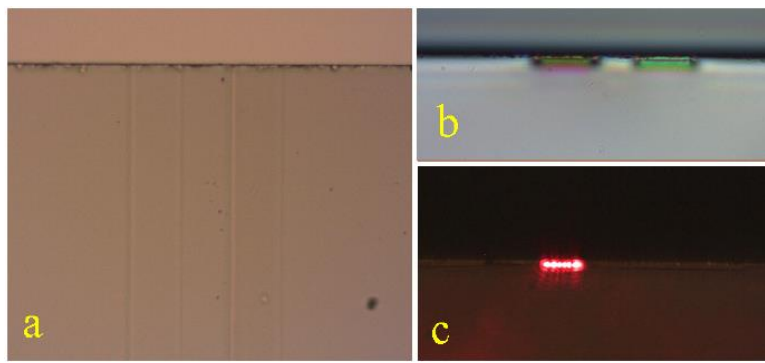


Fig 2. The a and b show the top channel waveguides and the output face waveguide taken with transmission microscope and c is the output waveguide with the light of the laser coupled.

CONCLUSIONS

In summary, we have studied the nonlinear optical response in spherical and elongated Ag NPs embedded in SiO₂ by mean the z-scan technique. We can see a clear anisotropy in the absorptive and refractive responses in the case of elongated NPs, being more pronounced in the nonlinear refraction. In the other hand, we are able to see the propagation of light and to measure the propagation losses of the channel waveguide.

ACKNOWLEDGMENTS

We want to acknowledge CONACyT-Mexico for partial funding through Grant No. 102937 and Scholarship No. 221750

REFERENCES

- [1] R. Rangel-Rojo, J. McCarthy, H. T. Bookey, A. K. Kar, L. Rodriguez-Fernandez, J. C. Cheang-Wong, A. Crespo-Sosa, A. Lopez-Suarez, A. Oliver, V. Rodriguez-Iglesias and H. G. Silva-Pereyra, *Optics Communications* 282, pp. 1909_1912 (2009).
- [2] H. Marquez, D. Salazar, R. Rangel-Rojo, J. L. Angel-Valenzuela, J. V. Vazquez, E. Flores-Romero, L. Rodriguez-Fernandez, and A. Oliver, *Optical Materials* 35, pp. 927_934 (2013).
- [3] G. Mattei, P. Mazzoldi and H. Bernas, *Topics in Appl. Phys* 117, (2010).
- [4] A. Meldrum, R. López, R. Magruder, L. Boatner and C. White, , *Topics in Appl. Phys.* 116, pp. 255_285 (2010).
- [5] B. Can-Uc, R. Rangel-Rojo, L. Rodriguez-Fernandez and A. Oliver, *Optics Materials Express* 3(12), pp. 2012_2021 (2013).
- [6] M. Sheik-Bahae, T. T. Said, T. Wei, D. J. Hagan, and E. W. Van Stryland, *IEEE Journal of Quantum Electronics* 26(4), pp. 760_769 (1990).
- [7] A. Oliver, J. A. Reyes-Esqueda, J. C. Cheang-Wong, C. E. Román-Velázquez, A. Crespo-Sosa, L. Rodríguez-Fernández, J. A. Seman, and C. Noguez, *Phys. Rev. B* 74, pp. 245425 (2006).

Interaction of silver nanoparticles with *Candida albicans*

Roberto Vazquez-Muñoz¹, Ernestina Castro-Longoria¹, Miguel Avalos Borja^{2,3}

¹Departamento de Microbiología, CICESE, Ensenada, B.C. México, ²IPICIT, División de Materiales Avanzados, San Luis Potosí, S.L.P. México, ³Centro de Nanociencias y Nanotecnología, UNAM, Ensenada, B.C.
vazquezm@cyn.unam.mx

INTRODUCTION

Bionanomedicine studies the application of nanomaterials to address several current challenges in the clinic, such as treatments for cancer, drug transport and infectious diseases. In this field, different nanostructures and their interaction with biological systems are studied. Silver nanoparticles (AgNPs) are among the most studied materials, due to the microbicidal properties of silver [1]. While colloidal silver has undesirable effects, AgNPs could be more biocompatible, preserving or enhancing the microbicidal action of silver [2]. Infectious diseases are a major problem worldwide. Among these diseases, fungal infections are the fourth leading cause of death, where candidiasis is the most common. This disease is generated by the dimorphic fungus *Candida* spp, with *Candida albicans* as the most common and representative [3]. The use of antibiotics is not enough to combat infectious diseases, so alternative treatments are studied, such as the use of nanotechnology [4]. This study evaluates the effect of AgNPs against *C. albicans*, due to the clinical importance of this fungus and the few studies that exist [5].

The inhibitory concentrations (MIC and IC₅₀) of AgNPs were determined by the modified microdilutions test M27-A2 of the Clinical Laboratory Standards Institute [6], using the reference strain *C. albicans* ATCC SC5314. To determine the intracellular distribution of AgNPs, fungal cells (2.5x10⁶*mL⁻¹) exposed to the MIC were fixed with 2% glutaraldehyde in phosphate buffer and post fixed with 1% OsO₄. After fixation, cells were dehydrated in ethanol series and embedded in Spur's resin to finally obtain ultrathin sections. Samples were examined under transmission electron microscopy without post-dyeing. Results show antifungal activity at low concentrations (MIC= 150 µg*mL⁻¹; IC₅₀= 60 µg*mL⁻¹), lower than those of fluconazole. Currently, the mechanism of action of AgNPs is

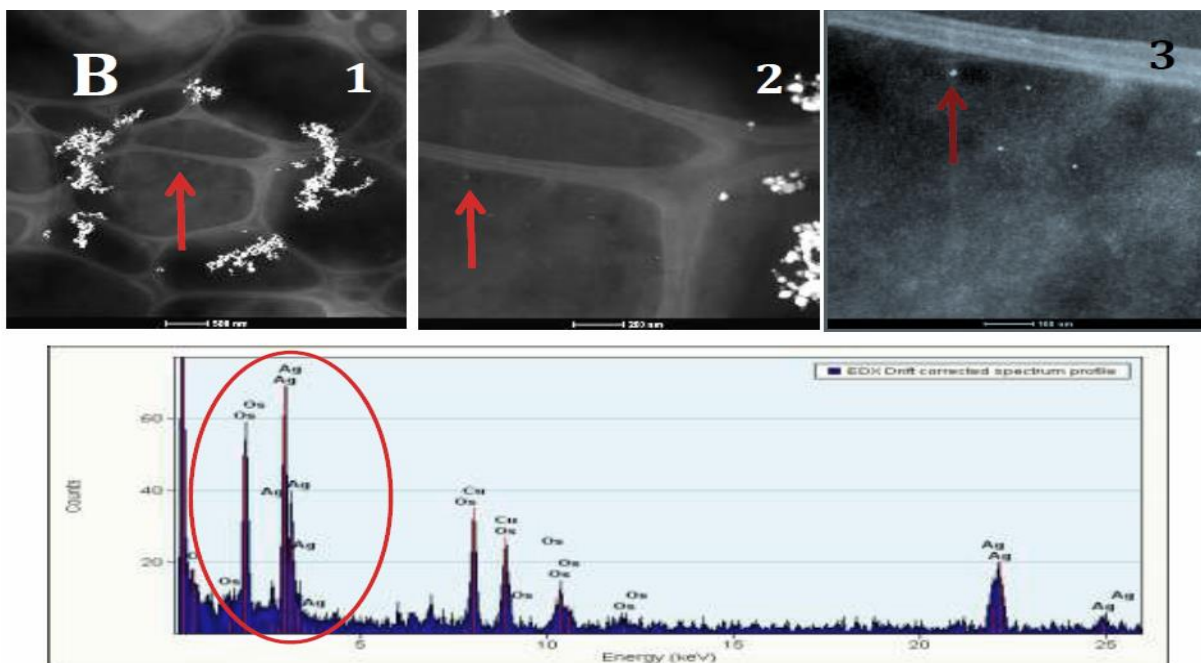


Fig. 1. Ultra structure analysis of the AgNPs-treated *Candida albicans* cells.

poorly understood. In order to increase the knowledge of how silver nanoparticles interact with the fungi, we determined the ultrastructural distribution of AgNPs in *C. albicans* cells. It was found that AgNPs, accumulate outside the cell but also smaller NPs localize throughout the cytoplasm. Energy dispersive spectroscopy (EDS) and

crystallography analysis confirms the presence of crystalline silver inside the cells. From the results obtained it is assumed that AgNPs used for this study do not penetrate the cell, but possibly free silver ions infiltrate into the cell and AgNPs are formed by reduction with soluble proteins present in the cytoplasm as no relationship was found with cell membrane or any membranous organelle.

ACKNOWLEDGMENT

We thank the Consejo Nacional de Ciencia y Tecnología (CONACyT) for a scholarship to RVM. We also thank Dr. Rosa Mouriño-Pérez for providing *C. albicans* strain, Dr. Nina Bogdanchikova for silver nanoparticles supply, Dr. Nicolás Cayetano for help with TEM work, and LINAN (IPICyT) for providing access to TEM facilities. Part of this work was funded by a SEP-CONACyT grant (CB2011/169154).

REFERENCES

- [1] Rai M. *et al.* *Biotech. Adv.* 27 (2009): 76-83.
- [2] Huh & Kwon (2011). *J. Control Release.* 156:128-145.
- [3] Pfaller & Diekema (2007). *Clinical microbiology reviews.* 20:133–63.
- [4] Taubes G. *Science* 321 (2008):356–61.
- [5] K-J Kim *et al.* *Biometals*, 22 (2009) 235–242.
- [6] CLSI, 2002

Encapsulation of Interference RNA by the CCMV capsid proteins

J.N. Zamudio-Ocadiz¹, R. Vazquez-Duhalt², R.D. Cadena Nava²

¹Centro de Investigación Científica y de Educación Superior de Ensenada, Ensenada, B.C. México, ²Centro de Nanociencias y Nanotecnología, Universidad Nacional Autónoma de México, Ensenada, B.C. México
jzamudio@cicese.edu.mx

ABSTRACT

The Cowpea Chlorotic Mottle Virus (CCMV) is a single-stranded RNA (ssRNA) icosahedral virus, which under certain conditions of pH and ionic strength have been disassembled and reassembled in vitro. In this work, we show the encapsidation of small interfering RNA (siRNA) with the capsid proteins of CCMV. The siRNA is a double-stranded RNA (dsRNA) molecule with 21 base pairs of length, the most notable role of siRNA is that can suppress the expression of a target gene with complementary nucleotide sequence. Synthesis of siRNA molecules was done in vitro, with a T7 RNA polymerase based system. The siRNA used in this work corresponds to a Renilla luciferase protein. Gel electrophoresis was performed to determine the synthesis of siRNA and the assembled nanoparticles were analyzed by Transmission Electron Microscopy (TEM). We observed spherical and tubular capsids with diameters of 21 and 16 nm respectively, as well as large and short tubes. We propose the use of protein shells from the Cowpea Chlorotic Mottle Virus (CCMV) to protect and delivery siRNA to target cells. The results obtained in this work could be used to improve the siRNA-based therapies.

Inhibitory effect of silver nanoparticles in bacteria of clinical interest

Roberto Vazquez-Muñoz¹, Alejandro Huerta Saquero¹, Roxana Ortiz², Emiliano Ventura Macías¹, Nina Bogdanchikova¹

¹Centro de Nanociencias y Nanotecnología, UNAM, Ensenada, B.C.; ²Facultad de Ciencias, UABC, Ensenada, B.C.
vazquezm@cnyunam.mx

ABSTRACT

Infectious diseases are the leading cause of death worldwide [1]. Bacterial infections are among the top of incidence. These diseases represent a significant proportion of public and private health resources, achieving cost of billions dollars [2]. Nowadays, antibiotics are the most effective way to treat infectious diseases, but there are many problems associated with their use [3], among them, the emergence of antibiotic-resistant microorganisms. In addition, there is no assurance that antibiotics are still generated at the pace required [4], so alternatives are sought in other technologies. Nanotechnology provides a platform for novel materials with property in the clinic.

Silver nanoparticles (AgNPs), are one of the most studied materials in biomedicine because of the clinical properties of silver. Its main application is as an antibiotic agent type, due to the well-known antimicrobial properties of silver, under the concept of "nanoantibiotics" [5]. There are many types of AgNPs, with different characteristics and properties, so it is important to study their effects and interactions against pathogens.

In this work, the inhibitory concentrations (MIC and IC₅₀) of AgNPs were determined by the modified microdilutions test M07-A9 y M45-A2 of the Clinical Laboratory Standards Institute [6], using the reference strains *Escherichia coli*, *Salmonella typhimurium* and *Staphylococcus aureus*. Bacterial cells were exposed to different concentrations of silver nanoparticles and silver nitrate. Cells treated with silver nanoparticles were cultured in media without treatments, in order to determine a bactericidal or bacteriostatic effect exerted by AgNPs over bacteria.

ACKNOWLEDGMENT

We thank to the Consejo Nacional de Ciencia y Tecnología (CONACyT) for a scholarship to RVM..

REFERENCES

- [1] NLM: National Library of Medicine. Infectious diseases
- [2] Scott D. (2009). The direct medical costs of healthcare-associated infections in U.S.
- [3] Fothergill *et al*, (2006). *Infect Dis Clin N Am* 20:699–709
- [4] Talyor *et al*, (2002). *Drug Discov. Today* 7(21):1086–1091.
- [5] Huh & Kwon (2011). *J. Control Release*. 156:128-145.
- [6] CLSI: Clinical Laboratory Standard Institute.

Enteral Administration of Bile Salt-Phosphatidylcholine Mixed Micelles Loaded with Clonazepam Improves the Anticonvulsant Response in Pentylentetrazole-Induced Seizures in Mice

Chavez Ramirez Daniela Silem^{1a}, Quintanar Guerrero David^{1b}, González Trujano Eva^{3c}, Leyva Gómez Gerardo²

¹Laboratory of Researching and Postgrade in Pharmaceutical Technology, Faculty of Higher Education Cuautitlán, National Autonomous University of Mexico. Av. 1° de Mayo s/n, Cuautitlán Izcalli, Estado de México, 54740, México, ²Laboratory of Connective Tissue, National Institute of Rehabilitation, Mexico City, Mexico, ³National Institute of Psychiatry. Ramón de la Fuente Muñiz. Research in Neuroscience. Av. México-Xochimilco 101, Col. Sn Lorenzo Huipulco, 14370. México, D. F. México.

^adaniela_silem@hotmail.com, ^bquintana@servidor.unam.mx, ^cevag@imp.edu.mx

ABSTRACT

In recent years, nanotechnology has changed the functionality of various materials to offer new alternatives to current challenges. One of the exemplary cases is medicine, where it is desired to design new medicines more efficient and with lower side effects. In this work, the anticonvulsant effectiveness of clonazepam (CLZ) loaded in bile salt – phosphatidylcholine mixed micelles (MM, CLZ-MM) administered by enteral route (oral, p.o.) in mice was investigated. Doses of CLZ and CLZ-MM at 0.01, 0.03, 0.1, 0.3 mg/Kg were administered by p.o. route to assess its anticonvulsant effect on pentylentetrazole (PTZ) induced seizures (80 mg/kg, i.p.) The occurrence of myoclonus, generalized seizures and tonic convulsions or mortality induced by the convulsant agent PTZ was registered. Statistical evaluation of latencies to seizures were evaluated as means by ANOVA and T Student tests (SigmaStat® SPSS). The size, zeta potential, shape and composition of mixed micelles were analyzed by light scattering, transmission electron microscopy (TEM), and high-performance liquid chromatography (HPLC). CLZ-MM of $22 \pm .59$ nm diameter, a zeta potential value at $-28.65 \pm$ mV, a spherical shape without drug crystal formation, an entrapment efficiency of 48.7% (w/) and drug loading of 10.3% (w/w) were obtained for this pharmaceutical formulation. A higher anticonvulsant effect on generalized and tonic seizures was obtained with CLZ-MM at 0.01 mg/kg. This carrier system could reduce side effects and is a proposal to improve efficiency of the drug dosage. These experiments are evidence that nanoparticulated pharmaceutical formulations offer several advantages in the transport of drugs to enhance their therapeutic activity.

Tomsk Polytechnic University – National Autonomous University of Mexico: 14 years of collaboration in nanoscience

Alexey Pestryakov¹, Nina Bogdanchikova², A.Simakov², E.Smolentseva², Vitalii Petranovskii², C. Almonaci²
¹ Tomsk Polytechnic University, Tomsk 634050, Russia, ² Centro de Nanociencias y Nanotecnología, Universidad Nacional Autónoma de México, Ensenada 22800, México
 pestryakov2005@yandex.ru

INTRODUCTION

Collaboration between TPU and CNyN-UNAM started in 2000. During 14 years researchers from Mexico and Russia executed seven mutual projects in the field of synthesis and investigation of catalysts based on metal nanoparticles (Ag, Au, Cu), as well as application of medicines based on colloidal silver. Long-term Russian-Mexican collaboration resulted in more than 50 articles, several patents, 6 PhD and MS thesis. This is an example of very effective and fruitful scientific cooperation between leading universities of two countries.

RESULTS

Nanogold catalysts for oxidation of CO and organic compounds

Supported gold nanoparticles attract great attention due to unique catalytic activity at low temperature in low-temperature CO oxidation, liquid phase oxidation of alcohols and other important processes for industry. Different factors (amount of defects, perimeter interface, strength of metal-support interaction, gold effective charge, etc.) are considered to influence strongly gold particle size, character of its interaction with the support and as a consequence its catalytic activity.

Catalytic tests in CO oxidation show several regions of the reduced samples with various catalytic behaviours: 20-200°C, 200-400°C and > 400°C; this situation is explained by the co-existence of gold active sites of different types. A comparative analysis among spectroscopic and catalytic data allows suggesting Auⁿδ⁺ clusters to be responsible for the activity in the low-temperature region (< 200°C); neutral Auⁿ clusters are active in the range 200-400°C; and gold nanoparticles may catalyze high-temperature CO oxidation. Au³⁺ ions are inactive in this process. The catalytic process seems to be very sensitive to Au effective charge; that is why gold catalysts are rapidly deactivated during storage in air. Our previous studies showed that in the samples Au/zeolite gold clusters are easily oxidized by air during long-term storage and effective charge of Au^{δ+} states exceeds the optimal one. At higher temperatures (> 150-200°C) bigger metal particles can participate in the catalytic process as well because under such conditions Au^{δ+} states may be formed on the gold surface as a result of reaction with the adsorbed oxygen.

Nanosized gold supported on modified mesoporous silica is an effective catalyst for the liquid-phase aerobic oxidation of benzyl alcohol. The catalysts exhibited high activity (TOFs of up to ca. 1000 h⁻¹), selectivity to the ester (up to 95%) and stability (TONs of up to ca. 4300). Among the studied modifiers, Ce and Ti oxides were found to be better promoters as compared with Fe oxide. The activation effect of the modifiers is associated with their influence on the electronic state, redox properties, and aggregation tendency of the supported gold, probably, due to the stronger support-catalyst interaction.

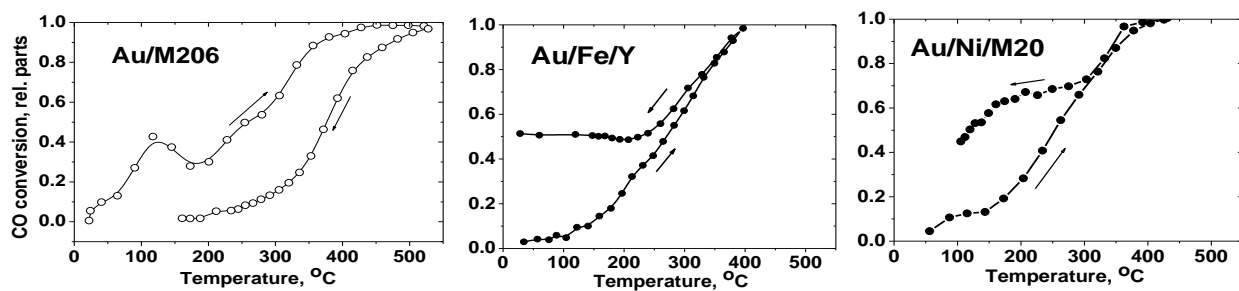


Figure 1. CO conversion versus temperature over Au/zeolite catalysts

Nanocopper catalysts supported on zeolites

Copper-containing systems are widely used as catalysts for processes of oxidation and hydrogenation of organic compounds. In spite of the long-term investigations, the nature of active sites of copper catalysts and the mechanism of interaction of the active component with the supports and modifiers is still under the discussion.

Different states of copper have been identified on the surface of $\gamma\text{-Al}_2\text{O}_3$, mordenite, erionite, clinoptilolite, pumice and bulk copper catalysts (foam copper) by spectroscopic methods. Spectroscopic experiments revealed that formation of copper active surface depends strongly on the nature of the support. In zeolites copper has the highest dispersion and the highest oxidizing ability, while on the surface of pumice and bulk metal the portion of the oxidized states of copper is small. Modifying additives exert a sufficient effect on the electronic states of copper as well. Thus, the experiments showed that additions of Ce and Zr oxides cause an electron-seeking effect on supported copper, stabilize the oxidized state of the metal and increase the effective charge of copper ions. In contrast, La and Cs oxides lower the effective charge of Cu^+ and $\text{Cu}_n^{\delta+}$ and favor their fast reduction at red-ox treatments. On low-surface supports, big particles of copper experience a minor influence of the modifiers. However, a part of the support surface (20-40 %) is not covered by big metal particles and contains highly-dispersed Cu^+ and $\text{Cu}_n^{\delta+}$ states. The modifiers produce a direct effect on electronic properties of these dispersed copper states.

High-effective medicines based on colloidal silver

The results of the present study showed that nanosilver in the form of gel and cream is effective for treatment of infected and not infected ulcers of diabetic legs of 1st Grade (classification of Wagner), I-B Grade (classification of Texas), as well as against condiloma acuminado (human Virus of papilloma) and acquired digital fibroma (histiocitoma recluse). The conventional treatments in these cases are longer, expensive and have complications.

Nanosilver containing gel and cream slows down the epithalization process in ulcers of diabetic patients; however one of the most important advantages is that the ulcers stay clean. The benefit of maintenance of the clean wound is better as compared to iodine, and colloidal silver liofilizada. It is necessary to point out that there was a reduction of the use of antimicrobial medicines if nanosilver products were applied in every treatment cycle. As regards condiloma acuminado and fibroqueratoma the result was favorable with tendency to the improvement.

Models of Porous Media Filling Using Sphere Packing Approach for Different Size Distributions

Larysa Burtseva^{1,a}, Alexey Pestryakov^{2,b}, Rainier Romero^{3,c}, Benjamín Valdez^{1,d}, and Vitalii Petranovskii^{4,e}

¹Instituto de Ingeniería, Universidad Autónoma de Baja California, Mexicali, B.C., México, ²Tomsk Polytechnic University, Tomsk, Russia, ³Universidad Politécnica de Baja California, Mexicali, B.C., México, ⁴Centro de Nanociencias y Nanotecnología, Universidad Nacional Autónoma de México. Ensenada, B.C. México.
burtseva@uabc.edu.mx

ABSTRACT

Macroscopic properties of a material such as elasticity, thermal conductivity or permeability are highly affected by its structure on the particle level. Therefore, the design of modern high-performance materials requires a comprehension of influence of structure on physical properties. Geometric models are powerful tools for studying these complex relations. Physical properties of the corresponding material should be simulated using a model of structure. Structure models with varying parameters allow to investigate the change of material properties and to obtain good candidates. The increasing capability of algorithms used, as well as computer power allows for high precision in the simulation results. In return, this produces new model structures and fitting procedures.

In many cases, the three-dimensional (3D) structural model of a matter can be represented as spheres packed in the available space. In case if the packing space is limited with a predetermine region, such as different types of matrices, filling of a porous structure (channels) with atoms and molecules of equivalent or comparable diameters (spheres), is commonly investigated through packing models. Packing of spheres belongs to the most-studied types of models.

The understanding of packing characteristics of particles is important in the modeling of structural properties of a material. Many factors affect the packing assumptions, such as particle size distribution, particle shape, inter-particle friction, surface chemistry, and agglomeration. Among these variables, the particle size distribution is probably most significant.

Considering spheres as objects to pack, the corresponding models can be classified into three categories: packings with monosized, bimodal and lognormal sphere size distributions. The particle size distribution is key issue of any investigation in this area; therefore, methodology, parameters measured and simulation algorithms are subjected to the type of particle size distribution. The common properties of each one of mentioned packing category are summarized in this study, and appropriate algorithms are listed.

ACKNOWLEDGMENTS

This research was supported by CONACYT, México, through grant 102907 and UNAM-PAPIIT through grant IN110713.

Second-Harmonic Generation from Gold Nanoparticles on Profiled Substrate

C.I. García-Gil¹, V.A. Verdugo-Gutiérrez¹, A.V. Khomenko, M.A. García-Zárate.
¹Centro de Investigación Científica y de Educación Superior de Ensenada, B. C.; México.
 akhom@cicese.mx

INTRODUCTION

Second-harmonic generation (SHG) is a nonlinear optical process in which two photons interact in a nonlinear material and one photon is generated. SHG has been used as a powerful tool for investigation of electronic and optical properties of metal nanoparticles of different sizes, shapes in colloids as well as for planar arrays of nanoparticles. One among the most common and simple methods for metal nanoparticles fabrication is a chemical method that results in colloidal suspensions of nanoparticles. The main obstacle to the application of SHG for investigation of colloids or randomly arranged on the substrate nanoparticles is extremely low efficiency of SHG. We report the experimental and numerical study of SHG from nanoparticles placed on the substrate with periodical structure of the surface to improve significantly the detection of SHG.

SAMPLES FABRICATION

To fabricate substrates with periodic surface profile we used crystalline silicon wafers that were recorded with photoresist. The grating was recorded on photoresist by interference lithography method using a laser with 406 nm wavelength and 0.5 W power; and then the silicon wafers were subjected to reactive ion etching.

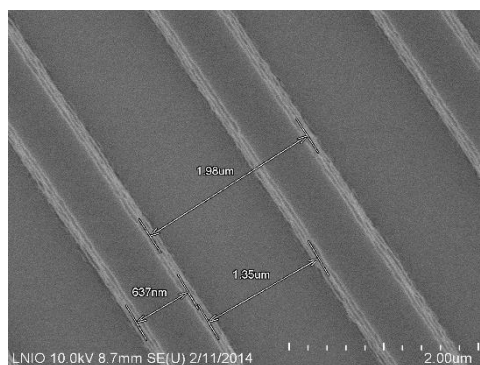


Fig. 1. Scanning electron microscopy image of the silicon substrate with periodical surface profile.

Figure 1 shows the electron microscope image of one of the fabricated substrate with 1.98 μm period and approximately 0.1 μm depth of the surface profile. In the next step of sample fabrication, the substrate is coated with nanoparticles from gold colloids.

SHG FROM PERIODICAL ARRAY OF METAL

For calculation of radiated second harmonic at far field we use the theoretical results presented in Ref. [1,2] that take into account dipole and quadrupole contributions and consider a plane wave pump beam. Figure 2 shows spatial distribution of SH power radiated by a single nanoparticle in forward and back directions. Figure 3 shows the same as Fig. 2a but for the 8x8 array of nanoparticles. When the number of the nanoparticles increases and they are arranged in a periodic structure such as shown in Fig. 1, the radiated power is redistributed due to interference. This leads to the increase of the peak intensity in the SG radiation pattern as N^4 , where N is the number of the nanoparticles.

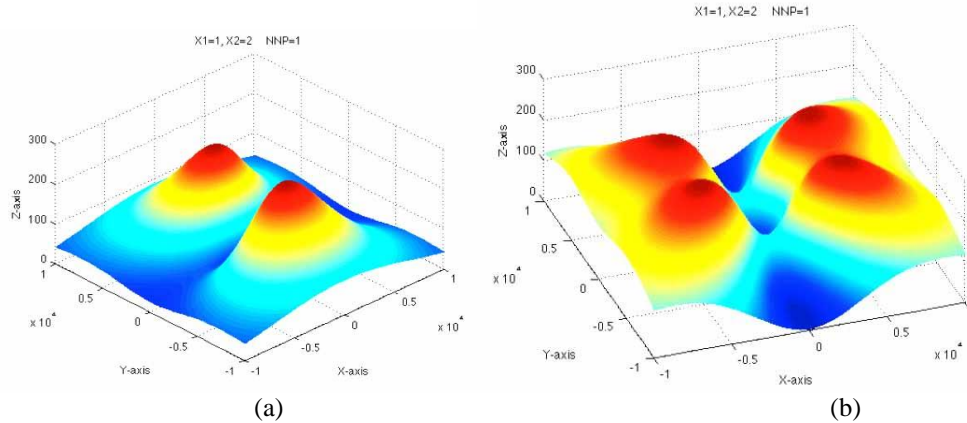


Fig. 1. SG radiation patterns of single metallic nanoparticle in forward (a) and back (b) directions.

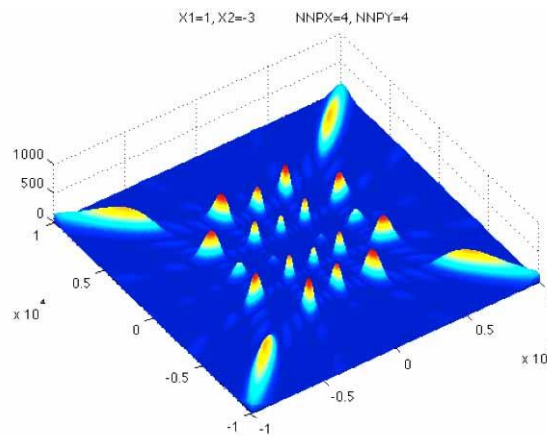


Fig. 2. SG radiation patterns from an 8x8 array of metal nanoparticles.

CONCLUSIONS

We propose a method that allows spatial localization and therefore increase the intensity of SHG radiation from metal nanoparticles fabricated by chemical method. The method involves the use of a substrate with a periodic surface profile (a diffraction grating) made coated with metal nanoparticles. We show that polarization and intensity of SH depend on polarization of pump beam that allows separate the contributions of different order in process of SHG.

ACKNOWLEDGMENTS

This work was supported by CONACYT through grant 129674. We acknowledge Rafael Salas Montiel (University of Technology of Troyes, France) for his great contribution to samples fabrication.

REFERENCES

- [1] J. I. Dadap, J. Shan, K. B. Eisenthal, and T. F. Heinz, "Second-harmonic Rayleigh scattering from a sphere of centrosymmetric material," *Physical review letters* 83, 4045-4048 (1999).
- [2] J. I. Dadap, J. Shan, and T. F. Heinz, "Theory of optical second-harmonic generation from a sphere of centrosymmetric material: small-particle limit," *Journal of the Optical Society of America B* 21, 1328-1347 (2004).

Time-resolved Z-scan technique for simultaneous measurements of nonlinear absorption, thermo-optic, and Kerr effect in nonlinear optical materials

Arturo S. Rojas, A. V. Khomenko, and M.A. García-Zárate.
 Centro de Investigación Científica y de Educación Superior de Ensenada, B. C., México
 jarojas@cicese.edu.mx

ABSTRACT

The dependence of the refractive index and absorption coefficient with the light intensity, known as optical Kerr effect, and nonlinear absorption respectively have several important applications, especially in devices for the control of ultrafast optical signals. Thus, there is a wide search for new materials with optimal nonlinear parameters for specific applications. The Z-scan technique is a relatively simple and reliable method for measure the Kerr coefficient and two-photon absorption. It has been shown that Z-scan allows distinguish between nonlinear effects with different physical mechanisms investigating the time response of the optical medium [1, 2]. This is important for applications where the signal has a high repetition rate and high average power. In this case, the ultrafast response can be affected by cumulative effects like slow thermo-optic effect.

The recent advances in the synthesis of complex nanostructures open the possibility to explore new electronic nonlinear optical properties. Nobel metal nanoparticles have attracted interest due to enhanced nonlinear optical response that can be used in new optoelectronic devices such as optical switches and limiters. The high-frequency and high-intensity operation of these devices make it necessary to use an experimental method that allows distinguishing between relatively slow thermo-optic and ultra-fast Kerr effects that contribute to the overall nonlinear response of the nanoparticles. We present the method that allows a simultaneous measurement of nonlinear absorption, thermo-optic, and Kerr effect.

Following [2], we developed a fully automated Z-scan experimental setup that allow a time-resolved simultaneous measurement of different nonlinear effects optical materials. Schematic of the experimental setup is shown in Fig. 1.

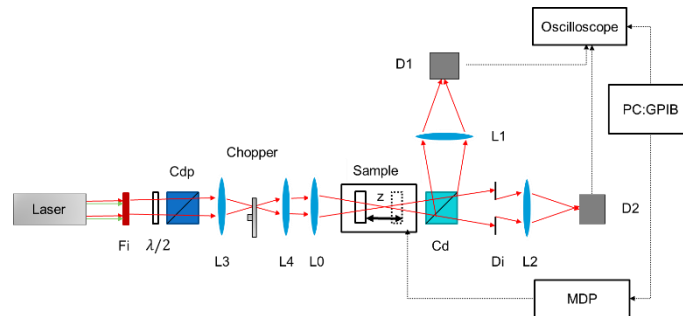


Fig. 1. Experimental setup. Fi filter, L0-4 lens, Cdp polarized beam-splitter cube, MDP computer translation stage, Cd beam-splitter cube, Di aperture y D's photodetectors.

The Ti:Sapphire laser delivered pulses at 835 nm wavelength with 88 MHz repetition rate. The FWHM pulse width was 120 fs. The pulse train was modulated by a mechanical chopper with the frequency of 50 Hz. The detection system includes ultra-fast photodiode and digital oscilloscope that allowed resolving each laser pulse at any Z-position during 0.5 ms. Thus the Z-scan signal temporal evolution was recorded during this time for further processing. To demonstrate experimental technique we present the results for Au-nanoparticle suspensions of different shapes. The method developed in the present work gives a basis for future studies on the nonlinear optical properties of the third order in suspensions of nanoparticles and solid samples allowing the search for nonlinear materials with optimal parameters for variety of applications.

ACKNOWLEDGMENT

This work was supported by CONACYT through grant 129674.

REFERENCES

- [1] Falconieri, M. (1999). Thermo-optical effects in Z-scan measurements using high-repetition-rate lasers. *Journal of Optics A: Pure and Applied Optics*, 1(6), 662.
- [2] Gnoli, A., Razzari, L., & Righini, M. (2005). Z-scan measurements using high repetition rate lasers: how to manage thermal effects. *Optics Express*, 13(20), 7976-7981.

Author index

- Abdulaeva, Liliia D. # **P-01**
Acosta Chávez, R. M. # **P-21**
Acosta, Brenda # **O-10, O-17, P-16**
Aguilar Tapia, A. # **P-17**
Almjasheva, O.V. # **P-03**
Almonaci, C. # **P-36**
Alonso Núñez, Gabriel # **K-01, O-01, O-04, P-08, P-24, P-30**
Antaschuk, Ksenia # **P-11**
Antúnez-García, Joel # **O-07, P-20**
Avalos Borja, Miguel # **P-32**
Avalos, L. # **P-28**
Badmaev B.B. # **K-09**
Bavrina, O.O. # **P-04**
Bedolla, Z. # **K-01, P-24**
Beloshapkin, S. # **O-10, O-11**
Bogdanchikova, Nina # **O-12, P-17, P-27, P-34, P-36**
Bugrov, A.N. # **P-03**
Burovikhina, A.A. # **P-02**
Burtseva, Larysa # **P-37**
Cabrera Ortega, J.E. # **P-17**
Cadena-Nava, Rubén Darío # **O-18, P-33**
Calvario, J.L. # **P-27**
Can-Uc, Bonifacio # **P-31**
Cardoza, M. # **K-01**
Castillón Barraza, F.F. # **O-14, P-19, P-22, P-23**
Castro-Longoria, Ernestina # **P-32**
Chaikina, E.I. # **P-28**
Chavez Ramirez, Daniela Silem, # **P-35**
Chávez Rivas, F. # **O-14, P-19**
Chislov, M.V. # **P-02**
Clegg, M.L. # **O-06**
Concepción Rosabal, B. # **P-19**
Contreras, Oscar E. # **K-01, O-01, P-28**
Córdova Rodríguez, V. # **P-21**
Córdova, Margoth # **O-03**
Cota E. # **O-08**
Damdinov, Bair # **K-09, O-20**
Dasgupta-Schubert, N. # **O-19**
de los Reyes, J.A. # **P-10**
Dembelova, Tuyana S. # **K-09**
Demidova, Yu. # **P-14, P-15**
Diaz de Leon, J.Noé # **P-08, P-09, P-10, P-24**
Domínguez, David # **K-01, O-01**
Driver S.M. # **O-06**
Estrada, Miguel # **O-05, O-10, O-11**
Evangelista, Viridiana # **O-10, O-17, P-16**
Farias, M.H. # **P-13**
Fruchart, Daniel # **P-05**
Fuentes Moyado, Sergio # **K-04, O-02, O-04, O-05, O-11, P-08, P-09, P-10, P-22**
Galván Martínez, D. Homero # **K-04, O-07, P-07, P-08, P-20**
García, Víctor # **K-01**
García-Gil C.I. # **P-38**
García-Zárate M.A. # **P-38, P-39**
Gómez-Rosas, G. # **P-29**
González Trujano, Eva, # **P-35**
Herrera Zaldivar, M. # **K-06, O-14**
Huerta Saquero, Alejandro # **O-12, P-27, P-34**
Jaime-Acuña, O. E. # **P-18**
Juárez-Moreno, Karla # **O-04**
Kalashnikov, Sergei, # **O-20**
Karakatsani, S. # **O-06**
Khomenko A.V. # **P-38, P-39**
King, D.A. # **O-06**
Klyukin, Konstantin # **P-05**
Kotolevich, Y. # **P-17**
Kovalyov, A.N. # **O-09, P-06**
Kultaeva, A.Y. # **O-09**
Kurenkova, Elena # **K-08, P-26**
Leyva Gómez, Gerardo # **P-35**
López Bastidas, Catalina # **K-07, O-13, P-30**
López Cisneros, M. # **O-11**
Lugo-Medina, Eder # **P-09**
Luna Vázquez R. # **O-12, P-27**
Machorro, Roberto # **K-07, O-13, P-30**
Martínez-Benítez, A. # **P-29**
Martinez-Castelo, J.R. # **P-13**
Martynyuk, O. # **O-12, P-17, P-27**
Maturano Rojas, V. # **P-17**
Mechtaeva, E.V. # **P-02**
Méndez Eugenio R. # **O-03, P-28**
Mikhailov, E.F. # **K-03**
Mikheenko, E.P. # **P-07**
Miridonov, Serguei # **O-17, P-16, P-22**
Mora, J. # **O-08**
Morales de la Garza, L. # **O-06**
Muñoz, Franklin # **K-01, O-01**
Murrieta-Rico, Fabian N. # **P-25**
Murzin, D.Yu. # **P-14, P-15**
Nomoev Andrei, # **O-20**
Obeso-Estrella, René # **P-09, P-22**
Oliver, Alicia # **P-31**
Ordóñez Peres, Carlos # **O-15, O-16**

Ortiz, Roxana # **P-34**
 Oseguera-Galindo, D.O. # **P-29**
 Penton Madrigal A. # **P-19**
 Perez, Omar # **K-01**
 Pérez Cabrera, L. # **K-04, P-08**
 Pérez-Centeno A. # **P-29**
 Pestryakov, Alexey # **O-12, P-17, P-27, P-36, P-37**
 Petranovskii, Vitalii # **O-07, O-09, O-13, O-14, P-06, P-10, P-18, P-19, P-20, P-21, P-22, P-24, P-25, P-30, P-36, P-37**
 Quintanar Guerrero, David, # **P-35**
 Ramírez-Garza, R.E. # **P-23**
 Rangel-Rojo, Raúl # **P-31**
 Raymond, Oscar # **P-18**
 Rodionov, I.A. # **P-02, P-03**
 Rodríguez-Fernández, Luis # **P-31**
 Rodríguez-Iznaga, I. # **O-14, P-19, P-21, P-23**
 Rojas, Arturo S. # **P-39**
 Rojas, F. # **O-08**
 Romanov, Nikolai # **O-20**
 Romero, Rainier # **P-37**
 Romo-Herrera, José M. # **K-01, O-01, P-28**
 Ruiz Medina, F. # **O-12, P-27**
 Rumynin V.G. # **O-15, O-16**
 Sánchez-Lopez, P. # **P-22**
 Santana-Aranda, M.A. # **P-29**
 Saraev, Alexander # **P-11, P-12**
 Sergiyenko, Oleg Yu. # **P-25**
 Shelyapina, Marina G. # **K-05, O-09, P-04, P-05, P-06, P-07, P-26**
 Simakov, Alexander # **P-12**
 Simakov, Andrey # **O-05, O-10, O-11, O-17, P-14, P-15, P-16, P-23, P-36**
 Simakova, Irina # **O-10, P-14, P-15**
 Smolentseva, Elena # **O-05, O-10, O-11, O-13, P-36**
 Smyslov, R.Yu. # **P-03**
 Soto, Gerardo # **O-01**
 Stepanov, Serguei # **P-30**
 Suresh, C. # **P-08**
 Tito Ferro, D. # **P-19**
 Tiwari, D. K. # **K-06, O-19**
 Tiznado, Hugo # **K-01, O-01, P-13, P-17**
 Tokarev, Igor # **K-03, O-15, O-15, P-11, P-12**
 Torres-Otañez, G. # **P-10**
 Utkina, T.D. # **P-02**
 Valdez, Benjamín # **P-37**
 Valenzuela, J. # **K-06**
 Vargas, Eunice # **O-05**
 Vazquez-Duhalt, Rafael # **O-04, P-33**
 Vazquez-Muñoz, Roberto # **P-32, P-34**
 Velarde, Juan J. # **P-30**
 Ventura Macías, Emiliano # **P-34**
 Verdugo-Gutiérrez V.A. # **P-38**
 Villaseñor Cendejas, L. M. # **O-19**
 Villavicencio, H. # **P-18**
 Zamudio-Ocadiz, J.N. # **P-33**
 Zanella Spesia R. # **P-17**
 Zavala-Sánchez, L.A. # **P-10**
 Zepeda, Trino A. # **O-12, P-08, P-09, P-10**
 Zhukov, Y.M. # **O-09**
 Zvereva, Irina # **K-02, P-01, P-02, P-03**